UNDERSTANDING THE BIOCHEMICAL BASIS OF TEMPERATURE INDUCED LIPID PATHWAY ADJUSTMENTS IN PLANTS

A Thesis Submitted to the College of
Graduate Studies and Research
In Partial Fulfillment of the Requirements
For the Degree of Doctor of Philosophy
In the Department of Biology
University of Saskatchewan
Saskatoon

By

QIANG LI

PERMISSION TO USE

In presenting this thesis/dissertation in partial fulfillment of the requirements for a Postgraduate degree from the University of Saskatchewan, I agree that the Libraries of this University may make it freely available for inspection. I further agree that permission for copying of this thesis/dissertation in any manner, in whole or in part, for scholarly purposes may be granted by the professor or professors who supervised my thesis/dissertation work or, in their absence, by the Head of the Department or the Dean of the College in which my thesis work was done. It is understood that any copying or publication or use of this thesis/dissertation or parts thereof for financial gain shall not be allowed without my written permission. It is also understood that due recognition shall be given to me and to the University of Saskatchewan in any scholarly use which may be made of any material in my thesis/dissertation.

DISCLAIMER

Reference in this thesis/dissertation to any specific commercial products, process, or service by trade name, trademark, manufacturer, or otherwise, does not constitute or imply its endorsement, recommendation, or favoring by the University of Saskatchewan. The views and opinions of the author expressed herein do not state or reflect those of the University of Saskatchewan, and shall not be used for advertising or product endorsement purposes.

Requests for permission to copy or to make other uses of materials in this thesis/dissertation in whole or part should be addressed to:

Head of the Department of Biology
University of Saskatchewan
112 Science Place
Saskatoon, Saskatchewan S7N 5E2
Canada

OR

Dean
College of Graduate Studies and Research
University of Saskatchewan
107 Administration Place
Saskatoon, Saskatchewan S7N 5A2
Canada

ABSTRACT

One of the cellular responses to temperature fluctuations in plants is the adjustment in the degree of membrane unsaturation. Glycerolipids are major constituents of cellular membranes. In higher plants, glycerolipids are synthesized via two major metabolic pathways compartmentalized in the ER and chloroplast. Adaptive responses in membrane lipids include alterations in fatty acid desaturation, proportional changes in membrane lipids as well as molecular composition of each lipid species. In this study, I systematically explored the significance of glycerolipid pathway balance in temperature induced lipid composition changes in three plant species that have distinctive modes of lipid pathway interactions through a combination of biochemical and molecular approaches including lipidomics and RNA-seq analysis. In *Arabidopsis thaliana*, a 16:3 plant, low temperature induces an augmented prokaryotic pathway, whereas high temperature enhances the eukaryotic pathway. *Atriplex lentiformis* reduces its overall lipid desaturation at high temperature and switches lipid phenotype from 16:3 to 18:3 through drastically increasing the contribution of the eukaryotic pathway as well as suppression of the prokaryotic pathway. In sync with the metabolic changes, coordinated expression of glycerolipid pathway genes, as revealed by RNA-seq also occurs. In *Triticum aestivum*, an 18:3 plant, low temperature leads to a reduced glycerolipid flux from ER to chloroplast. Evidence of differential trafficking of diacylglycerol (DAG) moieties from ER to chloroplast was uncovered in three plant species as another layer of metabolic adaptation under different temperatures. Taken together, this study has established a biochemical basis that highlights the predominance and prevalence of lipid pathway interactions in temperature induced lipid compositional changes.

ACKNOWLEDGEMENTS

I would like to express my gratitude to my supervisors and mentors, Dr. Jitao Zou and Dr. Yangdou Wei, for their full support, expert guidance, understanding and encouragement throughout my study and research. During the past five years, your immense knowledge and scientific attitude always pushed me forward; your kindness and patience always warmed me; your enthusiasm and motivation always encouraged me. I could not have imagined having better advisors and mentors for my Ph.D study.

Special thanks to my advisory committee, Dr. Peta C. Bonham-Smith, Dr. Gordon R. Gray and Dr. Kenneth Wilson for their support, guidance and helpful suggestions. I would also like to thank Dr. Owen Rowland for serving as my external examiner.

Members of Zou lab also deserve my sincerest thanks, their friendship and assistance has meant more to me than I could ever express. I am very grateful to Dr. Wenyun Shen for his help and advice, especially teaching me most of lab skills in lipid analysis and enzymatic assays, during my Ph.D. study. I would like to send many thanks to Dr. Liping Wang, Dr. Peng Gao, Ioannis Mavraganis and Jie Gao, who cheerfully answered my questions and maximally endured my habits in the lab. I should also mention the Aquatic and Crop Resource Development (ACRD)-Saskatoon, National Research Council Canada for allowing me to be part of a great professional community. I am glad to thank NSERC, NRC, and U of S for their financial support.

I would like to express my great appreciations to my parents, who gave me life and brought me up. Their love provided my inspiration and was my driving force. My wife, Qian Zheng, who selflessly supports my study and life; and my daughter, Kristina, who made me understand the true meaning of life. I also want to thank my parents-in-law for their unconditional support.

TABLE OF CONTENTS

LIST OF FIGURES

LIST OF TABLES

LIST OF ABBREVIATIONS

%	percentage
℃	degree Celsius
μ	micro-
μM	micromolar
C16	16-carbon
C18	18-carbon
2D-TLC	two dimensional thin layer chromatograph
AAPT1	aminoalchoholphosphotransferase 1
AAPT2	aminoalchoholphosphotransferase 2
ABC	ATP-binding cassette
ABRC	Arabidopsis Biological Resources Center
ACP	acyl-carrier-protein
ACT1	acyltranferase 1
BLAST	basic local alignment search tool
bp	base pair
CCT	phosphocholine cytidylyltransferase
cDNA	complementary DNA
CDP	cytidine diphosphate
CDP-DAG	cytidine diphosphate-diacylglycerol
CDS	cytidine diphosphate-diacylglycerol synthase
CK	choline kinase
CoA	coenzyme A
CTP	cytidine triphosphate
DAG	diacylglycerol
DBI	double bond index
DGD1	digalactosyldiacylglycerol synthase 1
DGD2	digalactosyldiacylglycerol synthase 2
DGDG	digalactosyldiacylglycerol
DHAP	dihydroxyacetone phosphate
ER	endoplasmic reticulum

ESI-MS/MS	electrospray ionization tandem mass spectrometry
FAD2,3,4,5,6,7,8	fatty acid desaturase 2,3,4,5,6,7,8
FAMEs	fatty acid methyl esters
FKPM	fragments per kilobase of exon per million fragments
G-3-P	glycerol-3-phosphate
GC	gas chromatography
GO	Gene Ontology
GPAT	glycerol-3-phosphate acyltransferase
GPDH	glycerol-3-phosphate dehydrogenase
hmACCase	homomeric acetyl-coenzyme A carboxylase
htACCase	heteromeric acetyl-coenzyme A carboxylase
KASI	β-Ketoacyl-[acyl carrier protein] synthase I
KASII	β-Ketoacyl-[acyl carrier protein] synthase II
KASIII	β-Ketoacyl-[acyl carrier protein] synthase III
LPA	lysophosphatidic acid
LPAAT	lysophosphatidic acid acyltransferase
MGD1, 2, 3	monogalactosyldiacylglycerol synthase 1, 2, 3
MGDG	monogalactosyldiacylglycerol
NaCl	sodium chloride
PA	phosphatidic acid
PAP	phosphatidate phosphatases
PC	phosphatidylcholine
PE	phosphatidylethanolamine
PEAMT	phosphoethanolamine N-methyltransferase
PECT1	phosphorylethanolamine cytidylyltransferase 1
PG	phosphatidylglycerol
PGP	phosphatidylglycerophosphate
PGPS1, PGPS2	phosphatidylglycerophosphate synthase 1, 2
PI	phosphatidylinositol
PIS1, PIS2	phosphatidylinositol synthase 1, 2
qRT-PCR	quantitative reverse transcription polymerase chain reaction

RNA-seq	RNA sequencing
SAD	Δ9 stearoyl acyl carrier protein desaturase
sn-1	carbon 1 position
sn-2	carbon 2 position
SQD1	UDP-sulfoquinovose synthase 1
SQD2	UDP-sulfoquinovose: DAG sulfoquinovosyltransferase
SQDG	sulfoguinovosyldiacylglycerol
TGD	trigalactosyldiacylglycerol
UDP	uridine diphosphate
UV	ultraviolet
v/v	volume/volume
VIPP1	vesicle-inducing protein in plastids 1
WT	Wild type

1 LITERATURE REVIEW

From the Sahara Desert to the Arctic Tundra, plants demonstrate extensive physiological and biochemical adaptation to large geographical differences in environmental temperatures. Owing to their sessile lifestyle, plants have evolved different mechanisms to help them cope with constantly changing temperatures. A key aspect of plant adaptation to temperature variations concerns remodeling of membrane lipids in order to maintain membrane integrity and the function of membrane-associated protein functions (Murata and Los, 1997; Wallis and Browse, 2002). The overall reason is probably related to the need to maintain membrane fluidity, which is directly affected by the unsaturation of the acyl lipid components of the bilayers (Harwood, 1991). Glycerolipids, which are major constituents of cellular membranes, have been a focus of attention since the 1960s for their roles in temperature adaptation in plants (Harwood, 1991; Wolfe, 1978). In plant cells, glycerolipid biosynthesis occurs primarily in the endoplasmic reticulum (ER) and chloroplast and involves a number of enzymatic reactions as well as metabolic intermediates (Ohlrogge and Browse, 1995). A considerable body of work has been focused on the process of fatty acid desaturation, namely, the activities of various fatty acid desaturases, in the *de novo* synthesis of glycerolipid molecules in response to temperature fluctuations (Iba, 2002; Murakami et al., 2000; Murata et al., 1992; Murata and Los, 1997; Wallis and Browse, 2002). It is equally apparent that alterations in the proportion of different membrane lipids as well as the molecular species for a given lipid class also facilitate plant adaptation at different temperatures.

1.1 Fatty acid biosynthesis in plants

Glycerolipids are major constituents of cellular membranes. The common characteristic of glycerolipids is the presence of a glycerol backbone. Fatty acyl groups are esterified in the *sn-1* and *sn-2* positions of the glycerol backbone to form a diacylglycerol moiety. In plants, the primary enzymes involved in the *do novo* fatty acid synthesis in plastids are acetyl-CoA carboxylase (ACCase) and the fatty acid synthase (FAS) complex. The first enzyme of fatty acid synthesis is ACCase, which initiates the ATP-dependent carboxylation of acetyl-CoA to form malonyl-CoA (Sasaki and Nagano, 2004). The malonyl group is then transferred to acyl

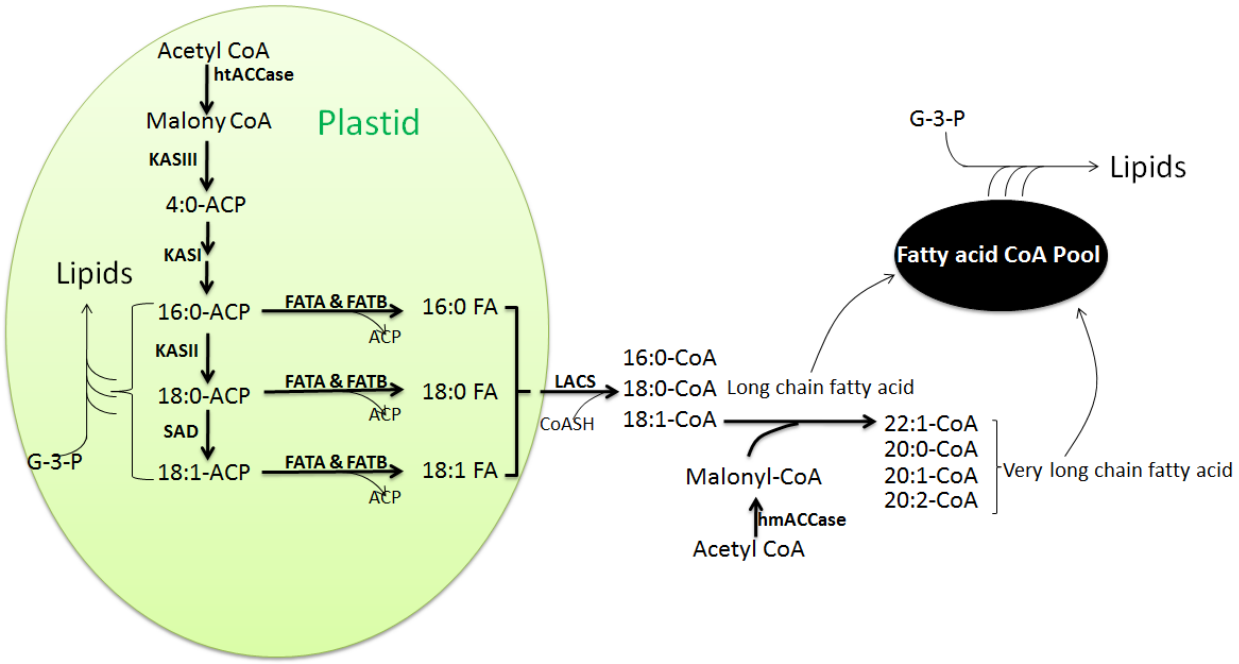

Figure 1.1 Scheme of reactions involved in fatty acid synthesis in plants.

Fatty acids are synthesized in plastids. Acetyl-CoA is first elongated to malonyl-CoA by acetyl-CoA carboxylase (ACCase) and then acetyl-CoA serves as a two-carbon unit to be added to malonyl-CoA for fatty acid chain elongation. 18:0-ACP is desaturated by a stearoyl-ACP desaturase (SAD) to generate 18:1-ACP. In plastids, terminal reactions of fatty acid synthesis include thioester bond hydrolysis by acyl-ACP thioesterases (FATA and FATB) to release the fatty acids from acyl carrier protein (ACP). Fatty acid products include stearic acid (18:0), oleic acid (18:1) and palmitic acid (16:0) are activated to CoA by long chain acyl-CoA synthetases (LACS) before exported to the ER for lipid synthesis. FA, fatty acids; ACP, acyl carrier protein; CoA, coenzyme A; CoASH, coenzyme A reduced form; KASI, β-ketoacyl-[acyl carrier protein] synthase I; KASII, β-ketoacyl-[acyl carrier protein] synthase II; KASIII, β-ketoacyl-[acyl carrier protein] synthase III; G-3-P, glycerol-3-phosphate. htACCase, heteromeric ACCase; hmACCase, homomeric ACCase.

carrier protein (ACP) to produce malonyl-ACP catalyzed by malonyl-CoA acyl carrier protein transacylase (Simon and Slabas, 1998). Malonyl-ACP is subsequently elongated into fatty acids through stepwise addition of two-carbon acetyl units by the FAS complex. As a result, the C2 subunits derived from malonyl-CoA are sequentially added to β-ketoacyl-ACP to form long chain fatty acyl-ACPs including 16:0-ACP and 18:0-ACP. 18:0-ACP is subsequently desaturated to 18:1-ACP by Δ-9 stearoyl ACP desaturase (Figure 1.1). The 16:0-ACP, 18:0-ACP and 18:0-ACP products are directly used for lipid synthesis in the plastids. On the other hand, fatty acids are released from ACP in the chloroplast stroma by chain-terminating acyl-ACP thioesterases (FATA and FATB) and then activated to fatty acyl-CoA esters by long chain acyl-CoA synthetases (LACS) in the plastid outer envelope before export to the ER for lipid synthesis (Chapman and Ohlrogge, 2012). Long chain fatty acids are further elongated to eicosenoic acid (20:1) and erucic acid (22:1) in seed tissues and up to 34 carbons for the biosynthesis of waxes and suberin (James et al., 1995; Kunst et al., 1992; Kunst and Samuels, 2009; Ohlrogge and Browse, 1995; Pulsifer et al., 2014; Roughan et al., 1979; Samuels et al., 2008).

1.2 Glycerolipid biosynthesis in plants

1.2.1 Two pathways for glycerolipid biosynthesis

Fatty acids synthesized in chloroplasts are mostly destined for esterification to glycerol-3-phosphate (G-3-P) to form glycerolipids (Ohlrogge and Browse, 1995). In higher plants, synthesis of glycerolipids can be accomplished through two parallel pathways, the prokaryotic and eukaryotic pathways, located in the chloroplast and the endoplasmic reticulum (ER), respectively (Figure 1.2) (Browse and Somerville, 1991; Hölzl et al., 2009; Ohlrogge and Browse, 1995). Biochemical and genetic studies with lipid mutants, particularly that of the model plant *Arabidopsis thaliana*, have contributed to our understanding of the pathways for glycerolipid biosynthesis in higher plants (Heinz and Roughan, 1983; Somerville and Browse, 1991; Wallis and Browse, 2002). Individual glycerolipids can be distinguished by different combinations of fatty acyl groups presented in the glycerol backbone. Fatty acyls synthesized in the chloroplast (16:0-ACP and 18:1-ACP) are partitioned between the chloroplast and the cytosolic compartment. A portion of the fatty acid flux is incorporated into non-phosphorous

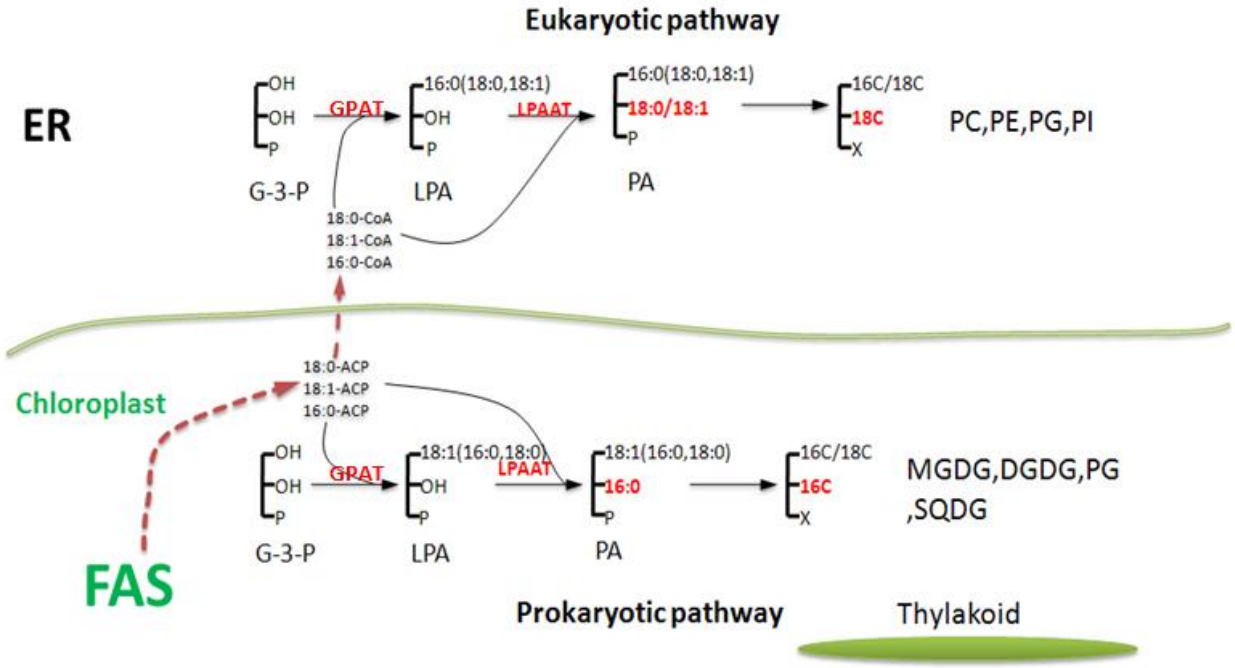

Figure 1.2 Prokaryotic and eukaryotic pathways for glycerolipid biosynthesis in plants.

The prokaryotic pathway occurs in chloroplasts while the eukaryotic pathway happens in the ER. In chloroplasts, acyl-ACPs are used as substrates and esterified mostly 16:0 at the *sn-2* position of G-3-P in the prokaryotic pathway. In contrast, the eukaryotic pathway in the ER utilizes acyl-CoAs as substrates and incorporates predominately 18:0/18:1 at the *sn-2* position of G-3-P. The sequential addition of fatty acyl groups to the *sn-1* and *sn-2* position of the glycerol backbone of G-3-P is catalyzed by glycerol-3-phosphate acyltransferase (GPAT) and lysophophatidic acid acyltransferase (LPAAT) to form lysophophatidic acid (LPA) and phophatidic acid (PA), respectively. X, head group; G-3-P, glycerol-3-phosphate; 16C, 16 carbon fatty acyls; C18, 18 carbon fatty acyls; DGDG, digalactosyldiacylglycerol; MGDG, monogalactosyldiacylglycerol; PC, phosphatidylcholine; PE, phosphatidylethanolamine; PG, phosphatidylglycerol; PI, phosphatidylinositol; SQDG, sulfoguinovosyldiacylglycerol.

glycerolipids including monogalactosyldiacylglycerol (MGDG), digalactosyldiacylglycerol (DGDG) and sulfoquinovosyldiacylglycerol (SQDG) in the chloroplast, while the remainder is activated with CoA at the chloroplast membranes and transported to the ER to be incorporated into phospholipids such as phosphatidylcholine (PC), phosphatidylinositol (PI) and phosphatidylethanolamine (PE). Phosphatidylglycerol (PG) is primarily synthesized in the chloroplast. The chloroplast pathway is also called the prokaryotic pathway as it was first identified in cynobacteria. On the other hand, the ER pathway is called the eukaryotic pathway (Shen et al., 2010).

1.2.2 Biosynthesis of phosphatidic acid (PA) and diacylglycerol (DAG)

As described above, fatty acyl groups generated from fatty acid synthesis are incorporated at the *sn-1* and *sn-2* positions of the G-3-P backbone by glycerol-3-phosphate acyltransferase (GPAT) and *lyso*phosphatidic acid acyltransferase (LPAAT) enzymes, giving rise to phosphatidic acid (PA) which serves as a common precursor for all glycerolipids (Figure 1.3). GPAT is the first enzyme in the pathway for the *de novo* synthesis of membrane and storage lipids. In *Arabidopsis*, there are 10 GPATs with distinct enzyme activities, substrate preferences and subcellular localization. GPAT usually catalyzes the transfer of a fatty acyl group to the *sn-1* position of G-3-P to form *lyso*phosphatidic acid (LPA). Recent studies showed that some GPATs possess *sn-2* acyltransferase activity as well (Yang et al., 2012). The *Arabidopsis* GPAT1, GPAT2, GPAT3 showed putative mitochondria targeting signals, however, only GPAT1 is located in the mitochondria and exhibits GPAT activity whereas no activities were detected with GPAT2 and GPAT3 (Zheng et al., 2003). GPAT1 has strong preferences for C16:0, C16:1, C18:0, C18:1 and C20:1 acyl CoAs (Yang et al., 2012). GPAT4, 5, 6, 7, 8 also showed GPAT activity but are mainly involved in cutin and suberin synthesis (Yang et al., 2012; Zheng et al., 2003). The chloroplast localized GPAT, ACT1, showed a strong substrate preference for 18:1-ACP. In the *act1* mutant, only minimal prokaryotic GPAT activity was detected and it was unable to synthesize diacylglycerol (DAG) moieties in the chloroplasts. In *act1*, the need of glycerolipids in chloroplasts is met by a compensatory increase in lipid flux from ER to chloroplasts through the eukaryotic pathway. GPAT9 is believed to be involved in non-chloroplast glycerolipid

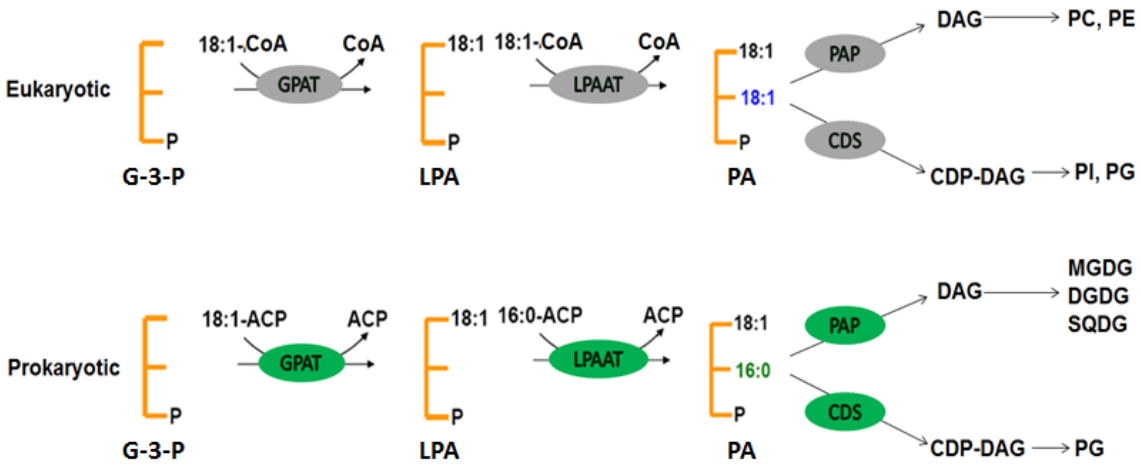

Figure 1.3 Biosynthesis of PA and DAG through the prokaryotic and eukaryotic pathway.

Two types of PA are produced in plants, prokaryotic pathway derived PA contains 16:0 at the *sn-2* position of the glycerol backbone while eukaryotic PA has 18-carbon fatty acids at the *sn-2* position. G-3-P, glycerol-3-phosphate; LPA, monoacylglycerol-phosphate; PA, phosphatidic acid; DAG, diacylglycerol; CDP-DAG, cytidine diphosphate-diacylglycerol; GPAT, glycerol-3-phosphate acyltransferase; LPAAT, *lyso*-phosphatidic acid acyltransferase; PAP, phosphatidate phosphatases; CDS, cytidine diphosphate-diacylglycerol synthase. Abbreviations for glycerolipids are defined in Figure 1.2.

synthesis in the ER. Unlike chloroplast GPAT which utilizes 18:1-CoA, GPAT9 can use 18:1 and 16:0-CoA.

LPAAT catalyzes the addition of a fatty acyl group to the *sn-2* position of the glycerol backbone to form PA. It is a pivotal enzyme controlling the destination of LPA to different types of PA in plants. Radioactive labeling experiments revealed that there are two types of PA used for glycerolipid synthesis in plants (Roughan and Slack, 1984). This discovery leads to the hypothesis of the two pathway model for glycerolipid synthesis in plants. PA produced via the prokaryotic pathway has 16:0 at the *sn-2* position and mostly 18:1 at the *sn-1* position of the glycerol backbone. On the other hand, PA synthesized in the ER contains 18:1 at the *sn-1* and *sn-2* positions, and in some cases 16:0 at the *sn-1* position. Isolation of *LPAAT* genes encoding chloroplastic and cytoplasmic LPAAT in different plant species verified the two pathway model (Kim et al., 2004; Kim et al., 2005). In *Arabidopsis*, there are five putative genes encoding LPAAT proteins (Kim et al., 2005). Only one gene, *LPAAT1*, encodes the chloroplast LPAAT which exhibits *in vitro* substrate preference for 16:0 over 18:1-CoA (Kim et al., 2005). *LPAAT2, 3, 4, 5* encode cytosolic LPAATs. *In vitro* enzymatic assay demonstrated that LPAAT2 exhibited the highest LPAAT activity among the four LPAATs and showed strong substrate preference for 18:1 over 16:0-CoA (Kim et al., 2005). Thus, LPAAT2 is responsible for the majority of the cytoplasmic LPAAT activity.

Dephosphorylation of PA by phosphatidate phosphatases (PAPs) yields DAG. In *Arabidopsis*, AtPAH1 and AtPAH2 are enzymes with confirmed PAP activity (Eastmond et al., 2010). DAG serves as a substrate for PC and PE biosynthesis. On the other hand, cytidine diphosphate-DAG (CDP-DAG) can be produced from cytidine triphosphate (CTP) and PA catalyzed by CDP-DAG synthase (CDS) (Haselier et al., 2010). In eukaryotes, CDP-DAG is a substrate for PI and PG biosynthesis (Zhou et al., 2013).

1.2.3 16:3 and 18:3 plants

Due to the substrate preference of chloroplast LPAAT to 16:0-ACP, the prokaryotic pathway incorporates primarily C16 fatty acids, at the *sn-2* position (Frentzen, 1993). In contrast, LPAAT

in the ER esterifies C18 fatty acids at the *sn-2*. Consequently, prokaryotic lipids contain C16 fatty acids at the *sn-2* position while eukaryotic lipids have C18 fatty acids. The C16 fatty acids at the *sn-2* position of MGDG originating from the prokaryotic pathway are subsequently desaturated to C16:3 fatty acids. As a result, leaf lipids of some plants possess a significant proportion of 16:3 fatty acids. They are generally called 16:3 plants to distinguish them from 18:3 plants wherein MGDG contains predominately 18:3 fatty acids (Gardiner and Rough, 1983; Schmidt and Heinz, 1993).

The relative abundance of 16:3 at the s*n-2* position of MGDG and DGDG can be considered as an indicator of the contribution from the prokaryotic pathway. The amount of 16:3 fatty acids in different plant species vary from 0 molar percentage (mol%) to ~40 mol% for MGDG and 0 mol% to ~22 mol% for DGDG. Generally, 16:3 plants are classified as those with more than 2 mol% of 16:3 in total fatty acids or 3 mol% and 1.2 mol% in MGDG and DGDG respectively (Mongrand et al., 1998). The divergent amount of 16:3 fatty acids in different plant species is an indication that contributions from the prokaryotic pathway and eukaryotic pathways for glycerolipid biosynthesis varied in nature. A survey of 468 plant species revealed that species belonging to the most primitive taxonomic groups, such as Bryophytes, Pteridophytes and Gymnosperms, are 16:3 plants (Mongrand et al., 1998). Both 16:3 and 18:3 plants are found in the dicotyledons while most monocotyledons are 18:3 plants. In the case of dicotyledons, the percentage of 16:3 plants in each of the different dicotyledon orders is not correlated with the order of evolution. Hence, it was proposed that the prokaryotic pathway was lost during evolution but at different rates (Mongrand et al., 1998).

1.2.4 Glycerolipid biosynthesis in the chloroplast

In higher plants, four major lipids are found in thylakoid membranes: MGDG and DGDG, PG and SQDG. All plants rely on the prokaryotic pathway for the assembly of thylakoid PG, but 16:3 plants, like *Arabidopsis*, also use the prokaryotic pathway for the synthesis of galactolipids (Figure 1.4, green block). In both 16:3 and 18:3 plants, the ER derived DAG moieties are transported to chloroplast envelope by unknown mechanisms to fulfill the requirements of

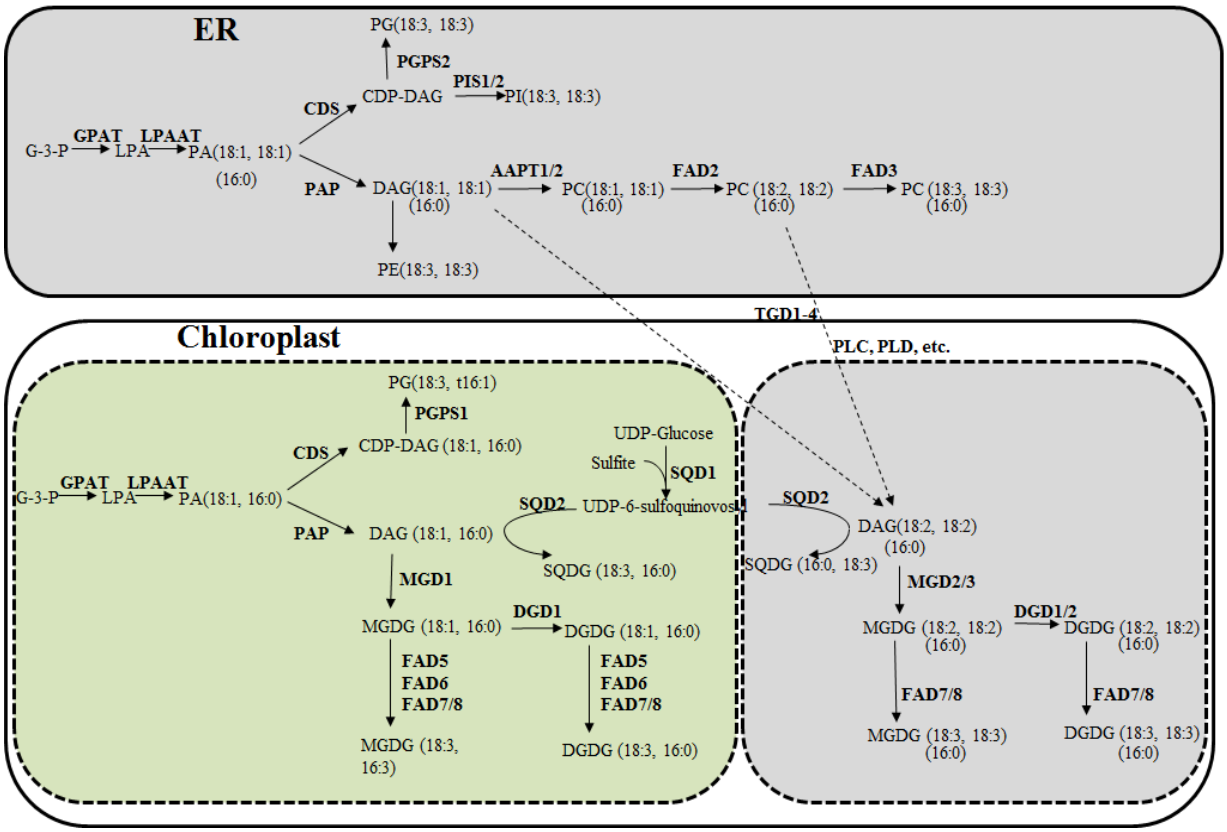

Figure 1.4 Glycerolipid biosynthesis pathways in plants.

The light green block represents the prokaryotic pathway while the grey blocks represent lipids synthesized from the eukaryotic pathway. Abbreviations for lipids and genes involved in glycerolipid synthesis are defined in Figures 1.1, 1.2 and 1.3. ER, endoplasmic reticulum.

galactolipids in thylakoids (Figure 1.4, grey blocks). Acyl lipids synthesized in the chloroplast are subjected to further desaturation by a series of membrane bound desaturases (Figure 1.4).

1.2.4.1 Biosynthesis of chloroplast galactolipids

In the membranes of chloroplast and other plastids, MGDG and DGDG are major constituents that are produced by stepwise galactosylation of DAG moieties. The most abundant membrane lipids in the chloroplast membranes are MGDG, which account for more than half of the lipids in thylakoid membranes in most organisms (Kobayashiet al., 2012; Shimojima et al., 2011). MGDG synthase belongs to the glycotosyltransferase superfamily and is also called uridine diphosphogalactose (UDP)-1,2-diacylglycerol galactosyltransferase. MGDG is synthesized by catalyzing the transfer of a galactosyl residue from UDP-1α-galactose to the *sn-3* position of DAG. In *Arabidopsis*, there are three genes (*MGD1*, *MGD2* and *MGD3*) encoding functional MGDG synthases that can be classified into two groups based on different substrate specificities to DAG moieties: the A-type (MGD1) and the B-type (MGD2 and MGD3) MGDG synthase (Figure 1.4). MGD1 is associated with the chloroplast inner envelope and is abundant in green tissues, whereas MGD2 and MGD3 are localized in the outer envelope and are more abundant in non-green tissues such as roots. Reverse genetics studies have shown that MGD1 is responsible for the synthesis of MGDG in the prokaryotic pathway while MGD2 and MGD3 are proposed to utilize the eukaryotic pathway derived DAG molecules (Figure 1.4). In 18:3 plants such as pea in which MGDG is derived from the eukaryotic pathway, the MGDG synthase is found in the outer envelope of chloroplast membranes exclusively (Benning and Ohta, 2005).

In plants, DGDG is synthesized by transferring one galactose from one molecule of MGDG to another by galactolipid:galactolipid galactosyltransferase (GGGT) (Kelly et al., 2003). Two genes (*DGD1* and *DGD2*) encoding DGDG synthase have been characterized in *Arabidopsis*. The major enzyme is DGD1which is located in the chloroplast outer envelope. Studies with *dgd1* mutants revealed that DGD1 is important for the synthesis of DGDG in the chloroplast (Figure 1.4). DGD2 is also localized in the chloroplast outer envelope and exhibited DGDG synthase activity in *in vitro* assay (Kelly and Dörmann, 2002). But it is UDP-galactose, not MGDG, that

serves as the galactose donor for DGD2. The expression of *DGD2* was very low in plant leaves but strongly induced under phosphate-limited conditions. Like MGD2 and MGD3 which are involved in MGDG synthesis in the outer envelope of chloroplasts, DGD2 also participates in mediating the synthesis of DGDG found in extrachloroplastic membranes (Benning and Ohta, 2005; Kelly et al., 2003).

1.2.4.2 Biosynthesis of SQDG

SQDG is a non-phosphorous lipid and is found exclusively in the chloroplast membranes in plants. SQDG has been proposed to be essential in balancing thylakoid membrane charges by substituting for PG under phosphate-limiting growth conditions in bacteria and plants (Yu et al., 2002). The synthesis of SQDG occurs in the chloroplast envelope (Sanda et al., 2001; Yu et al., 2002). In *Arabidopsis*, synthesis of SQDG involves two unique enzymes: UDP-sulfoquinovose synthase (SQD1) and UDP-sulfoquinovose: DAG sulfoquinovosyltransferase (SQD2) (Figure 1.4). Both SQD1 and SQD2 have been cloned and enzyme properties have been characterized (Sanda et al., 2001; Yu et al., 2002). SQD1 is responsible for the formation of UDP-sulfoquinovose from sulfite and UDP-glucose in the chloroplast stroma (Sanda et al., 2001). SQD2 is involved in transferring sulfoquinovosyl from a UDP-sulfoquinovosyl onto the head group of DAG to produce SQDG (Figure 1.4) (Yu et al., 2002).

1.2.4.3 Biosynthesis of chloroplast PG

In plants, PG is the only major phospholipid present in the thylakoid membranes of chloroplasts (Xu et al., 2002). The first step of PG synthesis is the conversion of PA to CDP-DAG by CDP-DAG synthase (CDS). CDP-DAG is then converted to PG by PG synthase (PGPS) (Figure 1.4). In plants, the majority of PG (>95%) is synthesized through the prokaryotic pathway in chloroplast while only a small portion (~5%) is produced in the cytosol and mitochondria (Heinz and Roughan, 1983). PG appears to be indispensable for photosynthesis systems. It has been reported that reduction or loss of PG content resulted in a significant

decrease in photosynthetic activity (Babiychuk et al., 2003; Hagio et al., 2002; Xu et al., 2002). In *Arabidopsis*, two PGPS encoding genes, *PGPS1* and *PGPS2*, have been identified. PGPS1 is localized in the chloroplast and chloroplastic PGP synthase activity was strongly reduced in the *pgp1* mutant. Disruption of *PGPS1* resulted in a significant reduction in PG content and impairment of photosynthesis (Babiychuk et al., 2003; Xu et al., 2002). The functionality of PGPS2 in plants is still unclear but PGPS2 in yeast was targeted to the ER (Babiychuk et al., 2003).

1.2.5 Phospholipid biosynthesis via the eukaryotic pathway

Phospholipids are basic building blocks of extraplastidial membranes in plants. PC, PE and PI are major phospholipids (> 90% of phospholipids) that are predominantly synthesized by the eukaryotic pathway (Ohlrogge and Browse, 1995; Shen et al., 2010). PC, PE and PI are synthesized from PA by two different mechanisms (Figure 1.4, Figure 1.5). PC and PE are produced by the Kennedy pathway, in which hydrolysis of the phosphate group from PA produces DAG, followed by DAG being utilized in the synthesis of PC and PE (Kennedy and Weiss, 1956). The second route utilizes CTP as an energy source to form a CDP-DAG molecule for PI production (Gibellini and Smith, 2010).

1.2.5.1 Biosynthesis of PC and PE

PC and PE are the most abundant phospholipids in eukaryotic cells. The *de novo* synthesis of PC and PE was first elucidated from landmark studies by Kennedy and Weiss (1956). PC and PE are mainly synthesized through two branches of the Kennedy pathway, the CDP-choline pathway for PC synthesis and the CDP-ethanolamine pathway for PE synthesis (Kennedy and Weiss, 1956) (Figure 1.5).

PC is a major constituent of cell membranes and plays critical roles both as a structural component as well as a messenger of cellular signaling (Cruz-Ramírez et al., 2004). The CDP-choline pathway consists of three enzymatic steps (Figure 1.5). First, choline kinase (CK) catalyzes the phosphorylation of choline to form phosphorycholine (PCho). In the second step,

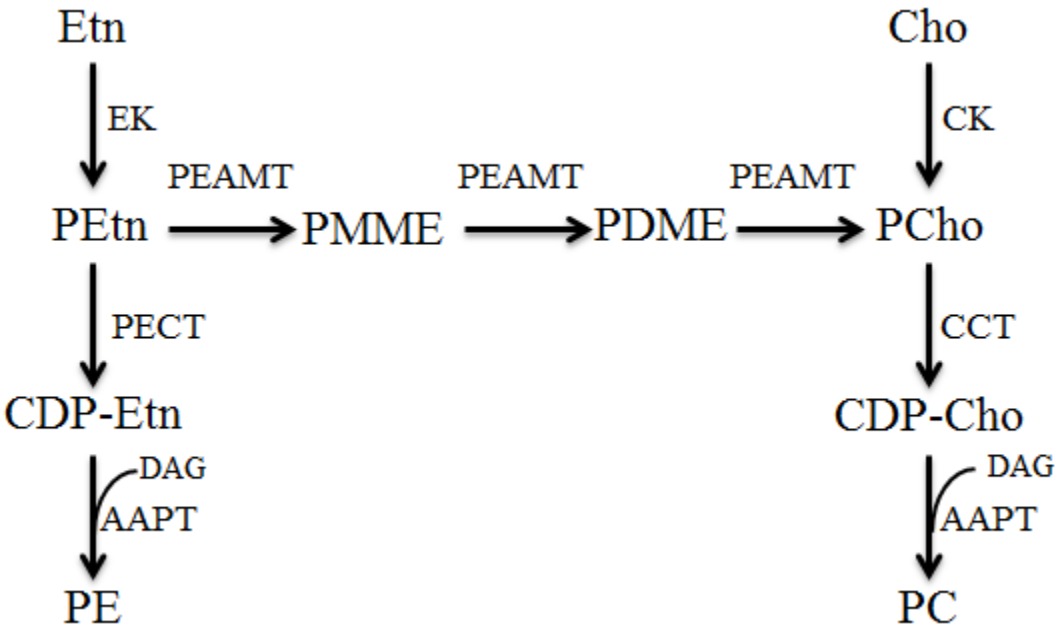

Figure 1.5 Synthesis of PE and PC in the ER.

Reactions in PE and PC synthesis (Gibellini and Smith, 2010). The abbreviations are: Etn, ethanolamine; PEtn, phosphoryl-ethanolamine; CDP-Etn, CDP-ethanolamine. Cho, choline; PCho, phosphocholine; CDP-Cho, CDP-choline; PMME, phosphatidylmonomethylethanolamine; PDME, phosphatidyldimethylethanolamine; PEAMT, phosphoethanolamine N-methyltransferase.

the rate limiting step in the Kennedy pathway, the CTP: phosphocholine cytidylyltransferase (CCT) uses PCho and CTP to generate CDP-Cho. The final step is catalyzed by aminoalchoholphosphotransferases (AAPT) which utilizes CDP-Cho and DAG to form PC. The CDP-choline pathway draws on PCho as a precursor in the synthesis of PC. Plants can produce PCho via either sequential methylation of phosphoryl-ethanolamine (PEtn) catalyzed by phosphoethanolamine N-methyltransferase (PEAMT) (BeGora et al., 2010; Bolognese and McGraw, 2000) or choline kinase (CK) (Figure 1.5). Three genes encoding PEAMT (*At1g48600*, *At1g73600*, and *At3g18000*) have been identified in *Arabidopsis* (Cruz-Ramírez et al., 2004) and three genes encoding CK, (*At1g74320*, *At1g74320* and *At4g09760*) have been isolated (Tasseva et al., 2004). Two *CCT* genes, *CCT1* and *CCT2*, were identified in plants (Inatsugi et al., 2009). AAPT1 and AAPT2 have been isolated in *Arabidopsis*, *Glycine max* and *Brassica napus* and are located in the ER (Goode et al., 1999; Qi et al., 2003). AAPT1 is capable of utilizing both CDP-Cho and CDP-Etn with some preference for CDP-Cho. AAPT2 also showed dual substrate specificity but it is unclear if it has preference for CDP-Etn (Qi et al., 2003).

PE is a non-bilayer phospholipid in cellular membranes that plays important roles in cell division and protein secretion (Mizoi et al., 2006). The pathway for PE synthesis involves the CDP-ethanolamine branch of the Kennedy pathway that uses a series of similar reactions, except for the involvement of ethanolamine instead of choline. *Arabidopsis* contains a single gene for a putative ethanolamine kinase (*EK*, *At2g26830*) but its function is still unknown (Easseva et al., 2004). Disruption of the *PHOSPHORYLETHANOLAMINE CYTIDYLYLTRANSFERASE 1 (PECT1)* gene in *Arabidopsis* resulted in embryonic lethality (Mizoi et al., 2006).

1.2.5.2 Biosynthesis of PI and PG via eukaryotic pathway

Phosphatidylinositol (PI) is a key phospholipid in non-photosynthetic plant cell membranes. PI also serves as the precursor of messenger molecules involved in the signal transduction pathways of calcium-dependent responses in plant cells (Collin et al., 1999). PI is synthesized from CDP-DAG and *myo*-inositol by the enzyme phosphatidylinositol synthase (PIS) (Figure 1.4). In *Arabidopsis*, two PISs, PIS1 and PIS2, have been characterized (Collin et al., 1999;

Löfke et al., 2008; Xue et al., 2000). These enzymes are located in the ER and Golgi apparatus. PIS1 has a preference for saturated CDP-DAG molecules while PIS2 prefers unsaturated CDP-DAG molecules (Löfke et al., 2008). A small portion (~5%) of PG can be produced via the eukaryotic pathway using CDP-DAG while the majority of PG is synthesized through the prokaryotic pathway in plants. Two PG synthase have been isolated from plants, PGPS1 and PGPS2. PGPS2 is thought to be responsible for PG synthesis through the eukaryotic pathway as it has been located in the ER in yeast (Müller and Frentzen, 2001).

1.2.6 Fatty acid desaturation

In all vegetative tissues, the major glycerolipids are first synthesized using only 18:1 and 16:0 acyl groups. However, the predominant fatty acids in cellular membranes are polyunsaturated with two to three double bonds (Ohlrogge and Browse, 1995). The monounsaturated 18:1 is produced in the plastid by a soluble enzyme, steroyl-ACP desaturase (SAD). Subsequent desaturation of acyl lipids to polyunsaturated forms is carried out by membrane-bound fatty acid desaturases (FADs) in the ER and chloroplasts (Harwood, 1988). Investigation of the regulatory properties of the membrane-bound desaturases by traditional biochemical techniques has been limited due to the difficulty in solubilizing and purifying them. Characterization of *Arabidopsis* desaturase mutants and heterologous expression in yeast systems has greatly enhanced our understanding of desaturation process in the ER and chloroplasts (Benning et al., 2006; Benning, 2009; Miquel et al., 1998).

In *Arabidopsis*, fatty acid desaturation through the prokaryotic pathway involves five desaturases, FAD4, FAD5, FAD6, FAD7 and FAD8. Two of these desaturases are highly substrate specific. The FAD4 inserts a *trans* double bond into 16:0 at the *sn-2* position of PG to generate an unusual *trans*-16:1 (Gao et al., 2009), whereas FAD5 is responsible for the desaturation of 16:0 to 16:1 at the *sn-2* position of MGDG and possibly DGDG (Heilmann et al., 2004; Hugly et al., 1989). In contrast, other chloroplast desaturases (FAD6, FAD7 and FAD8) act on acyl groups with no apparent specificity for chain length (C16 or C18), position on glycerol backbone (*sn-1* or *sn-2*) or lipid species (Wallis and Browse, 2002). FAD6 is an

18:1/16:1 desaturase (Browse et al., 1986; Schmidt and Heinz, 1993), while FAD7 and FAD8 are 18:2/16:2 desaturases (Heinz and Raughan, 1983; Ohlrogge and Browse, 1995). As a result, desaturation on PG (18:1/16:0) by FAD4 generates PG (18:1/*trans*-16:1) while MGDG (18:1/16:0) is converted to MGDG (18:1/16:1) by FAD5. Subsequent desaturation is carried out by FAD6, FAD7 and FAD8 to form PG (18:3/*trans*-16:1) and MGDG (18:3/16:3). Similar desaturation to 18:3 occurs in SQDG and DGDG. However, the desaturation of 16:0 to 16:3 occurs exclusively at the *sn-2* position of MGDG (McConn et al., 1994).

In the eukaryotic pathway, the 18:1 (FAD2) and 18:2 (FAD3) desaturases in the ER act on fatty acids at both *sn-1* and *sn-2* positions. 16:0 is not desaturated in the eukaryotic pathway (Hamada et al., 1998; Miquel et al., 1993). Though FAD2 and FAD3 have been characterized as PC desaturases, it is possible that they also act on other phospholipids (Wallis and Browse, 2002). In 16:3 plants, a portion of the ER-derived DAG moieties comprising highly unsaturated C18 fatty acids (18:2 and 18:3) are proposed to be transferred to the chloroplast for the synthesis of chloroplast galactolipids (Ohlrogge and Browse, 1995). Further desaturation of 18:2 to 18:3 in the ER-derived galactolipids occurs in chloroplast membranes by FAD7 and FAD8. Therefore, two pathways contribute to the production of galactolipids and give rise to varying amount of 18:3/16:3 and 18:3/18:3 molecular species of MGDG while DGDG is a mixture of 18:3/18:3 and 18:3/16:0 molecules. In 18:3 plants where the prokaryotic pathway only produces PG, the synthesis of chloroplast galactolipids entirely relies on the eukaryotic pathway (Browse et al., 1986). In these plants, the most abundant molecular species have 18:3 at both the *sn-1* and *sn-2* position of MGDG and DGDG.

1.3 Lipid transfer between the two glycerolipid pathways

1.3.1 Lipid transfer from ER to chloroplast

Biosynthesis of glycerolipids involves two parallel pathways compartmentalized in the ER and chloroplasts. Studies on lipid mutants indicated that even though enzymes are localized exclusively in the ER or chloroplast, composition of both chloroplast and ER lipids is affected by single mutation (Wallis and Browse, 2002).

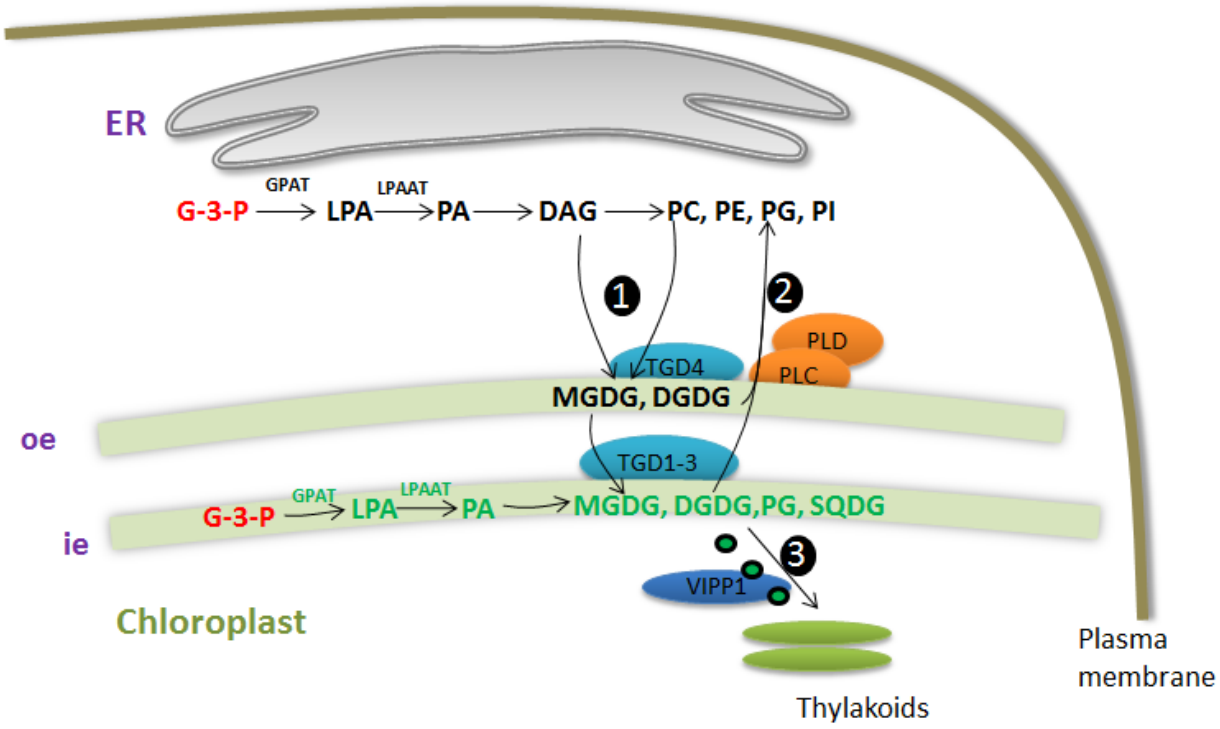

Figure 1.6 Lipid trafficking in plants.

Lipid trafficking in plants adapted from (Benning et al., 2009). ①, glycerolipids synthesized in the ER are transported to the chloroplast for galactolipid synthesis. ②, galactolipids are exported from chloroplasts to the extrachloroplastic membranes under phosphate-limiting conditions. ③,transportation of galactolipids from the chloroplast inner envelope to thylakoids. Abbreviations are defined in Figures1.1, 1.3 and Figure 1.4. oe, outer envelope; ie, inner envelope. PLC, phospholipase C; PLD, phospholipase D.

Two sources of DAG molecules are available for the synthesis of galactolipids in plants (Figure 1.6). DAG moieties assembled through the prokaryotic pathway in the chloroplast and DAG moieties assembled in the ER via the eukaryotic pathway but transported to the chloroplast envelope. Depending on the type of plants, chloroplast galactolipids MGDG and DGDG also contain varying amounts of fatty acids with eukaryotic configurations (C18 at the *sn-2* position of the glycerolipid backbone) (Browse et al., 1986). In 16:3 plants, both the prokaryotic and the eukaryotic pathways contribute almost equally to the production of chloroplast galactolipids while in 18:3 plants galactolipid production relies entirely on the eukaryotic pathway. Therefore, transportation of ER-derived lipids to the chloroplasts is required in plants.

Studies with *Arabidopsis* mutants confirmed lipid trafficking from ER to chloroplast. The *Arabidopsis act1* mutant is deficient in the activity of the chloroplast G-3-P acyltransferase, the first and committed enzyme of the prokaryotic pathway. The mutant has a severely decreased amount of 16:3 fatty acids but exhibited no detectable accumulation of its substrates, 18:1-ACP and 16:0-ACP. In addition, no distinguishable changes were observed in the amount of PE and PI compared to wild type plants, only that the amount of PC was slightly increased. Also, there was a minor decrease in chloroplast lipids like MGDG, DGDG and SQDG. Accompanying the greatly reduced 16:3 fatty acid level was an increased 18:3 level in MGDG. Thus, the *act1* mutation effectively blocked the prokaryotic pathway and converted *Arabidopsis* from a 16:3 plant to an 18:3 plant. Since the proportion of glycerolipids in *act1* were similar to that of wild type plants, it clearly showed that ER-lipids were transported into chloroplast to meet the requirements for lipid synthesis in chloroplasts (Kunst et al., 1988).

1.3.2 Lipid transfer from the chloroplast inner envelope to thylakoids

Galactolipids are the major constituents of thylakoid membranes, and are only detected in extrachloroplastic membranes in trace amounts and under certain conditions. About 75% of total thylakoid lipids are MGDG and DGDG. Since the biosynthesis of galactolipids occurs in the inner chloroplast envelope, a vesicular mechanism has been proposed for lipid transportation from the chloroplast inner envelope to thylakoids (Benning et al., 2006). VESICLE-INDUCING

PROTEIN IN PLASTIDS1 (VIPP1) has been demonstrated to play a critical role in this process. Sequence analysis showed that VIPP1 is a plastid-targeted protein that has high similarities with secretory proteins (Kroll et al., 2001). Disruption of VIPP1 in *Arabidopsis* resulted in a complete loss of internal thylakoid membranes in chloroplasts (Kroll et al., 2001; Zhang et al., 2012).

1.3.3 Lipid transfer from the chloroplast to extrachloroplastic membranes

Lipid exchange between the chloroplast and the cytosolic compartment is not one way in direction. Galactolipids, particularly DGDG, are no longer considered exclusively present in the chloroplast (Figure 1.6). Accumulation of DGDG in wild type *Arabidopsis* grown under phosphate-limiting conditions not only occurred in the chloroplasts but also in extrachloroplastic membranes, such as plasma membranes and mitochondria (Andersson et al., 2003; Andersson et al., 2005; Jouhet et al., 2004). Thus, the presence of non-phospholipids in extrachloroplastic membranes is a plant adaptation to phosphate deprivation. Though there is no direct evidence, it has been hypothesized that galactolipids are transported from chloroplasts to other organelles through sites of direct contact (Benning et al., 2006). In addition, a large number of phospholipases and galactolipid biosynthetic enzymes in the outer envelope of the chloroplast were up-regulated in this process which suggests active movement of lipids from chloroplasts to ER under phosphate-limiting conditions (Nakamura et al., 2005).

1.3.4 Factors involved in lipid transfer

TRIGALACTOSYLDIACYLGLYCEROL (TGD) proteins play an essential role in lipid transfer from ER to chloroplast (Awai *et al.*, 2006; Wang et al., 2013). In the *Arabidopsis tgd* mutants, transport of lipids from ER to chloroplast is disrupted (Benning et al., 2006). The TGD1, 2 and 3 form a bacterial-type ATP-binding cassette (ABC) transporter. *TGD1* is the first characterized *TGD* gene that encodes a membrane permease located in the inner envelope membrane of the chloroplast. Studies with *tgd1* mutants suggest that TGD1 is part of a multi-component ABC-type PA transporter that is required for the transfer of ER derived lipids to

chloroplasts (Awai et al., 2006; Xu et al., 2005). TGD2 is a substrate binding protein which, based on *in vitro* assays, specifically binds to PA while TGD3 is an ATPase. Unlike TGD1, 2 and 3 that transport ER-derived lipids through the inner envelope membrane of chloroplast, TGD4 binds PA specifically and resides in the outer chloroplast envelope (Roston et. al., 2012; Wang et al., 2013). Thus, PA is proposed to be the main lipid species transported from ER to chloroplast by TGD4.

Though TGDs play a role in transferring ER lipids to the chloroplast, the lipid species involved in this process remain unknown. DAG and PA synthesized in the ER are potential precursors transported to the outer envelope membranes, then reaching the TGD1, 2 and 3 proteins at the inner envelope membranes by unknown mechanisms (Benning et al., 2006). PC is also found in the outer envelope membranes of chloroplast. Lipid labeling studies show that the ER-derived PC can be converted to DAG for galactolipid synthesis in chloroplasts (Andersson et al., 2004). Therefore, mechanisms should exist for the transfer of PC molecules from their site of synthesis (the ER) to the chloroplasts, and the conversion of PC to DAG in the chloroplast membranes. Phospholipid transfer proteins might be involved in the transfer of PC molecules to the outer envelope membranes of chloroplasts (Kader, 1996). The conversion of PC to DAG or PA involves a large number of cytosolic lipases such as phospholipase C and D, however, many of them are still unknown. In addition, lipid flippases and lipid transporters could also be involved in lipid trafficking from ER to chloroplast. Hence, the precise mechanisms for the presence of ER-derived galactolipids in the membranes of chloroplasts remain a challenging question (Benning et al., 2006; Benning, 2008).

1.4 Lipid modifications in response to low and high temperatures

A number of changes in glycerolipid metabolism have been noted in plants grown at different temperatures. The physiochemical characteristics of membrane bilayers differ with the composition of lipid and fatty acid constituents, and their proportions change in response to environmental growth temperatures (McConn et al. 1994; Smolenska and Kuiper, 1977). The overall reason is probably related to the need to maintain membrane fluidity, which is directly

affected by the unsaturation of the acyl lipid components of bilayers (Harwood, 1991). Low temperature results in an increase in the degree of fatty acid unsaturation, while high temperature causes an opposite response (Wallis and Browse, 2002). In addition, changes in lipid composition are also observed. There may be relative alterations in the molecular species for a given lipid class as well as the proportion of different lipids (Harwood, 1994).

1.4.1 Lipid unsaturation and low temperature adaptation

Plants that are injured or killed by exposure to low, non-freezing temperatures in the range of 0 to 15℃ are referred to as chilling-sensitive (e.g. cotton and maize), whereas others, like *Arabidopsis*, are chilling-resistant among which some can tolerate temperatures even below 0℃ (Wolfe, 1978). The idea that membrane lipid unsaturation has a role in low temperature adaptation in plants originates from Lyons and Raison (Lyons, 1973; Raison and Lyons, 1986). They hypothesized that low temperature damage is associated with a transition from a liquid crystalline to a gel-like phase cellular membranes. Such a transition would reduce membrane fluidity and affect membrane integrity. However, in higher plants, cellular membranes of even chilling sensitive plants are highly unsaturated and do not seem to undergo a liquid crystalline to gel-like phase transition in the temperature range associated with chilling injury (Wolfe, 1979). Two concepts concerning lipid unsaturation have been proposed for low temperature adaptation in plants, though examples exist against both of them.

1.4.1.1 Polyunsaturated fatty acids and low temperature adaptation

It has been well documented that increased production of polyunsaturated fatty acids accompanies low temperature adaptation in many plants, and a positive correlation was found between a higher degree of unsaturation and cold tolerance (Wolfe, 1979). In *Arabidopsis*, the *fad2* mutant that is deficient in the activity of 18:1 to 18:2 desaturation displayed reduced polyunsaturated fatty acids in the ER along with reduced growth after 12 days at 6℃ (Miquel et al., 1993). Chlorophyll content of the mutant was reduced by about 50% during this period (Wu

et al., 1997). The *Arabidopsis fad5* mutant, deficient in a chloroplast fatty acid desaturase, accumulates a high level of 16:0, and the *fad6* mutant, that lacks an active desaturase responsible for the unsaturation of monounsaturated fatty acids, exhibits high levels of 16:1 and 18:1. These mutants, having reduced polyunsaturated fatty acids in chloroplast membranes, were indistinguishable from wild type plants when grown at 22℃ but displayed chlorotic lesions and decreased growth rate after a transfer to low temperature (6℃). Long term exposure of these mutants to low temperatures was lethal, while wild type plants survived (Miquel et al., 1993). The triple mutant *fad3/fad7/fad8* that is deficient in three genes responsible for the desaturation of 16:2 and 18:2 fatty acids completely lacks 16:3 and 18:3 fatty acids, and shows more chilling damage at low temperatures (20 to 5℃) (Wallis and Browse, 2002). An increase in polyunsaturated fatty acids (especially 16:3 and 18:3) is thought to enhance low temperature tolerance in plants (Murakami et al., 2000; Iba, 2002). Over-expression of the chloroplast FAD7 in tobacco increased the level of 16:3 and 18:3 fatty acids, and resulted in strong chilling tolerance in comparison to wild type (Kodama et al., 1994). However, transgenic tobacco with higher levels of polyunsaturated fatty acids due to over-expression of an ER-localized FAD3, showed no significant differences at low temperatures when compared to wild type (Hamada et al., 1998). Therefore, a specific role for polyunsaturated fatty acids in low temperature adaptation is not a universal phenomenon.

1.4.1.2 Disaturated phosphatidylglycerol (PG) and low temperature adaptation

Murata and colleagues (Murata et al., 1997) proposed that the level of disaturated PG which contains a combination of 16:0, 18:0 and 16:1-*trans* fatty acids in PG may be related to low temperature adaptability of plants. Generally, PG makes up 8-10% of chloroplast lipids and the majority of PG is found in the thylakoid membranes. Chilling-tolerant plants usually contain less than 20% of disaturated molecules, whereas chilling-sensitive species possess as high as 40 to 65% of disaturated PG (Murata et al., 1997). The amount of *trans*-16:1 in PG has been found to be decreased at low temperatures (Gray et al., 2005). These observations suggest that the disaturated PG molecules in the chloroplast membranes might be related to low-temperature adaptation in plants.

In chloroplast, PG usually contains 16:0 or *trans*-16:1 at the *sn-2* position of glycerol backbone. Due to the substrate selectivity of chloroplast GPAT, saturated 16:0 tends to be enriched in the *sn-1* position in chilling-sensitive plants while unsaturated 18:1 are preferentially esterified at the *sn-1* position in chilling-resistant plants. Hence, it has been proposed that the sensitivity to low temperature is caused by the substrate specificity of the GPAT enzymes (Iba, 2002). In transgenic *Arabidopsis* over-expressing a bacterial glycerol-3-phosphate acyltransferase gene (*plsB*), the level of disaturated PG content rose to 50%, compared to 5% in wild type. The chilling sensitivity of these transgenic plants was found to be increased (Iba, 2002), suggesting that plants with higher disaturated PG content are more sensitive to low temperatures.

However, a high level of disaturated molecules alone did not seem to be sufficient for inducing a chilling sensitive phenotype. The *Arabidopsis* mutant *fab1,* which is defective in converting 16:0-ACP to 18:0-ACP in the chloroplast, contained 43% of disaturated molecules in PG compared to 9% in wild type. However, the *fab1* mutants did not exhibit marked chilling injury when grown at 10 or 2℃ for two weeks (Wu et al., 1997). Hence, the level of disaturated PG is not the only determinant of low temperature tolerance in plants.

1.4.2 High temperature and fatty acid composition

Growth under high temperature is often accompanied by increased lipid saturation (Browse and Somerville, 1991; Iba, 2002). Decreasing the amount of polyunsaturated fatty acids in some studies showed enhanced high-temperature tolerance in plants. For example, a soybean mutant which is deficient in fatty acid unsaturation showed strong heat tolerance (Alfonso et al., 2001). One of the most dramatic phenotypes produced by an alteration of lipid changes in *Arabidopsis* is that of the *fab2* mutant in which the desaturation of 18:0-ACP to 18:1-ACP is blocked. The *fab2* mutant showed impaired growth as a result of the accumulation of 18:0 fatty acids. However, the mutant displayed similar morphology as wild type plants when grown at 35℃ (Lightner et al., 1994). Two *Arabidopsis* mutants, *fad5* which lacks 16:3 fatty acids, and *fad6,* which is deficient in dienoic and trienoic fatty acids, displayed increased thermal stability at high

temperatures. The *fad5* mutants also exhibited a higher growth rate under high temperature conditions than wild type (Wallis and Browse, 2002). In addition, both *fad7* and the *fad7/fad8* double mutants that are deficient in fatty acid desaturation for chloroplast lipids showed greater thermostability at 30℃ and 35℃ than wild type (Murakami et al., 2000).

1.4.3 Fatty acid desaturases respond to temperature fluctuations

Since lipid desaturation is reflected by the number of double bonds in the fatty acyl moiety, enzymes mediating the formation of the double bond, namely fatty acid desaturases, present themselves as the most likely factors controlling fatty acid desaturation during temperature adaptation. Temperature induced changes in fatty acid desaturase expression at both transcriptional and post-transcriptional levels have been widely explored. One example is the induction of the soluble Δ^9-stearoyl acyl carrier protein desaturase (*SAD*) at transcript level in potato during cold acclimation (Vega et al., 2004). Along with the increased expression of *SAD* was an increase in 18:2 in potato leaves. However, most membrane-bound desaturases involved in glycerolipid pathways are not regulated by temperatures at the transcript level. FAD8 is the only one that has been shown to be regulated by temperature at the transcript level (Gibson et al., 1994; McConn et al., 1994).

A post-transcriptional control mechanism was proposed to be involved in regulating FAD2 in *Arabidopsis*. *FAD2* is required for normal plant growth at low temperature (Miquel et al., 1993), but no transcript changes were observed when growing at 6℃ (Okuley et al., 1994). It has been proposed that post-transcriptional regulation participated in temperature-regulation of the soybean seed specific isoforms, GmFAD2-1A and GmFAD2-1B (Tang et al., 2005). Heterologous expression in yeast revealed that GmFAD2-1A was less stable and had a higher protein turnover rate than GmFAD2-1B. In addition, the enzyme activity of GmFAD2-1A and GmFAD2-1B might also be mediated through phosphorylation as a specific serine residue was identified in each sequence. At the transcript level, *GmFAD2-1A* and *GmFAD2-1B* decreased along with decreased levels of 18:2 in seeds during seed development at high temperature (Byfield and Upchurch, 2007). In wheat, the ER localized FAD3 has been shown to have

increased enzyme activity with increased 18:3 fatty acids at low temperatures though significant changes in transcript abundance has not been observed (Horiguchi et al., 2000). In *Arabidopsis*, FAD7 was later reported to be destabilized by high temperatures, hence implicating a post-transcriptional mechanism (Matsuda et al., 2005).

1.4.4 Lipid compositional changes in response to temperature fluctuations

Lipid changes at different temperatures in plants are not only observed in fatty acid composition but also in the proportion of glycerolipid species. The most common conversion is MGDG to DGDG, and such a metabolic change was proposed to aid survival at sub-optimal temperatures (Chen et al., 2006). A higher proportion of DGDG was observed at high temperatures in *Arabidopsis* (Chen et al., 2006), while low temperature induced the synthesis of MGDG in *B. napus* (Johnson and Williams, 1989). It has been postulated that DGDG had a tendency to stabilize the activity of photosynthetic system II (PSII) against heat stress (Yang et al., 2006). More MGDG was believed to be advantageous in regulation of fatty acid desaturation in the chloroplast, because the rate of desaturation of fatty acids in MGDG was significantly higher at all temperatures (Johnson and Williams, 1989). In addition, the process of desaturation on MGDG was faster at low temperatures than high temperatures in *B. napus* (Johnson and Williams, 1989). Thus, it was proposed that a higher proportion of MGDG would offer more advantages to the unsaturation of fatty acids in membranes.

In addition to the alterations in the proportion of glyceolipid species, changes were also observed in the same lipid species with different fatty acid combinations. As we know, in 16:3 plants like *B. napus*, the molecular profiles of MGDG is largely a mixture of 18:3/16:3 (prokaryotic) and 18:3/18:3 (eukaryotic) molecular species (Ohlrogge and Browse, 1995). An increase in MGDG (18:3/16:3) relative to MGDG (18:3/18:3) molecular species was observed in *B. napus* leaves grown at low temperature (Johnson and Williams, 1989). In contrast, a decrease in MGDG (18:3/16:3) relative to MGDG (18:3/18:3) was also observed in *Arabidopsis* grown at high temperatures (Chen et al., 2006). One explanation is that longer hydrocarbon chains (C18) which interact strongly with each other possess higher melting temperatures, whereas, shorter

chain length (C16) have a lower melting point since it reduces the tendency of hydrocarbon chains to interact with one another (Wolfe, 1978).

1.5 Proposed hypothesis

Modulation of membrane lipid composition under varying environmental conditions is an important part of plant stress adaptation. Membrane fluidity is greatly influenced by the degree of fatty acid desaturation; it is hence a truism without cladistic boundary that lower temperature results in an increased degree of desaturation whereas higher temperature causes an elevated degree of saturation of membrane lipid molecules (Iba, 2002; Murakami et al., 2000; Murata et al., 1992; Murata and Los, 1997; Wallis and Browse, 2002). To date, despite extensive studies on this subject, the link between fatty acid desaturases and desaturation under temperature fluctuations remains a weak one. Many studies have been focused on the degree of unsaturation in polyunsaturated fatty acids or several specific lipids. The fact is that, in membranes, fatty acids are almost never found in the form of free fatty acids but mostly esterified to glycerol to form glycerolipids (Ohlrogge and Browse, 1995). Changes in membrane lipid compositions and fatty acid combinations in each lipid species would also affect membrane fluidity (Johnson and Williams, 1989). Lipid redistribution between the two glycerolipid pathways as well as lipid exchanges between the ER and chloroplast are required in this process (Johnson and Williams, 1989). How the metabolic perturbation is hierarchically modulated between the two glycerolipid pathways, and precisely, what factors are involved in this process remain largely unknown. Hence, understanding the biochemical regulation in the context of glycerolipid pathways would provide more insights in temperature adaptation in plants.

The central hypothesis of this study is that a balance of glycerolipid pathways is critical for plant adaptation to temperature fluctuations. In addition, this study offers a biochemical basis to understand the increased fatty acid desaturation under low temperature and decreased fatty acid unsaturation at high temperature beyond the regulation of fatty acid desaturases.

1.6 Research objectives

The primary goal of this thesis is to understand the biochemical mechanisms of temperature induced lipid pathway adjustments in plants. A long-term goal is to explore a possible explanation of the reduced prokaryotic pathway contribution in plants during the evolutionary process. To achieve these goals, three plant species, *Arabidopsis thaliana, Atriplex lentiformis* and *Triticum aestivum*, that are known to be distinctly different in the mode of glycerolipid synthesis are employed in this study.

Objective 1: **Probe the biochemical and transcript responses in glycerolipid pathways in the typical 16:3 plant, *Arabidopsis*, when subjected to sub-optimal temperatures.** First, I comparatively investigated the balance of glycerolipid pathways in *Arabidopsis* at low (10℃), standard (22℃) and high temperature (30℃) conditions by thin layer chromatography (TLC)-based lipid profiling. Second, I performed transcript analysis of genes in the glycerolipid pathways to identify potential factors involved in regulating lipid changes. This will address my hypothesis by investigating lipid pathway adjustments in a typical 16:3 plant in response to low and high temperatures.

Objective 2: **Understand the metabolic conversion of *Atriplex lentiformis* from 16:3 to 18:3 lipid phenotype when grown at high temperature.** First, I comprehensively analyzed lipid molecules in *A. lentiformis* leaves grown at 23 and 43℃ to understand the lipid phenotype conversion; second, a comparative analysis of individual lipid molecular species within subsets of glycerolipid classes by lipidomics analysis; third, I employed RNA sequencing to understand the differential programming of the biosynthetic machinery required for lipid phenotype conversion. This will address my hypothesis by combining the biochemical and transcript changes in *A. lentiformis* at high temperature to understand the biosynthetic machinery required for the lipid phenotype conversion.

Objective 3: **Investigate the modulation of glycerolipid pathways in 18:3 plants at low temperature.** Lipid profiling and lipidomics were conducted to investigate the glycerolipid pathway adjustments in *Triticum aestivum* (18:3 plants) when grown at 23℃ and 4℃. This will address my hypothesis by investigating the lipid pathway adjustments in an 18:3 plant in

response to low temperature.

Objective 4: **Establish a model depicting the adjustments of fatty acid flux sharing between glycerolipid pathways in plants in response to temperature changes**. Identify the mode of fine tuning between glycerolipid pathways through systematic analysis of transcript and metabolic dynamics in these three plant species.

Objective 5: **Temperature treatment with *Arabidopsis* T-DNA mutants to further support the model.** Lipid mutants including *act1*, *gly1* and *fad5* which possess altered glycerolipid pathways were subjected to low temperature treatment. Biochemical and phenotypic changes were recorded. This will further test my hypothesis using *Arabidopsis* mutants.

2 MATERIALS AND METHODS

2.1 Description of plant materials used

In this study, three plant species were used: *Arabidopsis thaliana* (Columbia-0 ecotype, seeds were maintained in Dr. Jitao Zou's lab, National Research Council Canada), *Atriplex lentiformis* (Torr.) S.Wats (obtained from Stover Seed Company, USA) and *Triticum aestivum* L. cv. Manitou (Provided by Dr. Brian Fowler, University of Saskatchewan). *Arabidopsis* is a typical 16:3 plant. *A. lentiformis* is a native to southwest United States. It is a desert habitat shrub that has been well adapted to coastal and desert environments (Pearcy, 1978). *A. lentiformis* is a 16:3 plant capable of switching to 18:3 lipid phenotype when grown at high temperatures. *T. aestivum* is a typical 18:3 plant. All *Arabidopsis* lipid mutant lines used in this study are in the ecotype Columbia-0 (Col-0) genetic background and have been previously described as shown in Table 2.1.

Table 2.1 List of *Arabidopsis* lipid mutants used in this study.

Lipid mutants	Enzyme function	Glycerolipid pathway	ABRC Stock Number	References
fad5	16:0 to 16:1 desaturase on MGDG	Compromised prokaryotic pathway	CS206(*fad5-1*)	Hugly and Somerville, 1992
act1	Chloroplast glycerol-3-phosphate acyltransferase	Loss of prokaryotic pathway	CS200	Kunst et al., 1988
gly1	Chloroplast glycerol-3-phosphate dehydrogenase	Compromised prokaryotic pathway	SALK_111786C1	Miquel et al., 1998

2.2 Temperature treatments and plant growth conditions

Three growth chambers (Conviron, USA) with 16 hour light (~100 μmol m^{-2} s^{-1}) /8 hour dark regimes were employed for the experiments with *Arabidopsis* (Col-0). For temperature treatments, plants were grown at 22/17℃ (day/night temperature) in Sunshine Mix#3/LG3 soil (Sun Gro Horticulture, Canada) for one week after germination, then shifted to a 10/8℃ growth

chamber for low temperature and a 30/28℃ growth chamber for high temperature treatment for another 3 weeks. Hereafter referred to as 22, 10 and 30℃. Plants grown at 22℃ for four weeks were used as control. Fatty acid changes were observed at 10℃ and 30℃ in *Arabidopsis* (Ma and Browse, 2005; Maeda et al., 2006). A three week treatment ensures fatty acid turnover and resynthesis of new lipids to achieve the temperature-adapted composition (Falcone et al., 2004). In addition, the long-term treatment appears to be a key to understanding the importance of saturated and unsaturated fatty acids in plants at low and high temperature conditions (Wu et al., 1997). Three biological replicates for biochemical and transcript analyses were performed with leaf tissues harvested from plants at the rosette stage.

A. lentiformis plants (whose natural habitat is a desert in Death Valley, California, USA) were grown in a growth chamber (Conviron, USA) under either 23/18℃ or 43/30℃ day/night temperature regime with a 16 hour photoperiod and light intensity of 120 μmol m^{-2} s^{-1}. Hereafter referred to as 23℃ and 43℃. *A. lentiformis* plants have been shown lipid phenotype conversion and fatty acid changes at 43℃ (Pearcy, 1978). At least three biological replicates were conducted with leaves from eight week-old plants for lipid profiling, lipidomics and transcriptomic analysis.

Wheat (*T. aestivum* L. cv Manitou) plants were grown in Sunshine Mix#3/LG3 soil (Sun Gro Horticulture, Canada) at 23℃ growth chambers (Conviron, USA) for two weeks (three-leaf stage) after germination, then shifted to 4℃ growth chambers for cold treatment for another two weeks. Light intensity in both chambers was ~120 μmol m^{-2} s^{-1}. Above ground plant materials were harvested for lipid profiling (three biological replicates) and lipidomics analysis (four biological replicates). All samples were frozen in liquid N_2 immediately after harvesting and stored at -80℃.

For temperature treatment with *Arabidopsis* lipid mutants, plants including *gly1*, *fad5*, *act1* and wild type were grown in Sunshine Mix#3/LG3 soil (Sun Gro Horticulture, Canada) at 22℃ growth chamber (Conviron, USA) for one week after germination. Half of the plants were then shifted to a 5℃ growth chamber for low temperature while the other half were grown at 22℃ and used as control. 5℃ was selected for cold-treatment as the *fad5* mutants have been shown chlorosis (Hugly and Somerville, 1992). Three-week old rosette leaves were collected for biochemical analysis.

2.3 Growth stage assessment for *Arabidopsis*

Plants were grown in Sunshine Mix#3/LG3 soil (Sun Gro Horticulture, Canada) under long day (16 hour light /8 hour dark regimes, light intensity is ~100 μmol m^{-2} s^{-1}) conditions. Flowering time was measured by counting the total number of rosette leaves, excluding the cotyledons, once the bolt reached 5 cm. The number of days from sowing to bolting was also recorded. Six plants were analyzed for each genotype and the mean value ± standard deviation and student t-test were calculated.

2.4 Fatty acid analysis

For total fatty acid analysis, leaf samples (10-50 mg) were introduced into a Teflon-lined screw cap glass tube that was pre-rinsed with 2 mL dichloromethane. Then, 1 mL of 5% (v/v) sulfuric acid in methanol, 20 μL of 0.2% butylated hydroxy toluene in methanol and 300 μL of toluene were added as a co-solvent. The tubes were heated for 2 hours at 80°C. After the tubes were cooled, 1 mL of 0.9% (w/v) NaCl and 0.35 mL of hexane were added. The tubes were vortexed vigorously and centrifuged at 3,000 rpm for 3 min. The upper phase (organic phase) was transferred to a new tube and dried under nitrogen. After redissolving in hexane, the fatty acid methyl esters (FAMEs) were analyzed by gas chromatography.

2.5 Lipid analysis

Polar lipids were extracted from 0.5 g of harvested leaves. Leaf tissues were immediately immersed in liquid N_2 and ground under liquid N_2 with a mortar and pestle before extraction. After adding 4 mL of chloroform/methanol/formic acid (10:10:1, v/v/v), the extracts were transferred into a glass tube with a Teflon-lined screw cap. The mortar and pestle were washed with another 2 mL of chloroform/methanol/formic acid (10:10:1, v/v/v). The extracts were pooled, centrifuged at 2,500 rpm for 6 min and the upper phase was transferred into a new tube. The extracts were re-extracted with 2 mL chloroform/methanol/formic acid (5:5:1, v/v/v),

combined after centrifuging at 3,000 rpm using CL2 centrifuge (Thermo Scientific, USA), washed with 3 mL of 0.2 M H_3PO_4 and centrifuged for 8 min at 2,500 rpm.

Lipids were recovered in the organic phase and dried under nitrogen. After re-dissolving in chloroform, total lipids were separated by two dimensional thin layer chromatograph (2D-TLC) using the method of Shen et al., (2010). Polar lipids were separated on TLC plates with chloroform/methanol/50% ammonia hydroxide (65:25:2, v/v/v), and then plate rotated with chloroform/methanol/acetic acid/water (85:15:10:3, v/v/v/v). TLC pates were sprayed with 0.05% primulin in 80% acetone and lipids were visualized under UV light. Individual lipids were scraped off the TLC plates and transferred into a glass tube with a Teflon-lined screw cap. After adding 2 mL of 3N methanolic HCl, transmethylation of lipids was performed by heating at 80℃ for 2 hours. Fatty acid methyl derivatives of each lipid were extracted and determined by gas chromatographic analysis. An estimation of the membrane total unsaturation level by double bond index was calculated from mol% values of each fatty acid using the formula: DBI=[∑(number of double bonds x mol% of fatty acid)]/100 (Falcone et al., 2004).

2.6 Lipid class analysis

Lipid class analysis of MGDG, DGDG, PG and PC was performed according to Shen et al., (2010). Each lipid species was separated by 2D-TLC and eluted from the TLC plates by chloroform and methanol (2:1, v/v). Individual lipids were dissolved in 1 mL of 40 mM Tris-HCl buffer, pH7.2, 0.05% Triton X-100 containing 50 mM H_3BO_3. The reaction was initiated by adding 3000 Units of *Rhizopus arrhizus* lipase suspended in the same buffer. The mixture was incubated at 37℃ for 30-60 min. Lipids were extracted with 3.8 mL of chloroform and methanol (2:1, v/v) and 1 mL of 0.15 M acetic acid. The organic phase was collected and separated on TLC plates with chloroform/methanol/acetic acid/water (85:15:10:3, v/v/v/v). The *lyso*-lipids containing fatty acids at the *sn-2* position were scraped off the TLC plates for gas chromatographic analysis after transmethylation. Fatty acid composition at *sn-1* position was calculated based on the fatty acid composition of the original diacyl lipids and the lysolipids.

2.7 Lipidomics analysis

Lipid extractions for lipidomics analysis were performed according to the protocol from the Kansas Lipidomics Research Center (http://www.k-state.edu/lipid/lipidomics). Briefly, leaf tissues from *A. lentiformis* and *T. aestivum* plants were heated in 2 mL isopropanol with 0.01% butylated hydroxytoluene at 75°C for 10 min to inactivate the lipases. Chloroform and methanol (2:1, v/v) were added for extraction. After several extractions, the combined extracts were washed with 1 M KCl to remove proteins and carbohydrates. The chloroform phase was taken out and dried under a nitrogen stream. Lipid extracts were dissolved in chloroform for lipidomic analysis. Electrospray ionization tandem mass spectrometry (ESI-MS/MS) analysis was performed with three or five biological replicates for each growth condition at the Kansas Lipidomic Research Center. The data for each lipid molecular species are presented as mol% of the total lipids analyzed (Welti et al., 2002).

2.8 Real-time qRT-PCR analyses

Total RNA was extracted from leaves of *Arabidopsis* grown at 10, 22 and 30℃, respectively, using the Plant RNeasy Mini kit (Qiagen, Ontario, Canada). RNA quality and quantity was determined by spectrophotometry at 260 nm and 280 nm using NanoDrop 2000 (ThermoScientific, USA). cDNA synthesis was conducted with 1 μg of total RNA using QuantiTect Reverse Transcription kit (Qiagen, Ontario, Canada). Genes selected for qRT-PCR were chosen based on their potential significance in glycerolipid pathways. All primers used for qRT-PCR were designed to produce fragments between 75 and 130 bp. Primer specificity was checked with BLASTn searches against TAIR10 Transcripts (http://www.arabidopsis.org/). All transcripts were normalized with the endogenous control *ACTIN 2* (*At3g18780*) (Huang et al., 2007). Real-time qRT-PCR was performed with Power SYBR Green PCR Master Mix (Applied Biosystems, USA) and amplification was monitored with ABI StepOne Real-time PCR Systems (Applied Biosystem, USA). Each 20 ul reaction contained 1 x Power SYBR Green PCR Master Mix, 50 nM of each primer, and cDNA template. Data acquisition and analysis were performed using StepOne software 2.0. Each sample was conducted with three independent biological

replicates and each reaction contains four technical replications. The primers used for qRT-PCR are listed in Table 2.2.

Table 2.2 Primer pairs used for qRT-PCR.

Gene Name	AGI ID	Forward primer (5'→3')	Reverse primer (5'→3')
ACTIN2	AT3G18780	AACCCAAAGGCCAACAGAGA	AAGGTCACGTCCAGCAAGGT
AAPT1	AT1G13560	GGGAACGCGGAAGAAACGCA	CCCCTATAGAGAGCGGCGAA
AAPT2	AT3G25585	TTTGGATTCCTTGTGGGAAG	GAACCCCGTCGTTGAGTCTA
ATPIS1	AT1G68000	GGCTTTGACATTGTTCGGTT	GATCAAGGCTTCTGCTGCT
ATPIS2	AT4G38570	CTGTGGATGGATGGTGCGCT	AGAAGACAGGCTGTGCTGAC
NMT1	AT3G18000	CCCGATTCGACGTTGTGCGA	TGGCCTTCGACGGCGAGTCT
PECT1	AT2G38670	TTCTGGCGTGCCGCTACGTG	GCTCTCGGCTACTGTCCCAT
FAD2	AT3G12120	CCTTCCTCCTCGTCCCTTAC	CTCTTTCGAGGGATCCAGTG
FAD3	AT2G29980	TCAAACCCTTTCTTCACCACA	TTGGTCCATAGCAACAACCA
PGPS2	AT3G55030	TGTCGCCACCGCCCTTCTTC	TCCACCGTCGCGGTGTCTTC
MGD2	AT5G20410	ACGGTCATGGCCCTTGCAGA	CCGTCGCCGCTTGTTACGGA
MGD3	AT2G11810	CACTGATTTGCGGCCTCCCA	GGGTGAAAACTCCAGCCCCA
DGD1	AT3G11670	GTGCAAGAAGCAATGACGA	GTTGCTGCTTCCCAAGAGAG
DGD2	AT4G00550	GTGTGTTTGCGTCATCTTC	CCAAAAGCTGTTCTGGAAG
ACT1	AT1G32200	TTCTCGCGGCGGCGTTAGTG	GCTCACTCGGCGTCTCACCG
ATS2	AT4G30580	GCCAACGGGTAGTGAAGGTA	GTTGCAAAGAACATCCGCTT
PGP1	AT2G39290	TCTTCACCGCCTCCGTCGCA	GCGGCGACACGACCAAGTGT
PAP1	AT2G01180	GTCAAGGAAGGCCACAAGAG	GCCTTGATTTTGCCAGAGAG
MGD1	AT4G31780	GTTACATCGCTGGTCAAGAG	TGCCGGTCCAAACCAATCCG
FAD5	AT3G15850	TGGGTTTTGGTTCAGTCACA	TAGGTGGTTCGAAGGAATCG
FAD6	AT4G30950	CCGTGGTATCTGCTACCGTT	TAGGAAGGCGAGAGTACCCA
FAD7	AT3G11170	TCGCTATCGTCTTTGCATTG	GCCAATAGAGAGGCCAAACA
FAD8	AT5G05580	TCCTTTGCCTGAAAGCATCT	GAAAGGGTATGCGAGCATTG
SQD1	AT4G33030	CCCGGCAAAAGCTGGTGAGT	GCCCAAGCTTTGAACCCGCT
SQD2	AT5G01220	GCAAGCTCCGCTTCTGTGGA	AGCGGCGCATCAATCTCCGA

2.9 RNA extraction, library preparation and Illumina sequencing

Total RNA was extracted from *A. lentiformis* leaf tissues grown at 23 and 43℃ using Agilent Plant RNA isolation Kit (Agilent technologies, USA). The yield and RNA quality were

determined by a NanoDrop 2000 (Thermo scientific, USA). Total RNA was redissolved in RNA-free water to a final concentration of 200 ng/µL. Eight complementary DNA libraries were constructed from leaves with four biological replicates for each growth condition using TruSeq RNA Sample Preparation Kit v2 (Illumina, Inc., USA). Sequencing reactions were conducted on Illumina HiSeq2000 at the National Research Council, Aquatic and Crop Resource Development (ACRD)-Saskatoon, Canada. Each fragment used pair-end sequencing from a 200 bp insert library, and the length of each sequence read was 101 bp. All sequence files generated in this study are available at the NCBI Gene Expression Omnibus under accession number GSE52913.

2.10 *De novo* assembly, transcript annotation and differential expression analysis

After removing sequencing adapters and trimming low-quality reads by Btrim program (Kong, 2011), repeat masking was performed by removing reads with hits against the TIGR Plant Repeats Database (Ouyang and Buell, 2004) using Bowtie2 with a maximum fragment length of 1000 nt (Langmead and Salzberg, 2012). All Illumina reads were then assembled into contigs using Trinity program (version 2013-02-25) using default parameters following the protocol documented in Grabherr et al. (2011) and Haas et al. (2013). Using paired-end reads, contigs from the same transcript were connected and extended in both ends using the CAP3 program to remove redundancy (Huang and Madan, 1999). In total, 144, 456 unique sequences with an average length of 1,109 bp were constructed. Illumina reads were then mapped back onto the contigs using the alignReadsl.pl script that is a part of the Trinity program. Transcripts with at least 50 reads per transcript across eight samples were defined as expressed and used for differential expression analysis. Normalized transcript expression levels were estimated according to the transcript features (length, depth of sequencing and reads) and sample size in units of FPKM (Fragments Per Kilobase of exon per Million fragments) (Gentleman et al., 2004, Robinson et al., 2010). For each transcript, the mean $\log_2$ fold change and corresponding *p*-value were calculated using edgeR package (Robinson et al., 2010) from the average of four biological replicates of each experimental condition. False discovery rate (FDR) correction (Benjamini and Hochberg, 1995) was applied to account for testing of multiple transcripts. Transcripts were considered differentially regulated if the *p*-value was less than 0.01 and the fold change in

expression level was greater than 4.

Putative functions of all transcripts were assigned using BLASTx searches (E-value cut-off of 10^{-6}) against *Arabidopsis* TAIR10 database for downstream analysis. Of the 46,493 transcripts, 30, 204 (65%) were successfully annotated. In some cases, more than one *A. lentiformis* transcript matched the same AGI protein in *Arabidopsis*. These transcripts could have resulted from non-overlapping sequence fragments from the same mRNAs or distinct homologous sequences in *A. lentiformis*. In these cases, the transcript with the highest FPKM normalized read counts, which presumably has the highest expression levels, was assigned as the representative transcript of the group. Customized glycerolipid pathways were generated using MapMan program (Thimm et al., 2004). MapMan BINcodes for glycerolipid genes in *A. lentiformis* were manually assigned.

3 RESULTS

3.1 Biochemical and transcript changes in glycerolipid pathways in response to sub-optimal temperatures in *Arabidopsis*

3.1.1 Glycerolipid compositions are relatively stable during leaf development

To investigate whether glycerolipid compositional changes in leaves grown at low and high temperatures are caused by developmental differences or temperatures, it is important to determine the proportion of each lipid species during leaf development. Leaf numbers and growth stages of *Arabidopsis* grown at standard growth conditions (22℃, long day) as well as at low (10℃) and high (30℃) temperatures were recorded (Figure 3.1a). Results suggested that three-week, four-week and five-week old plants grown at standard growth conditions (22℃, long day) shared similar growth stages as of plants grown at 10, 22 and 30^{o}C respectively after temperature treatments (Figure 3.1b). Rosette leaves from the three-week, four-week and five-week old plants grown at 22℃ were then collected separately for lipid analysis to assess the effects of developmental stages on lipid compositions.

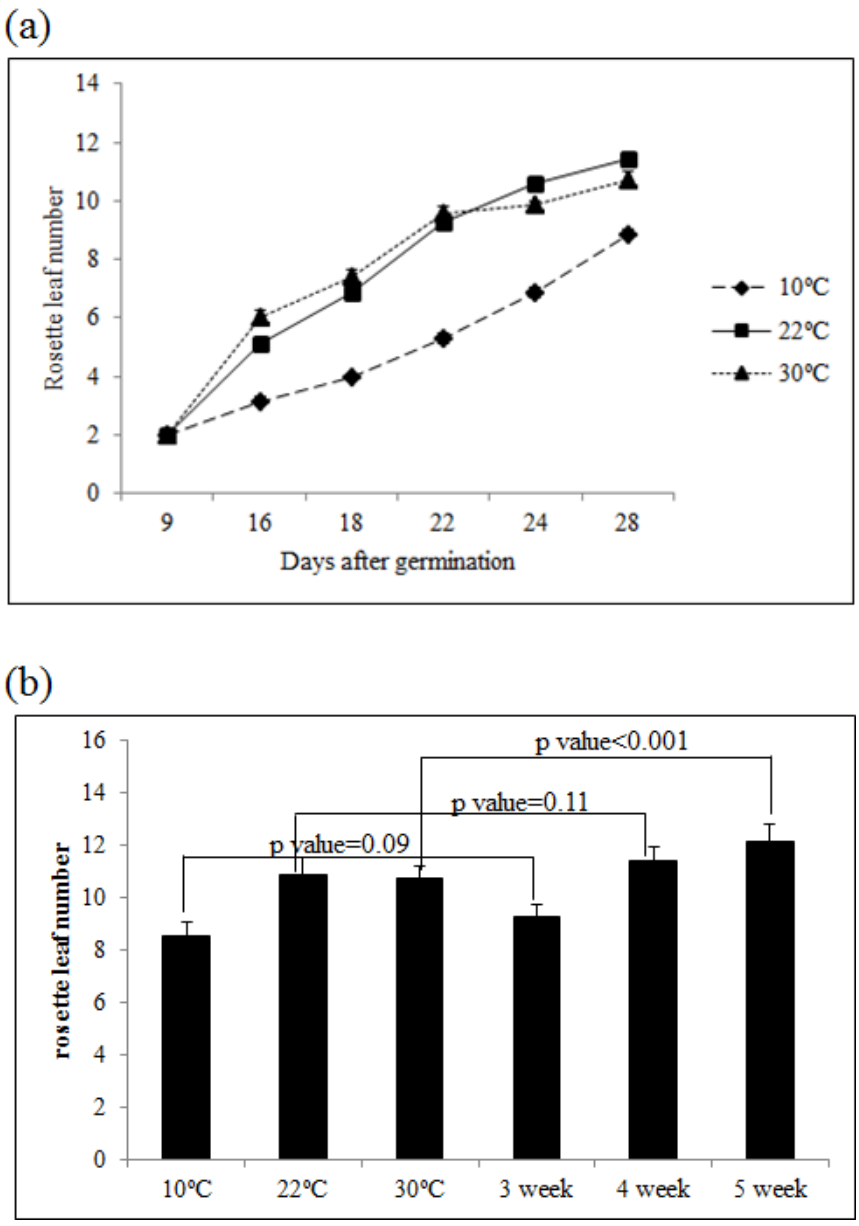

Figure 3.1 Growth stage analysis of plants raised at 10, 22 and 30℃.

(a) Leaf number of *Arabidopsis* grown at 10, 22 and 30℃ during temperature treatments. Plants were grown at 22℃ for one week and then transferred to 10℃ and 30℃ for another three weeks. Rosette leaves of *Arabidopsis* are numbered for true leaves that were at least 10 mm in length. Values are average of counting six individual plants. (**b)** Assessment of plant growth stage at the end of temperature treatments. Leaf numbers of temperature-treated plants (left panel) were counted and compared to plants grown at standard conditions (22℃) at three, four and five weeks (right panel), respectively. P values are calculated by two-tailed student t-test. Values are mean ± SD of six individual plants.

On a total fatty acid basis, molar percentage (mol%) of 18:3 increased with a concomitant decrease in 18:2 as leaf maturity advanced (Table 3.1). Analysis of seven major glycerolipid species showed that, while the proportion of each glycerolipid species was generally static, subtle changes in the mol% were detectable during leaf development (Table 3.2). MGDG and DGDG were slightly increased 1.13 mol% and 0.98 mol% respectively in five-week old leaves compared to three-week old leaves. In contrast, PC, PE, PG, SQDG and PI showed minor decrease (less than one mol%) in the amount of total lipids. Small differences (< 3.08 mol%, Table 3.2) were observed in fatty acid compositions of MGDG, DGDG, PG, PI and SQDG. 18:2 in PC showed a significant decrease of 7.7 mol% and 18:3 were increased by 6.9 mol% in five-week old leaves compared to three-week old leaves. These results suggested that, though subtle changes were observed in fatty acid composition of each lipid species during leaf development, the proportion of each glycerolipid species in cell membranes is relatively stable.

Table 3.1 Total fatty acid composition analysis during *Arabidopsis* leaf development at 22℃.

Values are mean ± SD from three biological replicates from three individual plants. DBI, Double Bond Index.

	Fatty acid composition (mol%)									
	16:0	16:1[a]	16:2	16:3	18:0	18:1	18:2	18:3	C16/C18	DBI()
2 week	15.6 ± 0.60	6.0 ± 0.33	1.1 ± 0.05	11.5 ± 0.17	1.2 ± 0.04	7.2 ± 0.38	18.2 ± 0.24	42.1 ± 0.33	0.5 ± 0.00	2.1 ± 0.02
3 week	17.2 ± 0.37	5.5 ± 0.47	1.1 ± 0.05	11.8 ± 0.48	1.4 ± 0.04	6.5 ± 0.47	17.6 ± 0.53	41.6 ± 1.03	0.5 ± 0.01	2.1 ± 0.02
4 week	15.9 ± 0.56	4.6 ± 0.93	0.9 ± 0.12	12.6 ± 0.37	1.1 ± 0.09	5.5 ± 0.83	15.7 ± 0.41	45.1 ± 0.74	0.5 ± 0.01	2.2 ± 0.02
5 week	15.8 ± 0.60	3.4 ± 0.04	0.7 ± 0.01	13.0 ± 0.29	1.1 ± 0.05	4.0 ± 0.05	14.3 ± 0.31	49.4 ± 0.46	0.5 ± 0.01	2.2 ± 0.02

[a] represents sum of *cis* and *trans*-16:1

Table 3.2 Glycerolipid composition analysis of *Arabidopsis* during leaf development.

Values represent averages of three independent pools of leaf tissues and expressed as mean ± SD.

Glycerolipids		Total Polar Lipids (%)	Fatty acid composition (mol%)								C16/C18
			16:0	16:1[a]	16:2	16:3	18:0	18:1	18:2	18:3	
DGDG											
	3 week	16.4 ± 0.18	12.3 ± 0.21	0.2 ± 0.01	0.7 ± 0.01	2.8 ± 0.03	1 ± 0.04	1.5 ± 0.16	4.8 ± 0.35	76.8 ± 0.36	0.19 ± 0.00
	4 week	17.0 ± 0.10	13.1 ± 0.19	0.3 ± 0.08	0.6 ± 0.01	2.5 ± 0.03	1.1 ± 0.12	1.9 ± 0.12	4.8 ± 0.05	75.7 ± 0.5	0.20 ± 0.00
	5 week	17.5 ± 0.41	12.6 ± 0.63	0.1 ± 0.04	0.5 ± 0.01	2.3 ± 0.06	0.9 ± 0.01	1.5 ± 0.08	4.8 ± 0.2	77.3 ± 0.63	0.18 ± 0.01
MGDG											
	3 week	42.3 ± 0.14	0.9 ± 0.08	1.1 ± 0.03	1.9 ± 0.02	34.4 ± 0.85	0.1 ± 0.05	1.2 ± 0.12	2.9 ± 0.19	57.4 ± 0.49	0.62 ± 0.01
	4 week	42.9 ± 0.82	0.8 ± 0.02	1.2 ± 0.04	1.8 ± 0.01	34.2 ± 0.69	0.1 ± 0	1.2 ± 0.13	2.5 ± 0.09	58.3 ± 0.42	0.61 ± 0.01
	5 week	43.3 ± 0.41	1 ± 0.01	0.6 ± 0.02	1.3 ± 0.02	34.1 ± 0.03	0.1 ± 0	0.7 ± 0.07	2.2 ± 0.54	59.9 ± 0.48	0.59 ± 0.00
PC											
	3 week	16.0 ± 0.43	20.6 ± 0.48				2.9 ± 0.05	8.2 ± 0.08	37.2 ± 0.29	31.1 ± 0.67	0.26 ± 0.00
	4 week	15.9 ± 0.52	21.1 ± 0.4				2.7 ± 0.09	7.6 ± 0.07	35.8 ± 0.07	32.8 ± 0.36	0.27 ± 0.00
	5 week	16.0 ± 0.54	23.7 ± 1.15				2.8 ± 0.53	4.5 ± 0.1	31 ± 0.68	38 ± 1.63	0.31 ± 0.01
PE											
	3 week	9.4 ± 0.20	29.5 ± 0.69				2.4 ± 0.1	4 ± 0.22	40 ± 0.33	24.2 ± 0.25	0.42 ± 0.01
	4 week	9.2 ± 0.28	29.5 ± 0.06				2.3 ± 0.07	3.8 ± 0.01	39.2 ± 0.06	25.2 ± 0.08	0.42 ± 0.00
	5 week	8.8 ± 0.18	29.5 ± 0.13				2.2 ± 0.04	2.8 ± 0.12	38.2 ± 0.53	27.3 ± 0.3	0.42 ± 0.00
PG											
	3 week	11.0 ± 0.34	26.3 ± 0.07	26.8 ± 0.03			1 ± 0.05	6.4 ± 0.02	8.6 ± 0.03	31 ± 0.13	1.13 ± 0.00
	4 week	10.9 ± 0.48	27.6 ± 0.06	25.7 ± 0.08			1 ± 0	7 ± 0.04	9 ± 0.04	29.7 ± 0.06	1.14 ± 0.00
	5 week	10.5 ± 0.20	28.6 ± 0.34	24.5 ± 0.15			1 ± 0.11	5.8 ± 0.11	10 ± 0.17	30.1 ± 0.39	1.13 ± 0.01
PI											
	3 week	3.1 ± 0.05	44.6 ± 0.93				3.4 ± 0.25	3.3 ± 0.32	26.3 ± 0.22	22.4 ± 0.16	0.81 ± 0.02
	4 week	2.6 ± 0.29	43.8 ± 2.64				3.4 ± 0.06	3.8 ± 1.27	26.1 ± 1.13	22.9 ± 0.24	0.78 ± 0.05
	5 week	2.4 ± 0.13	47.4 ± 0.71				2.9 ± 0.84	1.9 ± 0.26	23 ± 0.64	24.9 ± 0.59	0.90 ± 0.01
SQDG											
	3 week	1.7 ± 0.19	40.3 ± 1.4				2 ± 0.11	2 ± 0.05	5.6 ± 0.13	50.1 ± 1.64	0.67 ± 0.02
	4 week	1.4 ± 0.05	41.5 ± 1.27				2.4 ± 0.41	2.4 ± 0.61	6.5 ± 0.82	47.3 ± 0.57	0.71 ± 0.02
	5 week	1.4 ± 0.15	42.1 ± 1.23				2.8 ± 1.05	1.2 ± 1.03	6.9 ± 0.32	47 ± 1.56	0.73 ± 0.02

[a] represents sum of 16:1 *cis* and *trans* in MGDG and DGDG
[b] represent sum of 18:1 *cis* and *trans* fatty acids.

3.1.2 Lipid changes in *Arabidopsis* leaves grown at high and low temperatures

3.1.2.1 Changes in total fatty acid composition of leaves of *Arabidopsis* grown at high and low temperatures

Changes in mol% of major fatty acid species in *Arabidopsis* plants grown at 10, 22 and 30℃ are shown in Table 3.3. Both 16:3 and 18:3 polyunsaturated fatty acids decreased at 30℃, while the polyunsaturated 18:3 exhibited a significant increase at 10℃. The proportion of 18:2 showed an opposite trend to 18:3, with a significant increase at 30℃ and a substantial decrease at 10℃. The monounsaturated 18:1 exhibited an increase at both 10 and 30℃. The degree of unsaturation in total fatty acids can be estimated by the Double Bond Index (DBI) that is calculated based on double bonds (as described in Chapter 2, Section 2.6) (Falcone et al., 2004). There was a decrease in DBI at 30℃ and an increase of DBI at 10℃. These results suggested an overall decrease in the degree of unsaturation in membrane lipids at 30℃ and an increase in the degree of unsaturation at 10℃.

Table 3.3 Total fatty acid composition in leaves of *Arabidopsis* plants grown at 10, 22 and 30℃.

Values are means ± SD of mol% (n = 4 individual plants). Statistically significant differences (two-tailed student t-test; *, $p < 0.05$) were calculated by comparisons between temperature treatments (10 and 30℃) and the standard growth condition (22℃), respectively. DBI, double bond index. C16 represents the sum of 16: 0, 16: l, 16:2 and 16:3; C18 represents the sum of 18:0, 18:1, 18:2 and 18:3.

	Fatty acid composition (mol%)								C16/C18	DBI
	16:0	16:1[a]	16:2	16:3	18:0	18:1	18:2	18:3		
10℃	17.9 ± 0.39	2.0 ± 0.14*	0.7 ± 0.01	12.4 ± 0.19	0.8 ± 0.05*	5.9 ± 0.34*	13.5 ± 0.18*	46.9 ± 0.11*	0.49 ± 0.01*	2.14 ± 0.00*
22℃	17.6 ± 0.34	3.6 ± 0.13	0.8 ± 0.09	12.2 ± 0.07	1.2 ± 0.02	3.8 ± 0.41	16.3 ± 0.4	44.4 ± 0.44	0.52 ± 0.00	2.12 ± 0.00
30℃	18.9 ± 0.12*	4.7 ± 0.06*	1.1 ± 0.04*	9.5 ± 0.12*	2.0 ± 0.07*	5.4 ± 0.44*	20.5 ± 0.24*	37.8 ± 0.75*	0.52 ± 0.00	1.95 ± 0.01*

[a] represents sum of 16:1 *cis* and *trans.*

3.1.2.2 Glycerolipid compositional changes in *Arabidopsis* grown at high and low temperatures

Analysis of individual lipids extracted from *Arabidopsis* leaves revealed distinctive impacts of higher and lower growth temperatures on the relative proportion of glycerolipid species. At 10℃, there was a significant increase in MGDG while an increase in DGDG at high temperature (30℃) was evident (Table 3.4). Increases in MGDG at low temperatures and DGDG at high temperatures have been observed in *B. napus* (Johnson and Williams, 1989) and *Arabidopsis* (Chen et al., 2006), respectively, but controlled comparisons between the effects of both high and low temperatures have not been reported. The major phospholipids, PC and PE, decreased in mol% irrespective of high or low temperature conditions. Therefore, in *Arabidopsis* the proportion of galactolipids was increased, whereas the level of phospholipids was reduced under both low and high temperature.

3.1.2.3 Fatty acid compositional changes of glycerolipid species in response to high and low temperatures

Fatty acyl composition of individual lipids was analyzed (Table 3.4). The most notable change was an increase in the 18:3 to 18:2 ratios at 10℃ in most glycerolipid species. Conversely, the 18:3/18:2 ratios decreased at 30℃. Calculation of DBI for each lipid species showed a uniform trend of changes with an increase at 10℃ and a decrease at 30℃ in each lipid species (Figure 3.2).

In higher plants, the predominant fatty acids have chain lengths of 16 or 18 carbons. As previously demonstrated, MGDG is a mixture of eukaryotic type (C18/C18) and prokaryotic type (C18/C16) molecules (Ohlrogge and Browse, 1995). Thus, the ratio of C16/C18 in glycerolipids would roughly reflect the contribution of two pathways to the production of MGDG. The C16/C18 ratios were calculated for each glycerolipid species (Table 3.4). DGDG and SQDG showed a lower C16/C18 ratio at 10℃ and a higher ratio at 30℃ when compared to 22℃. MGDG, on the other hand, showed the opposite response, with an increased C16/C18 ratio at 10℃ and decreased C16/C18 ratio at 30℃.

Table 3.4 Glycerolipid composition in leaves of *Arabidopsis* plants grown at 10, 22 and 30℃.

Value represents average of five independent samples. Statistically significant differences (two-tailed student t-test; *, $p < 0.05$) were calculated by comparisons between temperature treatments (10 and 30℃) and standard growth condition (22℃), respectively. C16 represents the sum of 16: 0, 16: l, 16:2 and 16:3; C18 represents the sum of 18:0, 18:1, 18:2 and 18:3.
[a] represents sum of 16:1 *cis* and *trans* in MGDG and DGDG.

Glycerolipids		Total Polar Lipids (%)	Fatty acid composition (mol%)								C16/C18
			16:0	16:1[a]	16:2	16:3	18:0	18:1	18:2	18:3	
DGDG											
	10℃	15.9 ± 0.15	10.7 ± 0.71*	0.3 ± 0.12	0.6 ± 0.02*	3.1 ± 0.07*	0.5 ± 0.07*	0.9 ± 0.24*	3.6 ± 0.13*	80.3 ± 0.81*	0.17 ± 0.01*
	22℃	16.0 ± 0.32	12.6 ± 0.31	0.4 ± 0.14	0.6 ± 0.01	2.8 ± 0.02	0.8 ± 0.03	1.3 ± 0.34	6.3 ± 0.27	75.3 ± 0.31	0.20 ± 0.00
	30℃	17.9 ± 0.39*	17.9 ± 0.10*	0.8 ± 0.23	0.7 ± 0.04	1.7 ± 0.08*	1.5 ± 0.12*	2.1 ± 0.27*	9.9 ± 0.26*	65.6 ± 0.35*	0.27 ± 0.00*
MGDG											
	10℃	41.1 ± 0.49*	0.8 ± 0.09*	0.4 ± 0.06*	1.3 ± 0.03*	37.5 ± 0.30*	0.1 ± 0.05	0.4 ± 0.12*	2.0 ± 0.12*	57.4 ± 0.18*	0.67 ± 0.01*
	22℃	38.0 ± 0.83	1.4 ± 0.11	0.8 ± 0.04	1.5 ± 0.02	34.9 ± 0.19	0.1 ± 0.03	0.7 ± 0.14	3.7 ± 0.20	56.9 ± 0.36	0.63 ± 0.01
	30℃	38.7 ± 0.60	2.2 ± 0.17*	1.6 ± 0.04	2.2 ± 0.02*	29.8 ± 0.35*	0.2 ± 0.08*	1.5 ± 0.18*	5.9 ± 0.14*	56.6 ± 0.21	0.56 ± 0.00*
PC											
	10℃	16.6 ± 0.39*	26.1 ± 0.78*				1.5 ± 0.03*	4.7 ± 0.32	30.1 ± 0.23*	37.6 ± 1.04*	0.35 ± 0.01*
	22℃	17.6 ± 0.64	28.5 ± 0.50				2.0 ± 0.03	5.0 ± 0.29	31.0 ± 0.44	33.6 ± 0.75	0.40 ± 0.01
	30℃	16.1 ± 0.30*	28.6 ± 0.19				3.4 ± 0.09*	5.3 ± 0.41*	34.3 ± 0.42*	28.4 ± 0.50*	0.40 ± 0.00
PE											
	10℃	11.4 ± 0.25*	30.2 ± 0.52*				1.0 ± 0.04*	4.1 ± 0.41*	34.9 ± 0.16*	29.8 ± 0.48*	0.43 ± 0.01*
	22℃	12.4 ± 0.18	34.4 ± 0.55				1.8 ± 0.06	2.9 ± 0.37	36.0 ± 0.28	24.9 ± 0.48	0.52 ± 0.01
	30℃	10.6 ± 0.11*	36.5 ± 1.25*				3.3 ± 0.20*	2.8 ± 0.57	38.9 ± 0.60*	18.5 ± 0.66*	0.58 ± 0.03*
PG											
	10℃	10.1 ± 0.49	41.3 ± 0.50*	18.1 ± 0.38*			0.6 ± 0.05*	2.4 ± 0.37*	7.6 ± 0.25*	30.0 ± 0.80*	1.46 ± 0.05*
	22℃	10.1 ± 0.17	32.4 ± 0.71	28.5 ± 0.78			1.0 ± 0.10	5.2 ± 0.74	11.5 ± 0.47	21.4 ± 0.51	1.56 ± 0.04
	30℃	10.3 ± 0.02	29.5 ± 1.50*	33.4 ± 0.91*			1.3 ± 0.12*	9.0 ± 1.00*	14.8 ± 0.90*	11.9 ± 0.83*	1.70 ± 0.13*
PI											
	10℃	3.0 ± 0.17	54.9 ± 1.26				1.7 ± 0.45	2.3 ± 1.47	18.9 ± 0.50*	22.1 ± 1.01	1.22 ± 0.06
	22℃	3.5 ± 0.24	54.4 ± 1.10				1.9 ± 0.11	2.4 ± 0.71	20.3 ± 0.10	21.1 ± 0.45	1.19 ± 0.05
	30℃	3.5 ± 0.12	55.0 ± 0.70				2.7 ± 0.20*	2.1 ± 0.81	23.9 ± 1.16*	16.4 ± 0.71*	1.22 ± 0.03
SQDG											
	10℃	2.0 ± 0.20	44.7 ± 1.87				1.2 ± 0.33*	2.5 ± 2.20	3.9 ± 0.42*	47.6 ± 1.99*	0.81 ± 0.06
	22℃	2.3 ± 0.09	46.8 ± 2.71				1.6 ± 0.18	3.0 ± 0.66	9.7 ± 0.68	38.9 ± 1.65	0.88 ± 0.10
	30℃	2.8 ± 0.13	49.8 ± 2.83				2.6 ± 0.29*	4.6 ± 2.50*	16.6 ± 1.08*	26.5 ± 1.47*	1.00 ± 0.12

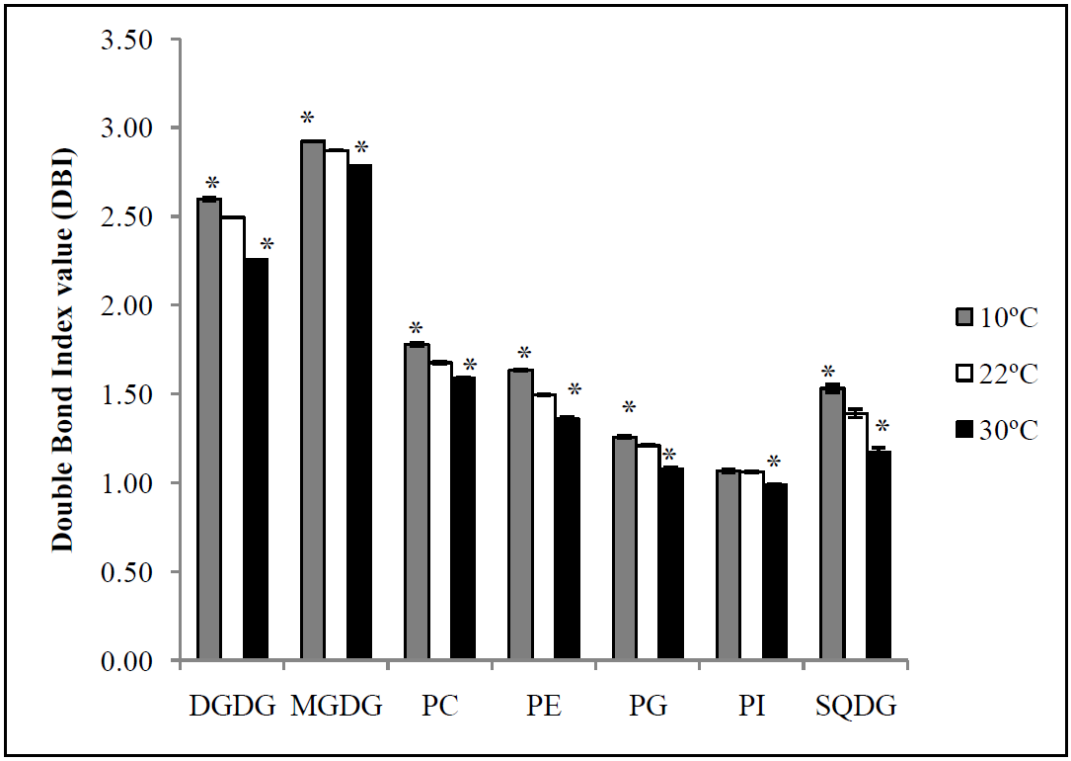

Figure 3.2 Double bond index (DBI) values in individual lipid species of *Arabidopsis* grown at 10, 22 and 30℃.

DBI values were calculated as described in Materials and Methods. Values are mean ± SD from three biological replicates. *, p value < 0.05 (two-tailed student t-test)

3.1.3 Rebalancing of the glycerolipid pathways by a distinct lipid flux at high and low temperatures in *Arabidopsis*

In *Arabidopsis*, both MGDG and DGDG are composed of C18/C16 (prokaryotic) and C18/C18 (eukaryotic) molecular species. The contrasting pattern of C16/C18 ratio displayed by MGDG and DGDG under different temperatures provided the impetus to quantify the relative contributions of the eukaryotic pathway and prokaryotic pathway (Browse et al., 1986). Purified lipids were digested with *Rhizopus sp.* lipase to remove fatty acyl groups at the *sn-1* position and fatty acid compositions of *lyso*-derivatives were determined (Figure 3.3). A previously detailed analysis of wild-type *Arabidopsis* showed that for every 1000 fatty acid molecules produced in the chloroplast, 615 enter the eukaryotic pathway (Miquel et al., 1998). A similar analysis with temperature-treated plants was conducted to gain an overall view of the flux of glycerolipids at 10, 22 and 30℃ (Table 3.5). This revealed a higher flux through the prokaryotic pathway at 10℃. At 30℃, the increased DGDG could be mostly accounted for by increased flux to the eukaryotic pathway. The total lipid flux from ER to chloroplast was reduced at 10℃ (229 mol/1000 mol) and increased at 30℃ (276 mol/1000 mol) when compared to plants grown at 22℃ (242 mol/1000 mol) (Table 3.5). Hence, fatty acid flux sharing between the two pathways was altered both at 10 and 30℃. High temperature enhanced the eukaryotic pathway contribution to DGDG synthesis in the chloroplast, while low temperature enhanced the prokaryotic pathway primarily contributing to more MGDG.

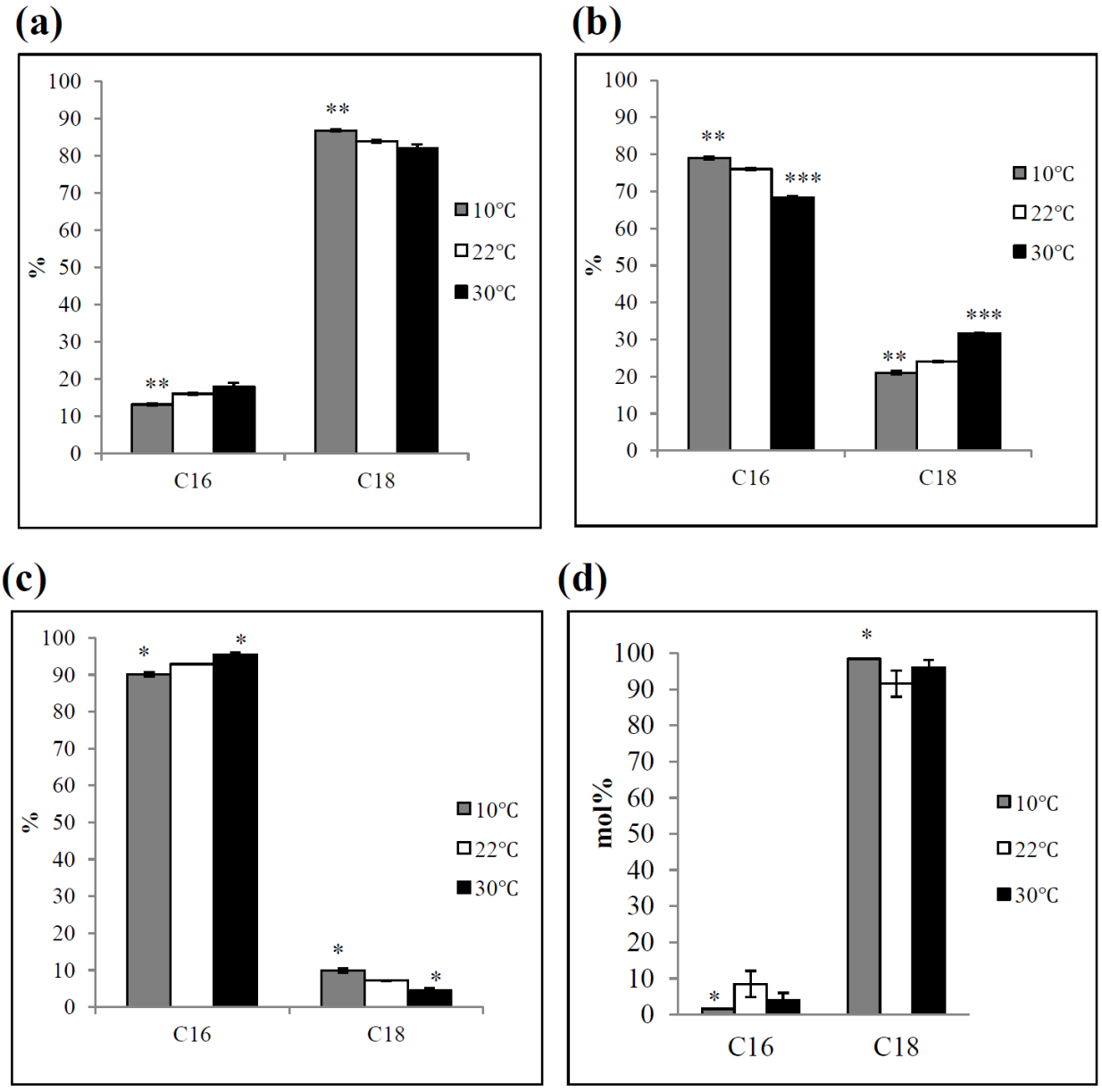

Figure 3.3 Lipid class analysis of glycerolipids originating from both the eukaryotic and prokaryotic pathways.

The *lyso*-lipids (represent the *sn-2* position of the parent lipid) were purified by TLC and derivatized using 3 N methanolic HCl, and analyzed by gas chromatography. C16 represents the sum of 16: l, 16:2 and 16:3; C18 represents the sum of 18:0, 18:1, 18:2 and 18:3. **(a)** DGDG; **(b)** MGDG; **(c)** PG; **(d)** PC. Values are means ± SD (n = 3). Statistically significant differences were calculated between temperature treatments (10℃ and 30℃) and standard growth condition (22℃), respectively. Two-tailed student t-test; *, $p < 0.05$; **, $p < 0.01$; ***, $p < 0.001$.

Table 3.5 Mass composition and flux of leaf lipids from *Arabidopsis* plants grown at 10, 22 and 30℃.

Data were calculated based on the results of Table 3.4 and Figure 3.3 according to methods of Browse *et al.*, (1986) and Shen et al., (2010). C16 represents the sum of 16:0, 16:l, 16:2 and 16:3; C18 represents the sum of 18:0, 18:1, 18:2 and 18:3.

	Mass of fatty acid (mol/1000mol)[a]	*sn*-2 position (%)[b]		Flux to prokaryotic pathway (mol/1000 mol fatty acid)	Flux to eukaryotic pathway(mol/1000 mol fatty acid)
		C16	C18		
MGDG					
10℃	411	79	21	324	86
22℃	380	76	24	289	91
30℃	387	68	32	265	122
DGDG					
10℃	159	13	87	21	138
22℃	160	16	84	26	134
30℃	179	18	82	32	147
PC					
10℃	166	2	98	3	163
22℃	176	8	92	15	162
30℃	161	4	96	6	155
PG					
10℃	101	90	10	91	10
22℃	101	93	7	94	7
30℃	103	95	5	98	5
PE					
10℃	114	0	100	0	114
22℃	124	0	100	0	124
30℃	106	0	100	0	106
PI					
10℃	30	0	100	0	30
22℃	35	0	100	0	35
30℃	35	0	100	0	35
SQDG					
10℃	20	100	0	0	20
22℃	23	100	0	0	23
30℃	28	100	0	0	28
Total					
10℃				439	561
22℃				423	577
30℃				402	598

[a] An original input of 1000 mol of fatty acids synthesized in the chloroplast as acyl-ACP species.
[b] Each lipid species was divided between the prokaryotic and eukaryotic pathway on the basis of content of C16 at the *sn*-2 position.

3.1.4 Gene basis of glycerolipid pathway adjustments under different temperatures

To gain insight into metabolic readjustments at the gene expression level, I selected 24 genes encoding enzymes of the glycerolipid pathways (Shen et al., 2010) for analyses by real-time qRT-PCR. The genes were categorized into three major groups according to the subcellular localization and biological function of their protein product, nine of which were from the eukaryotic pathway, four were localized in the chloroplast envelope, and 11 were involved in the prokaryotic pathway (Figure 3.4).

A decreased level of the *FATTY ACID DESATURASE 2* (*FAD2*) (2.3 fold) was detected at 10℃, the most significantly perturbed gene in the eukaryotic pathway (Figure 3.4). In the prokaryotic pathway, the expression of *ACT1*, the first enzyme of the prokaryotic pathway, showed a significant increase (1.6 fold) at 10℃. Several genes involved in MGDG synthesis were induced, among which *MONOGALACTOSYL DIACYLGLYCEROL SYNTHASE 1* (*MGD1*, 1.6 fold), *FATTY ACID DESATURASE 5* (*FAD5*, 4.6 fold) and *FATTY ACID DESATURASE 8* (*FAD8*, 1.8 folds) were the most significantly increased. The two digalactosyldiacylglycerol synthase genes, *DGD1* and *DGD2*, responded contrastingly at 10℃, with a increase for *DGD1* and a decrease for *DGD2*.

High temperature presented different pathway dynamics. Several genes of the eukaryotic pathway were induced. These included enzymes involved in PC synthesis, such as *AMINOALCOHOLPHOSPHOTRANSFERASE* gene *AAPT1* (1.7 fold, p value = 0.08), *PHOSPHORYLETHANOLAMINE CYTIDYLYLTRANSFERASE* gene *PECT1* (1.3 fold, p value = 0.07) and *FAD2* (1.8 fold). *PHOSPHATIDYLINOSITOL SYNTHASE 1*, *ATPIS1*, which utilizes DAG originating from the eukaryotic pathway, also showed a 1.6 fold increase. In the chloroplast, *LYSOPHOSPHATIDIC ACID ACYLTRANSFERASE* (*ATS2*) showed a 1.7 fold increase. Transcript level of *DGD1* and *DGD2* were significantly increased 2.3 fold and 1.2 fold respectively. Expression of the two SQDG synthases, *SQD1* and *SQD2*, were both induced at 30℃.

Conventional wisdom on the control of desaturase expression would suggest an induction at low temperatures and repression at high temperatures. *FAD5*, the protein of which utilizes

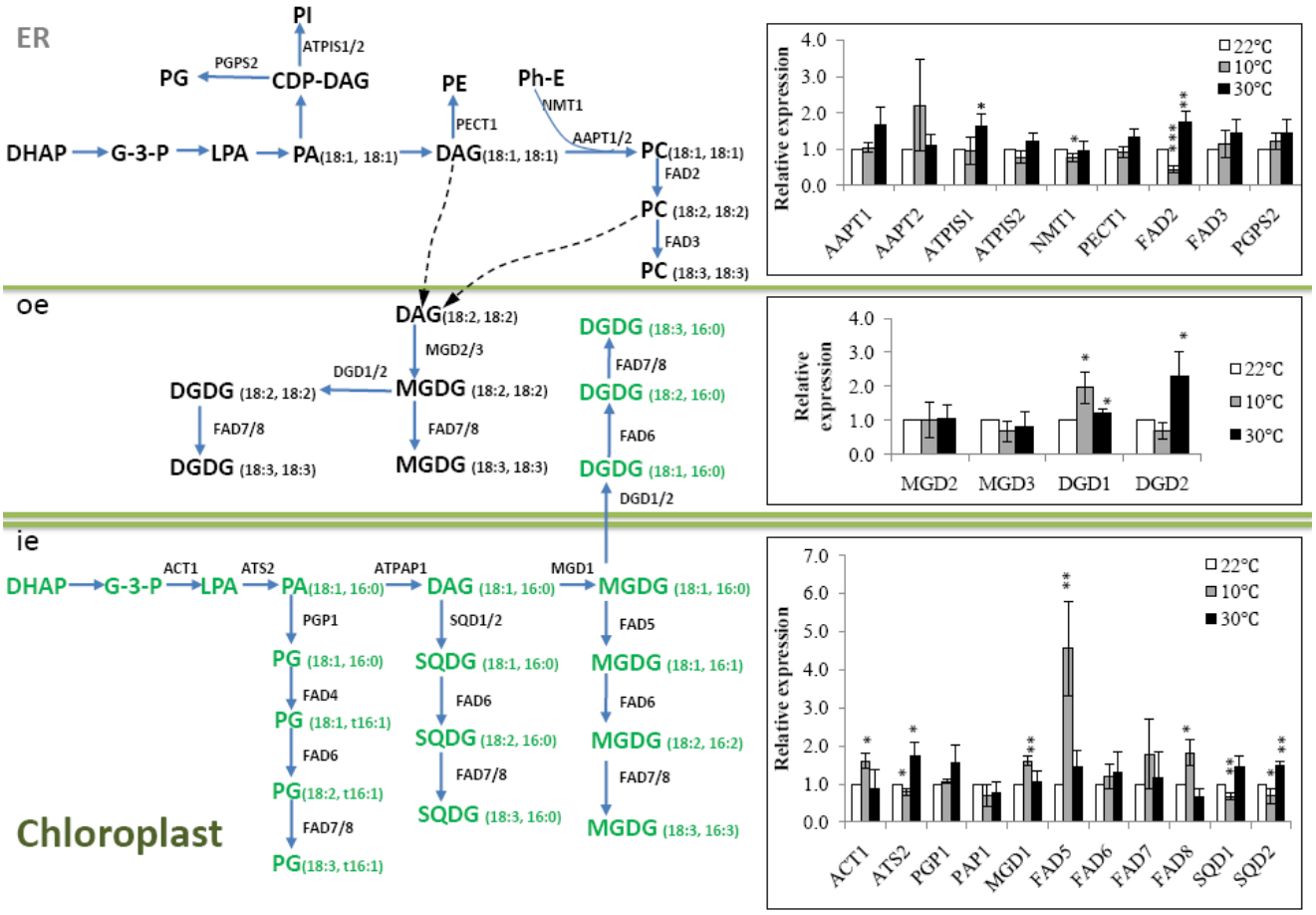

Figure 3.4 Glycerolipid metabolism pathways integrated with qRT-PCR results.

Different lipid species are derived either from the eukaryotic (*sn-1*/*sn-2*, C18/C18 or C16/C18) or prokaryotic pathway (*sn-1*/*sn-2*, C18/C16). Dash lines represent possible channeling between the ER and chloroplast (Benning, 2009). Relative expression levels of all genes were analyzed by real-time qRT-PCR using cDNA from *Arabidopsis* grown at 10 (grey bar), 22 (white bar) and 30 ℃ (black bar) as templates. For comparison, expression values from plants grown at 22℃ were normalized to 1 using StepOne software 2.0 (Applied Biosystems). Relative expression values (means ± SD , n = 3) from low- and high-temperature-treated plants were presented as fold change against plants grown at 22℃. *, p value < 0.05; **, p value < 0.01 (two-tailed student t-test) compared with values for control (plants grown at 22℃). Abbreviations are defined in Figures1.1, 1.3 and Figure 1.4. ie, inner envelope; oe, outer envelope. DHAP, dihydroxyacetone phosphate.

MGDG as substrate exclusively, was considerably up-regulated in plants grown at 10℃. This was also in line with the increased proportion of MGDG through the prokaryotic pathway that was detected at low temperature. Counter intuitively, however, is the expression of *FAD2* that encodes the *ω-6* desaturase responsible for the conversion of 18:1 to 18:2 utilizing PC in the ER. It displayed an opposite pattern to that of *FAD5*, in that it was up-regulated at 30℃ and down-regulated at 10℃. Underscoring the significance of these *FAD2* transcript level changes were the decrease at 10℃ and increase at 30℃ of 18:2 in PC and the total fatty acid composition of leaves (Table 3.3 and Table 3.4).

3.2 Conversion of *A. lentiformis* from a 16:3 to 18:3 plant at high temperature is a result of rebalancing the glycerolipid pathways

Despite a clear definition of 16:3 and 18:3 plants, classification of the two categories relies on a defined threshold of 16:3 (Mongrand et al., 1998). In nature, there are species capable of switching their lipid phenotype from 16:3 to 18:3. *A. lentiformis* is a notable example, a 16:3 plant that exhibits an 18:3 lipid profile when grown at high temperature (Pearcy, 1978). I was interested in how the change in lipid phenotype of *A. lentiformis* is brought about at high temperatures. Both 2D-TLC and lipidomics were utilized to dissect the biochemical changes in glycerolipid pathways. Whole genome transcriptomics were employed to identify the major genes involved in modulation of glycerolipid pathways in *A. lentiformis*.

3.2.1 Glycerolipid changes in *A. lentiformis* grown at high temperatures

Total fatty acid analysis of leaves of *A. lentiformis* confirmed a dramatic decrease in 16:3 fatty acid, which was at 5.5 mol% at 23℃, but only 0.9 mol% at 43℃ (Table 3.6). 16:3 plants are classified as those with more than 2 mol% of 16:3 in total fatty acids or 3 mol% and 1.2 mol% in MGDG and DGDG respectively (Mongrand et al., 1998). Therefore, *A. lentiformis* plants were switched from 16:3 plants to 18:3 plants based on the total fatty acids.

Significant changes in the proportion of individual glycerolipid species were also observed (Table 3.7). The compositions of DGDG, PC and PI increased while the percentage of MGDG and PG decreased at 43℃. The decreased 16:3 fatty acids occurred in both MGDG (from 14.6 mol% at 23℃ to 2.7 mol% at 43℃) and DGDG (2.5 mol% at 23℃ to 0.2 mol% at 43℃) (Table 3.7). At 43℃, the composition of 16:0 in almost all lipids was significantly increased while the proportion of 18:3 was reduced. A simultaneous increase of 18:1 and 18:2 were observed in galactolipids (DGDG and MGDG) and SQDG. Eukaryotic lipids such as PC, PE and PI showed an increase of 18:1 while 18:2 and 18:3 decreased. In PG, the amount of 18:1 also increased but 18:2 were not changed at 43℃.

Table 3.6 Total fatty acid compositions of leaves of *A. lentiformis* grown at 23 or 43℃.

Values represent averages of four independent biological replicates. Statistically significant differences were calculated between 43 and 23℃ (two-tailed student t-test; *, $p < 0.05$). DBI, double bond index. C16 represents the sum of 16: 0, 16: l, 16:2 and 16:3; C18 represents the sum of 18:0, 18:1, 18:2 and 18:3.

	Fatty acid composition (mol%)								C16/C18	DBI
	16:0	16:1[a]	16:2	16:3	18:0	18:1	18:2	18:3		
23℃	16.2 ± 1.9	2.8 ± 1.2	1.1 ± 1.3	5.5 ± 0.5	1.4 ± 0.4	4.2 ± 2.1	12.7 ± 1.4	56.5 ± 3.3	0.34 ± 0.02	2.20 ± 0.08
43℃	21.8 ± 1.2*	2.7 ± 0.6	0.3 ± 0.3	0.9 ± 0.2*	2.4 ± 0.3*	13.1 ± 2.4*	13.2 ± 1.3	45.6 ± 1.9*	0.35 ± 0.02	1.82 ± 0.06*

[a] represents sum of *cis* and *trans*-16:1

Table 3.7 Glycerolipid composition of leaves from *A. lentiformis* grown at 23 or 43℃.

Values are means ± SD (*n* = 3). Statistically significant differences (two-tailed student t-test; *, p value < 0.05) were calculated between 43 and 23℃. C16 represents the sum of 16: 0, 16: l, 16:2 and 16:3; C18 represents the sum of 18:0, 18:1, 18:2 and 18:3.

Glycerolipids		Total Polar Lipids (%)	Fatty acid composition (mol%)								C16/C18
			16:0	16:1[a]	16:2	16:3	18:0	18:1[b]	18:2	18:3	
DGDG											
	23ºC	21.7 ± 0.42	13.9±1.18	0.4±0.05	0.1±0	2.5±0.07	1.4±0.06	2.5±0.12	4.8±0.14	74.4±1.16	0.20 ± 0.02
	43ºC	26.0 ± 0.13*	26.8±0.5*	0.5±0.01	0.1±0	0.2±0*	4.2±0.04*	8.6±0.27*	13.7±0.16*	45.8±0.39*	0.38 ± 0.01*
MGDG											
	23ºC	41.9 ± 0.31	1.5±0.21	0.4±0.02	0.6±0	14.6±0.25	0.2±0.03	1.7±0.24	2.3±0.3	78.6±0.46	0.21 ± 0.00
	43ºC	35.9 ± 0.62*	7.6±0.21*	0.7±0.02*	0.8±0*	2.7±0.01*	0.8±0.01*	5.5±0.16*	10.9±0.06*	71±0.42*	0.13 ± 0.00*
PC											
	23ºC	14.8 ± 0.80	26.1±1.83				2.5±0.64	17.8±0.49	28.3±1.12	24.5±1.46	0.37 ± 0.03
	43ºC	16.4 ± 0.51*	30.6±0.62*				2.6±0.05	37.8±0.76*	13.6±0.26*	14.5±0.58*	0.46 ± 0.02*
PE											
	23ºC	6.8 ± 0.25	23.9±0.45				1.8±0.29	9.7±0.66	42.7±0.55	21.5±0.19	0.32 ± 0.01
	43ºC	6.8 ± 0.23	31.5±0.54*				2.6±0.3*	20.9±0.35*	25.3±0.35*	19.2±0.2*	0.47 ± 0.01*
PG											
	23ºC	8.9 ± 0.22	35.5±0.26	23.6±0.4			1.1±0.16	4±0.15	13.4±0.39	22.2±0.42	1.45 ± 0.03
	43ºC	7.0 ± 0.19*	45±0.48*	23.4±0.22			2.3±0.04*	10.2±0.16*	13.2±0.27	5.8±0.28*	2.17 ± 0.07*
PI											
	23ºC	2.4 ± 0.06	46.8±1.91				3.7±0.8	8.1±0.22	23.1±1.57	18.4±1.01	0.88 ± 0.07
	43ºC	4.1 ± 0.28*	47.5±0.75				3.4±0.26	14.7±0.14*	17.3±0.11*	17.1±0.47	0.90 ± 0.03
SQDG											
	23ºC	3.6 ± 0.83	48.5±0.78				1.8±0.18	2.8±0.31	11.8±0.16	35.1±1.13	0.94 ± 0.03
	43ºC	3.7 ± 0.57	54.1±5.48				3.4±0.09*	10.6±1.27*	14.4±2.11	17.4±2.05*	1.20 ± 0.25

[a] represents sum of 16:1 *cis* and *trans* in MGDG and DGDG
[b] represent sum of 18:1 *cis* and *trans* fatty acids.

3.2.2 Fatty acid flux sharing between glycerolipid pathways was rebalanced in *A. lentiformis* grown at high temperature

Since DGDG, MGDG and PG can be synthesized by both pathways, I performed stereospecific fatty acid composition analysis at the *sn-2* position of these lipids. There was a significant decrease in the proportion of C16 lipids in DGDG (Figure 3.5a) and MGDG (Figure 3.5b) at 43℃, thereby confirming that the synthesis of MGDG and DGDG through the prokaryotic pathway in the chloroplast was suppressed. The proportion of C16 and C18 lipid moieties at the *sn-2* position of PG (Figure 3.5c) was not significantly changed compared to plants grown at 23℃. As expected, the majority (more than 96%) of the fatty acyl moieties at the *sn-2* position in PC were identified as C18 fatty acids (Figure 3.5d). The proportion of 18:1 at the *sn-2* position of PC was substantially increased while 18:2 and 18:3 were decreased at 43℃ relative to plants grown at 23℃.

I compared the relative contributions of the two glycerolipid pathways in *A. lentiformis* grown at 23 or 43℃ using data in Table 3.7 and Figure 3.5. As shown in Table 3.8, at 43℃, the contribution from the prokaryotic pathway was clearly reduced while that of the eukaryotic pathway was enhanced. Significant reduction in fatty acid flux was observed in prokaryotic MGDG and PG while the synthesis of DGDG and PI via the eukaryotic pathway was increased. These results are consistent with an enhanced lipid flux from ER to chloroplast at high temperature in *Arabidopsis*. Reduction in the amount of 16:3 in *A. lentiformis* plants grown at 43℃ was the direct consequence of the repression of the prokaryotic pathway. The conversion of *A. lentiformis* from 16:3 plants to 18:3 plants under high temperature is hence a consequence of a rebalancing of the glycerolipid pathways.

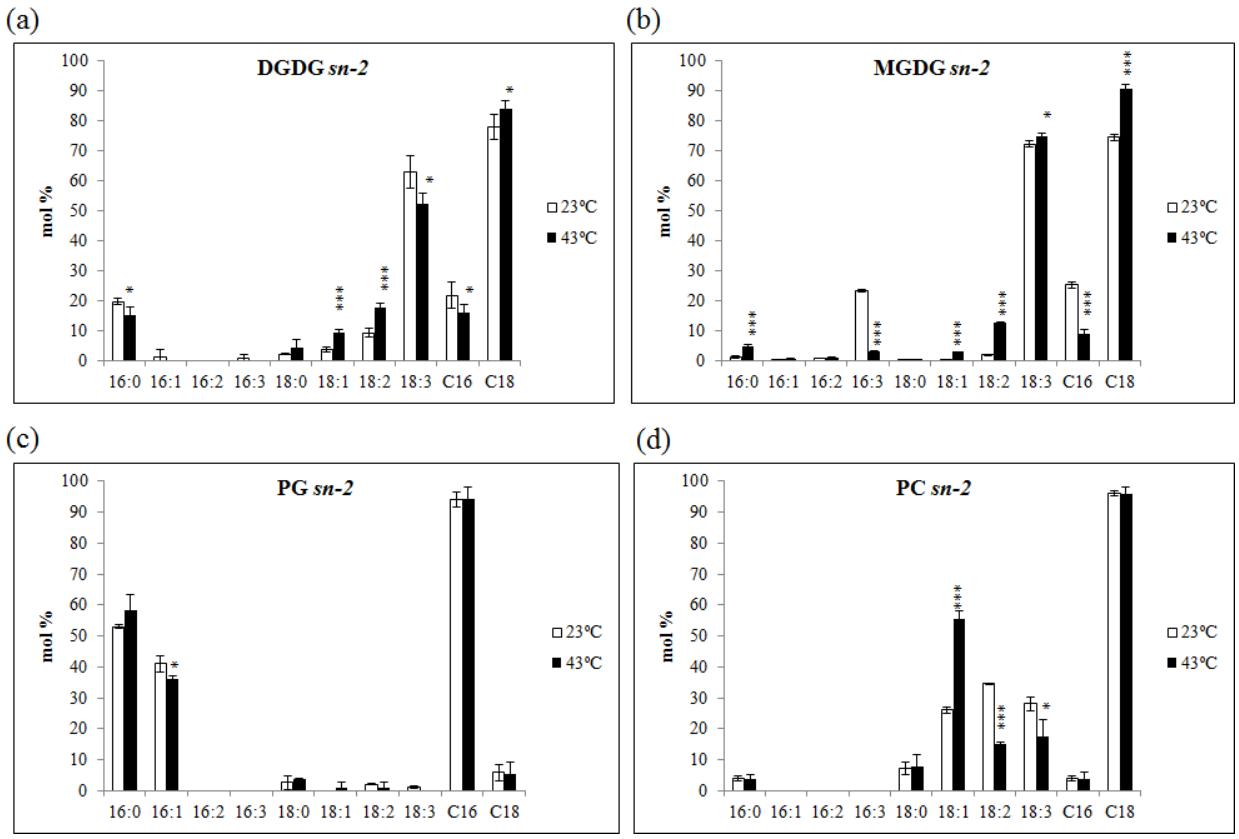

Figure 3.5 Lipid class analysis in leaves from *A. lentiformis* plants grown at 23 or 43°C.

Individual lipids were purified by two dimensional TLC (2D-TLC) on silica gel 60, eluted from the gel, and incubated with *Rhizopus* lipase as described in "Materials and Methods." C16 represents the sum of 16:l, 16:2 and 16:3; C18 represents the sum of 18:0, 18:1, 18:2 and 18:3. **(a)** DGDG; **(b),** MGDG; **(c),** PG; **(d),** PC. Values are means ± SD (n = 3). Two-tailed student t-test; *, $p < 0.05$; **, $p < 0.01$; ***, $p < 0.001$.

Table 3.8 Mass composition and flux of leaf lipids from *A. lentiformis* plants grown at 23 or 43℃.

The data were calculated based on the results of Table 3.7 and Figure 3.5 according to Browse *et al.*, (1986) and Shen et al., (2010). C16 represents the sum of 16: 0, 16: l, 16:2 and 16:3; C18 represents the sum of 18:0, 18:1, 18:2 and 18:3.

	Mass of fatty acid (mol/1000 mol)[a]	*sn*-2 position (%)[b]		Flux to prokaryotic pathway (mol/1000 mol fatty acid)	Flux to eukaryotic pathway (mol/1000 mol fatty acid)
		C16	C18		
MGDG					
23℃	419	25.4	74.7	107	313
43℃	359	9.1	90.9	33	326
DGDG					
23℃	217	21.8	78.0	47	169
43℃	260	16.0	84.0	42	218
PC					
23℃	148	3.9	96.1	6	142
43℃	164	3.8	96.2	6	158
PE					
23℃	68	0	100	0	68
43℃	68	0	100	0	68
PG					
23℃	89	94.1	5.9	84	5
43℃	70	94.4	5.6	66	4
PI					
23℃	24	0	100	0	24
43℃	41	0	100	0	41
SQDG					
23℃	36	100	0	36	0
43℃	37	100	0	37	0
Total					
23℃				279	722
43℃				184	815

[a] An original input of 1000 mole of fatty acids synthesized in the chloroplast as acyl-ACP species.

[b] Each lipid species was divided between the prokaryotic and eukaryotic pathway on the basis of C16 content at the *sn*-2 position.

3.2.3 *A. lentiformis* lipidomics analysis

Comparative analysis of individual lipid species within subsets of glycerolipids should shed new light on the alternations of the glycerolipid pathways. To this end, a lipidomic survey of lipid molecular species in *A. lentiformis* grown at 23 or 43℃ was conducted. Lipidomics is a targeted metabolomics approach which provides a comprehensive analysis of lipid species within a cell or tissue. The analysis based on electronspray tandem mass spectrometry (ESI-MS/MS) is capable of providing quantitative data of lipid molecular species to the level of head group, carbon chain length and double bonds of the acyl groups (Welti et al., 2002). Composition of each lipid species at 43℃ was similar in trend to 2D-TLC data where there was an increase in DGDG and a decrease in MGDG (Figure 3.6a). The proportions of PC and PI were increased. Analysis of fatty acyl moieties of individual lipids revealed that levels of DGDG (34:6) and MGDG (34:6) containing DAG moieties of 34:6 were significantly reduced. These 34:6 moieties should only have a fatty acid composition of the 18:3(*sn-1*)/16:3(*sn-2*) and should originate from the prokaryotic pathway (Figure 1.4, Figure 3.6b and 3.6c). Together with the aforementioned lipid class analysis, and in line with the pathway adjustment observed in *Arabidopsis* that high temperature represses the prokaryotic pathway, these results further confirmed that the prokaryotic pathway was repressed at 43℃.

It is interesting to note that *Arabidopsis* phospholipids have been shown to contain barely detectable level of 34:1 lipid molecular species (Shen et al., 2010), while *A. lentiformis* plants grown at 23℃ had 34:1 levels of 12 mol% in PC. The proportion of C34:1 lipid species was further increased in *A. lentiformis* grown at 43℃, reaching 33 mol% in PC (Figure 3.6d). The increase of the monounsaturated lipid (34:1) with the decrease of polyunsaturated fatty acids, might be beneficial for plants grown at high temperatures.

(a)

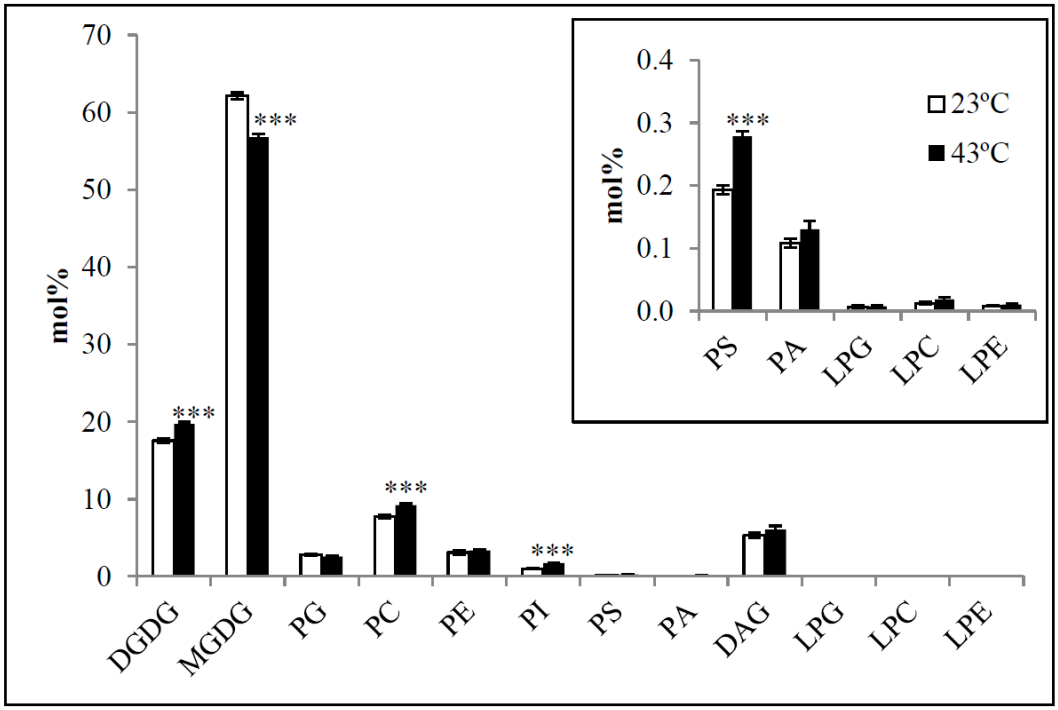
mol%
70
60
50
40
30
20
10
0
***
DGDG
MGDG
PG
PC
PE
PI
PS
PA
DAG
LPG
LPC
LPE
0.4
0.3
0.2
0.1
0.0
23ºC
43ºC
PS
PA
LPG
LPC
LPE

(b)

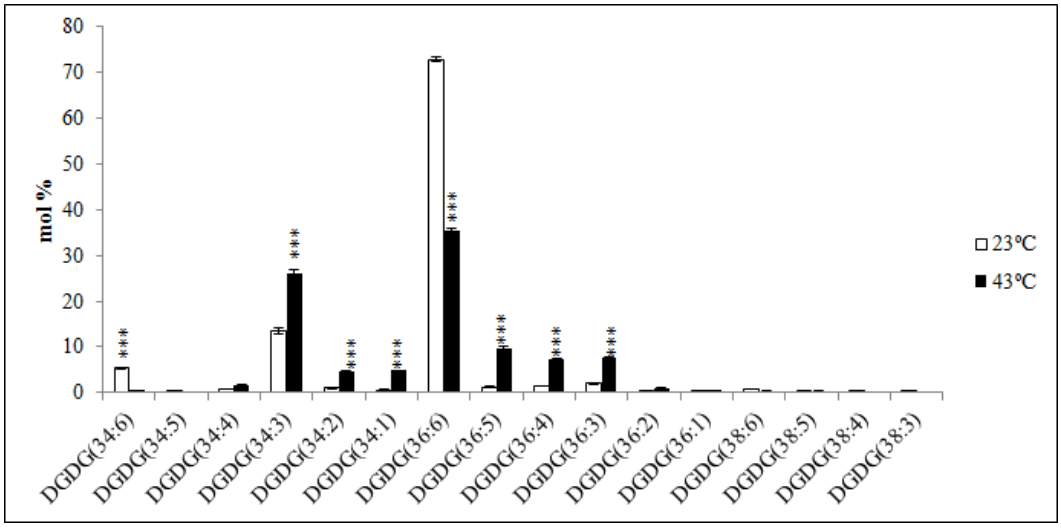
mol %
80
70
60
50
40
30
20
10
0
23ºC
43ºC
DGDG(34:6)
DGDG(34:5)
DGDG(34:4)
DGDG(34:3)
DGDG(34:2)
DGDG(34:1)
DGDG(36:6)
DGDG(36:5)
DGDG(36:4)
DGDG(36:3)
DGDG(36:2)
DGDG(36:1)
DGDG(38:6)
DGDG(38:5)
DGDG(38:4)
DGDG(38:3)

(c)

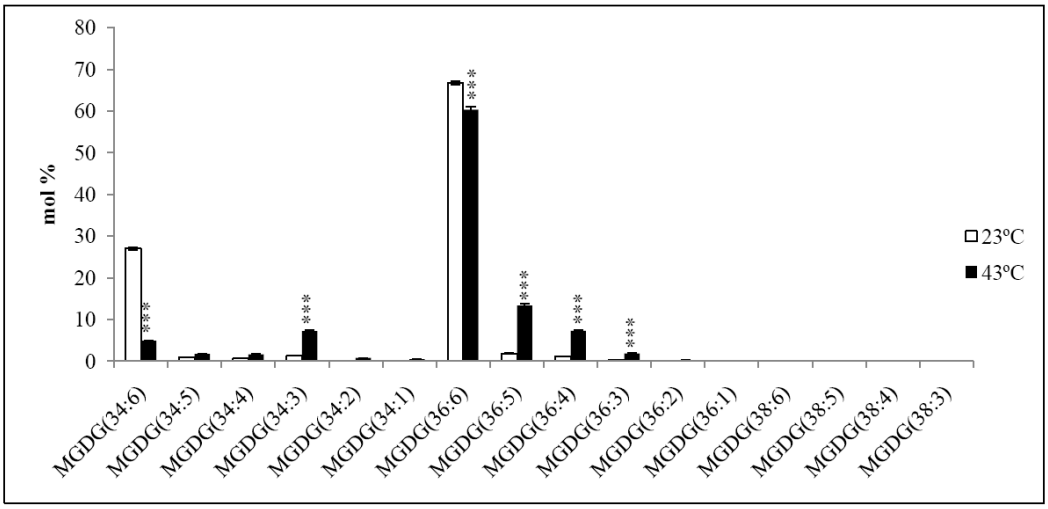

(d)

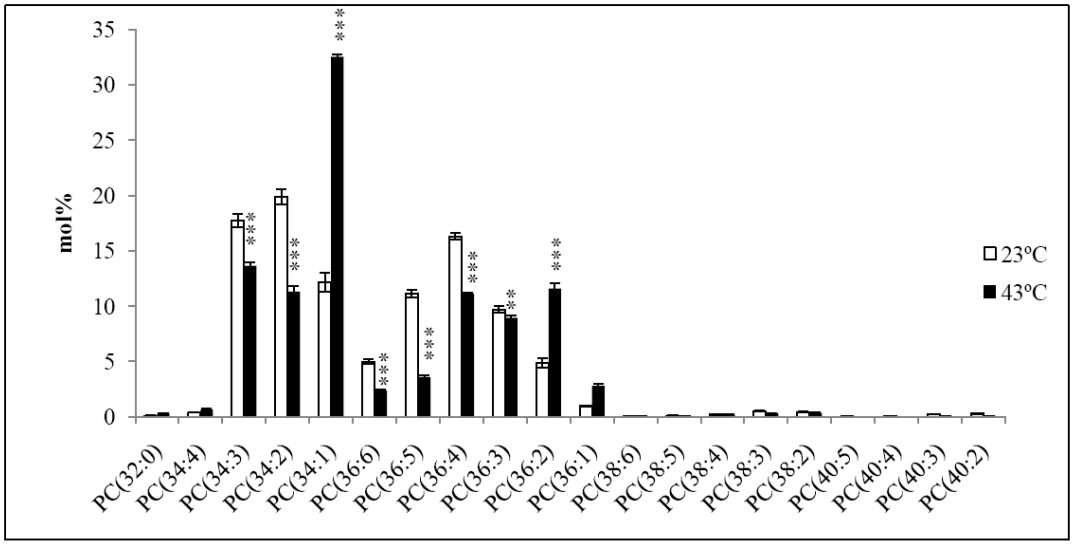

Figure 3.6 ESI-MS/MS analysis of glycerolipid species in leaves of in *A. lentiformis* grown at 23 or 43℃.

ESI-MS/MS analysis was performed at the Kansas Lipidomic Research Center as indicated in "Materials and Methods". **(a)**, relative content (mol %) of different lipid species in leaves of *A. lentiformis* grown at 23 or 43℃. Molecular species of DGDG **(b)**, MGDG **(c)** and PC **(d)** (mol% of lipid molecular species in individual glycerolipids) in leaves of *A. lentiformis* grown at 23 and 43℃; Values are means ± SD (n = 5). Student t-test; *, $p < 0.05$; **, $p < 0.01$; ***, $p < 0.001$.

3.2.4 Differential channeling of DAG moieties from ER to chloroplast

MGDG in *A. lentiformis* had a significant decrease in total C34 lipids (C16/C18 and/or C18/C16) with a corresponding increase in C36 lipids (C18/C18) at 43℃ (Figure 3.7). In fact, the decrease of total C34 lipids in MGDG could be almost entirely accounted for by the reduction of MGDG (34:6). At the same time, a significant increase in C16 containing lipid molecular species (C34 lipids in DGDG, PC, PE and C32 in PG) were detected in most of the other major lipids at 43℃. PG had a higher proportion of C32 lipids (C16 plus C16) and lower C34 lipid species in plants grown at 43℃ (Figure 3.7). Thus, there was increased accumulation of C16 lipid molecules that were mainly derived from the eukaryotic pathway as the prokaryotic pathway was substantially suppressed in plants grown at high temperatures (Section 3.2.2 and 3.2.3).

Along with the accumulation of 34:1 lipid molecules in eukaryotic PC, there were corresponding increases of 34:3 lipid molecular species in both MGDG and DGDG with the DGDG increase being particularly pronounced (Figure 3.6b, c). Since the percentage of C16 fatty acids at the *sn-2* position of DGDG was already known to be reduced at 43℃ (Figure 3.5a), the increased DGDG (C34) lipid molecules were expected to contain a higher proportion of 16:0 moieties at the *sn-1* position. To verify this, fatty acyl moieties at the *sn-1* position were calculated based on the *sn-2* positional analysis and total fatty acid composition. This confirmed that, at 43℃, there was a consistent significantly increased 16:0 distribution at the *sn-1* position of DGDG, MGDG, PC and PG (Figure 3.7). I was prompted to re-examine the distribution of 16:0 at the *sn-1* position in DGDG in *Arabidopsis* based on these observations. It was confirmed that an increase of 16:0 at the *sn-1* position of DGDG at 30℃ and a decrease in 16:0 at the *sn-1* position of DGDG at 10℃, supporting the existence of differential channeling in *Arabidopsis* (Table 3.9). Since PC and DAG are potential precursors for DGDG and MGDG synthesis in the chloroplast, I conclude that the increased DGDG was derived, in large proportion, from the eukaryotic lipids with 16:0 at the *sn-1* position. It also should be noted that the C16/C18 ratio was increased significantly at 30℃ (Table 3.4) indicating an overall reduction of DAG moieties with C18 fatty acids used for DGDG synthesis in the chloroplast. Thus, differential channeling of DAG moieties (C34 and C36) from the ER to the chloroplast provides an additional means of metabolic adjustment during temperature adaptation in plants.

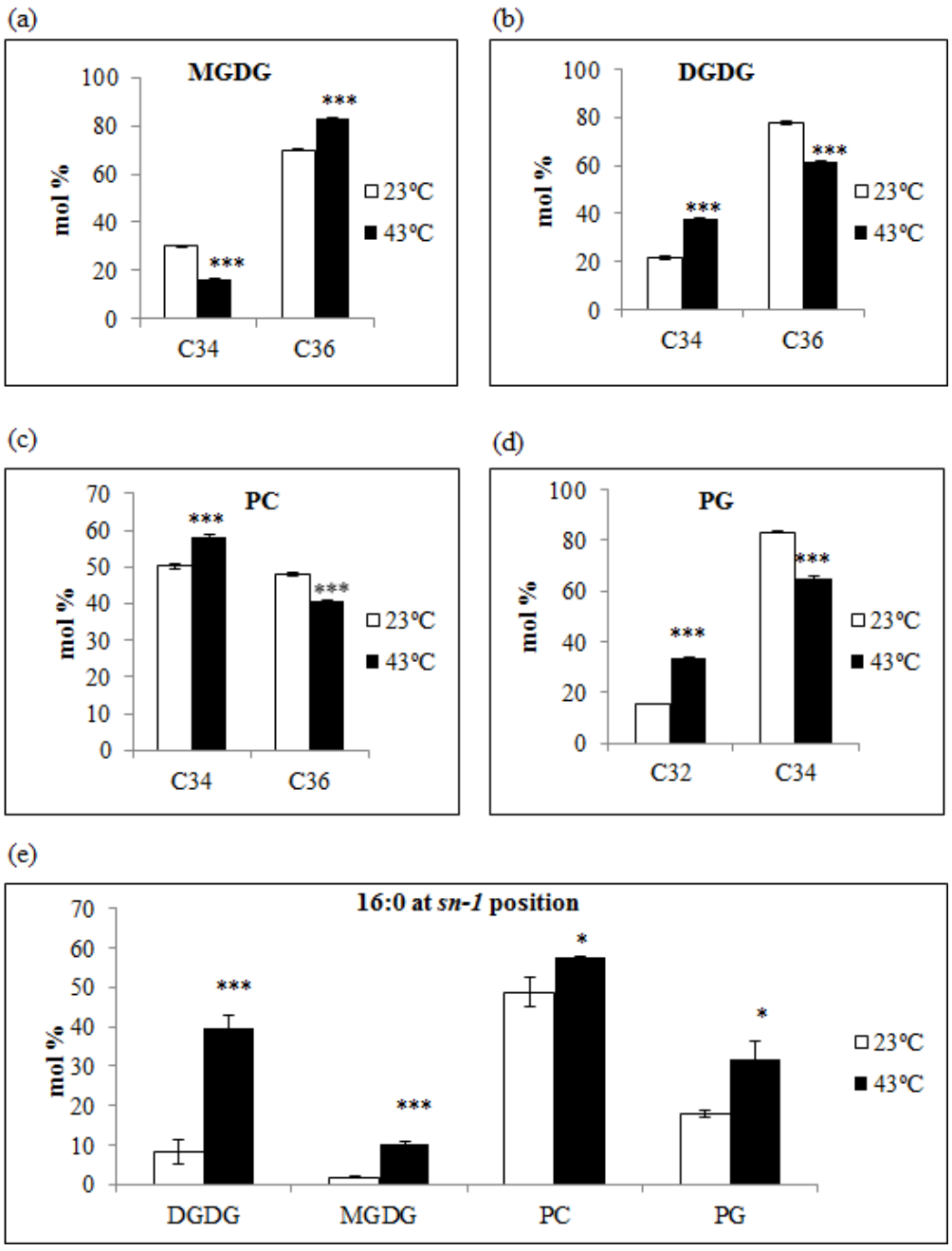

Figure 3.7 Changes in subpools of glycerolipid species in *A. lentiformis* grown at 23 or 43°C.

Subpool size of MGDG **(a)**, DGDG **(b)**, PC **(c)** and PG **(d)** in leaves of *A. lentiformis* grown at 23 or 43°C. **(e)** Percentage of 16:0 at *sn-1* position was calculated based on the *sn-2* positional analysis and original fatty acid composition of individual lipids. C32 represents C16/C16 lipid molecules; C34 represents C16/C18 and C18/C16 lipid molecules; C36 represents C18/C18 lipid molecules. Values are means ± SD (n = 5). Student t-test; *, $p < 0.05$; **, $p < 0.01$; ***, $p < 0.001$.

Table 3.9 Fatty acid composition at the *sn-1* position of DGDG in *Arabidopsis*.

Lipid class analysis of *sn-2* position of DGDG was performed according to "Materials and Methods". Fatty acid composition at *sn-1* was calculated from three replicates based on the formula: [*sn-1* position] = 2 x [parent mol%]-[*sn-2* position]. Values are mean ± SD (n=3). Statistical differences were calculated by comparisons between temperature treatments (10 and 30℃) and standard growth condition (22℃), respectively. *, P value < 0.05 (two-tailed student t-test)

Fatty acid	DGDG *sn-1* position (mol %)		
	10℃	22℃	30℃
16:0	10.7 ± 0.25*	12.2 ± 0.35	20.1 ± 1.75*
16:1	0.4 ± 0.07	0.6 ± 0.33	1.3 ± 0.42
16:2	0.8 ± 0.06	0.7 ± 0.02	0.7 ± 0.15
16:3	3.6 ± 0.14*	3.2 ± 0.08	1.8 ± 0.19*
18:0	0.4 ± 0.11*	1.2 ± 0.07	2.2 ± 1.11
18:1	1.7 ± 0.17	1.6 ± 0.70	2.8 ± 0.44
18:2	4.6 ± 0.25*	6.8 ± 0.36	10.0 ± 0.95*
18:3	78.0 ± 0.28*	73.8 ± 0.66	61.0 ± 2.55*

3.2.5 RNA sequencing of the *A. lentiformis* transcriptome

3.2.5.1 Illumina sequencing and *de novo* assembly

To seek further insight into the factors controlling the shift from a 16:3 to 18:3 lipid profile in *A. lentiformis*, I conducted RNA sequencing (RNA-seq) analysis to assess gene expression in plants grown at 23 and 43℃. Total RNA were extracted from eight week old *A. lentiformis* leaf tissues with four biological replicates for each growth condition, resulting in a total of eight complementary DNA (cDNA) libraries. Pair-end sequencing was performed from a 200 bp insert library, and the length of each sequence read is 101 bp. A total of 170,266,371 reads were generated from the eight libraries. After filtering short reads (less than 100 bp) and repeated sequences, 155,365,454 reads (100 bp in length) were used for further analysis (Table 3.10). Due to the absence of reference genome information for *A. lentiformis*, *de novo* assembly of the filtered Illumina reads using Trinity program was applied to construct transcripts (Grabherr et al., 2011 and Haas et al., 2013). Using paired-end reads, contigs from the same transcript were

connected and extended at both ends to remove redundancy by the CAP3 program (Huang and Madan, 1999). A total of 144, 456 unique sequences with an average length of 1,109 bp were constructed (Figure 3.8).

Table 3.10 Total reads obtained from RNA sequencing

Plant species	Temperature	Library name	Total reads	Quality pass	Repeat mask
A. lentiformis	23℃	23-1	28,661,697	26,917,056	26,765,776
		23-2	15,275,121	14,376,055	14,305,927
		23-3	17,799,234	16,756,851	16,677,289
		23-4	16,374,100	15,394,834	15,322,866
	43℃	43-1	35,511,645	32,514,455	32,101,857
		43-2	16,058,741	14,778,233	14,517,486
		43-3	22,295,284	20,489,021	19,629,344
		43-4	18,290,549	16,755,987	16,044,909

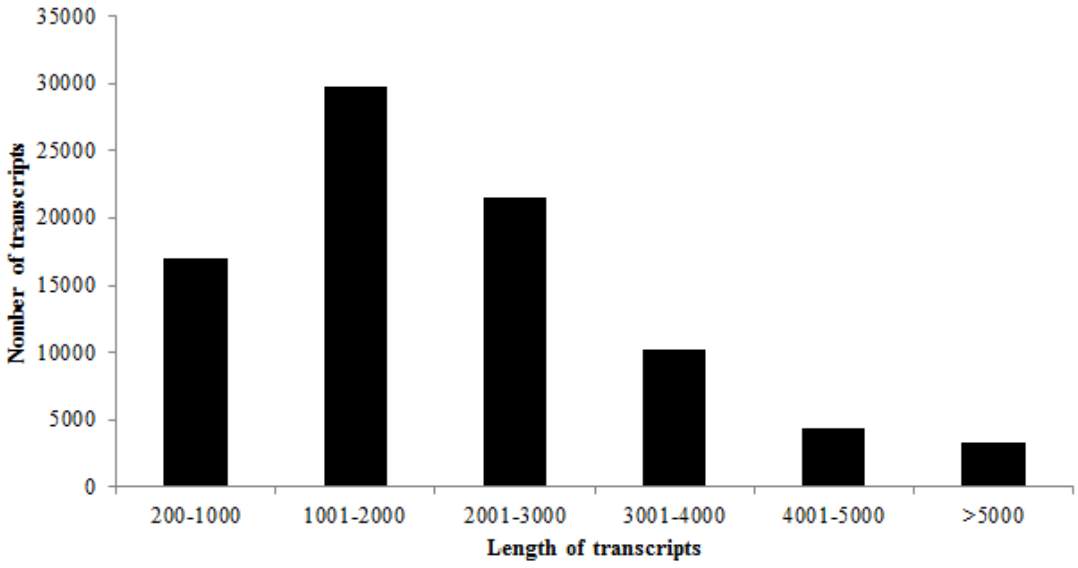

Figure 3.8 Distribution of assembled contigs length generated from RNA-seq.

3.2.5.2 Transcript annotation and differential expression analysis

To assign expression levels to different transcripts, Illumina reads were individually mapped back onto the transcripts using the Trinity program (Grabherr et al., 2011 and Haas et al., 2013). Transcripts with at least 50 reads per transcript across eight samples were defined as expressed to eliminate extremely low expression values. Of the 144,456 transcripts, 46,493 transcripts met the criteria and were used for further analysis. Normalized transcript expression levels were estimated according to the transcript features (length, depth of sequencing and reads) and sample size in units of FPKM (Fragments Per Kilobase of exon per Million fragments) (Gentleman et al., 2004; Robinson et al., 2010). Putative functions of transcripts were assigned using BLASTx searches against the TAIR10 database using a cut-off E-value of 10^{-6}. Of the 46,493 transcripts, 30,203 (65%) were successfully annotated. In some cases, more than one *A. lentiformis* transcript matched the same AGI protein in *Arabidopsis*. These transcripts could be the result of non-overlapping sequence fragments from the same mRNAs or distinct homologous sequences in *A. lentiformis*.

Differentially expressed transcripts between *A. lentiformis* grown at 43 and 23℃ were identified using the edgeR package (Robinson et al., 2010). Of the annotated transcripts, 1,494 were significantly down-regulated and 2,249 were significantly up-regulated based on stringent criteria (fold change cutoff = 4, FDR < 0.01). Gene Ontology (GO) terms were subsequently assigned to differentially expressed transcripts based on their sequence matches to AGI proteins (Figure 3.9). The GO database (http://www.geneontology.org/) is a controlled vocabulary that describes the roles of genes and proteins in all organisms. The ontology covers three domains: cellular component, the parts of a cell or its extracellular environment; molecular function, the elemental activities of a gene product at the molecular level such as binding or catalysis; and the biological process, operations or sets of molecular events. Detailed description of GO terms can be found in TAIR website (ftp://ftp.arabidopsis.org/home/tair/Ontologies/Gene_Ontology). Up-regulated and down-regulated transcripts were assigned to at least one GO term in three categories by using the batch retrieval of GO annotation in TAIR, respectively (http://www.arabidopsis.org/tools/bulk/go/index.jsp). GO cellular component analysis showed that most differentially expressed transcripts were in the nucleus, other cytoplasmic components, intracellular components and chloroplast (Figure 3.9a). A large number of transcripts belonging

(a)

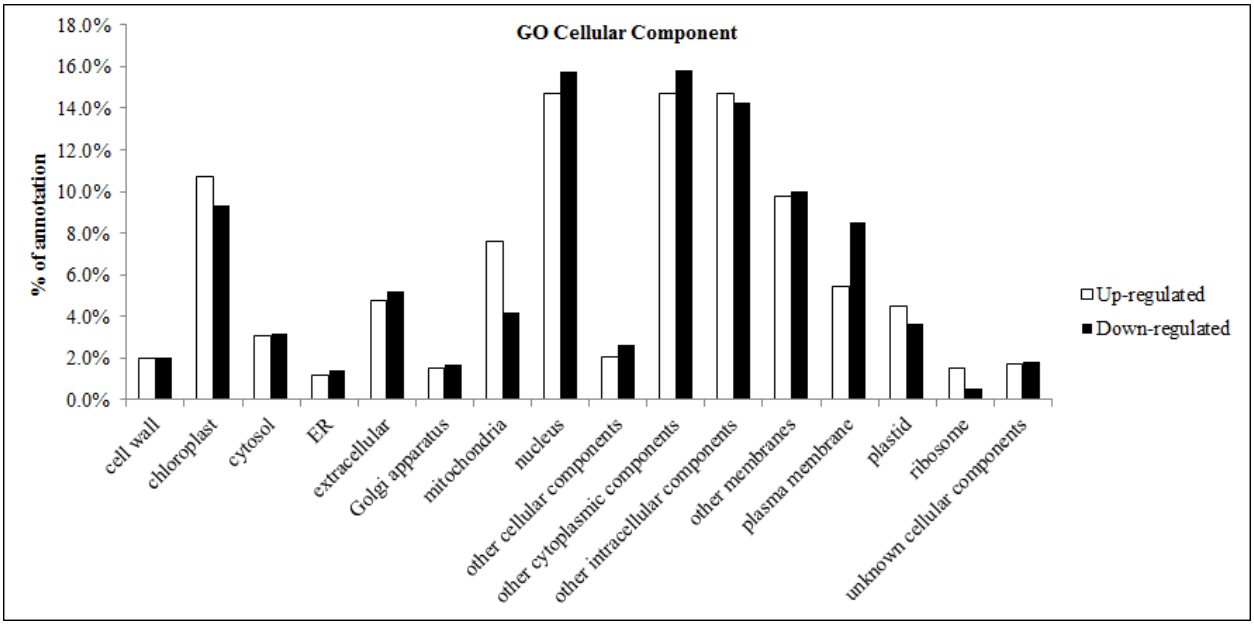
GO Cellular Component
% of annotation
18.0%
16.0%
14.0%
12.0%
10.0%
8.0%
6.0%
4.0%
2.0%
0.0%
cell wall
chloroplast
cytosol
ER
extracellular
Golgi apparatus
mitochondria
nucleus
other cellular components
other cytoplasmic components
other intracellular components
other membranes
plasma membrane
plastid
ribosome
unknown cellular components
Up-regulated
Down-regulated

(b)

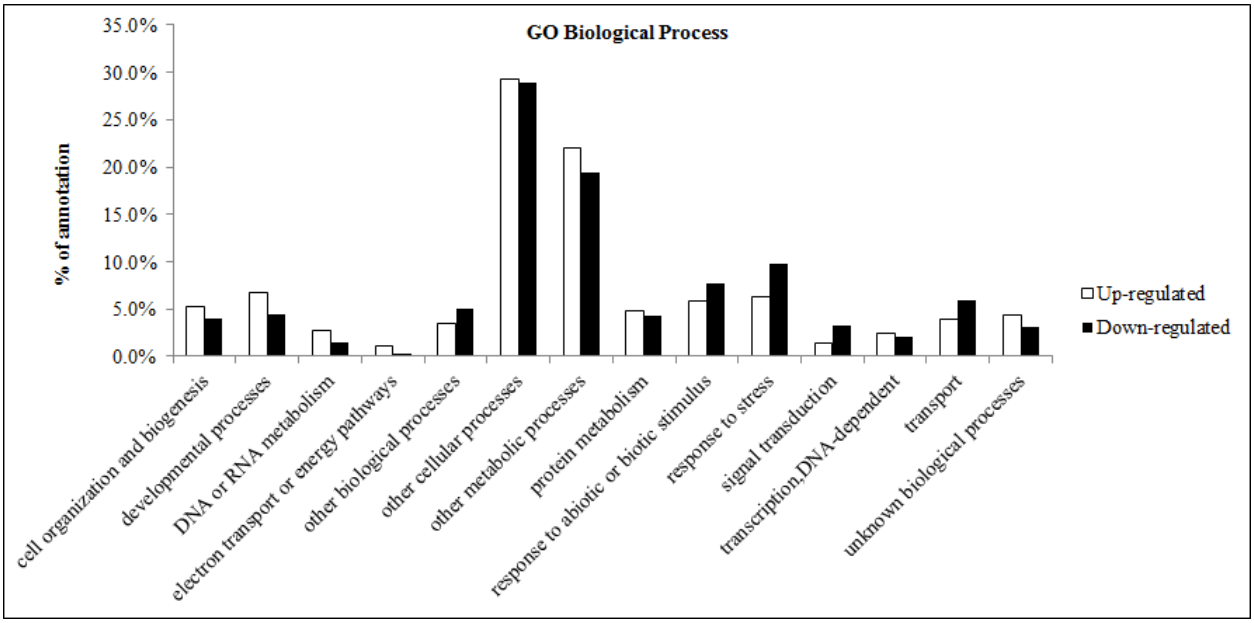
GO Biological Process
% of annotation
35.0%
30.0%
25.0%
20.0%
15.0%
10.0%
5.0%
0.0%
cell organization and biogenesis
developmental processes
DNA or RNA metabolism
electron transport or energy pathways
other biological processes
other cellular processes
other metabolic processes
protein metabolism
response to abiotic or biotic stimulus
response to stress
signal transduction
transcription,DNA-dependent
transport
unknown biological processes
Up-regulated
Down-regulated

(c)

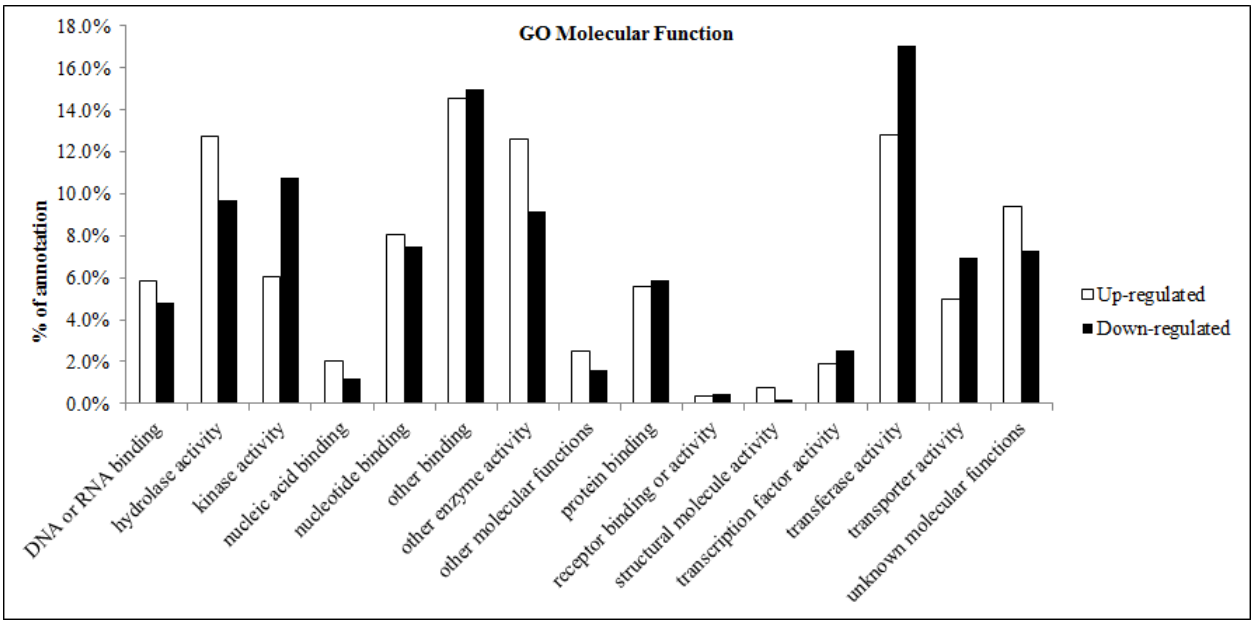

Figure 3.9 GO classification of differentially expressed transcripts.

Bar chart illustrating GO terms (ftp://ftp.arabidopsis.org/home/tair/Ontologies/Gene_Ontology/) assigned to putative peptides from *A. lentiformis* inferred from RNA-seq data. Functional categorization was expressed as percentage of annotations in total annotations in this category. GO terms are categorized by **(a)** cellular component, **(b)** biological process and **(c)** molecular function. Up-regulated and down-regulated represents significantly induced and repressed transcripts, respectively.

to metabolic processes, cellular processes and response to stress were also revealed by GO biological process categorization (Figure 3.9b). The categorization based on GO molecular function uncovered a number of differentially expressed transcripts encoding transfereases and hydrolases (Figure 3.9c). These results suggested *A. lentiformis* plants grown at high temperature were undergoing extensive metabolic activities.

3.2.6 Key genes in lipid pathways are differentially regulated to achieve the lipid phenotype conversion

Expression levels of lipid metabolism genes were compiled according to the Arabidopsis Acyl-Lipid Metabolism database (http://aralip.plantbiology.msu.edu) (Beisson et al., 2003; Li-Beisson et al., 2013). A total of 766 transcripts were identified and categorized based on their biological functions in lipid metabolism. Of the 776 transcripts, 131 were identified as significantly differential expressed transcripts (fold change cutoff > 4; FDR < 0.01) from nine categories (Appendix A). Approximately 50% of them (67 of 133) were identified as lipid signaling and lipid transfer proteins, suggesting active lipid turnover events. As the major constituents of plant barrier to environmental stimuli, temperature effects on wax and cutin production has been observed in numerous plants (Shepherd and Griffiths, 2006). A number of transcripts such as O-acyltransferase (WSD1-like) family proteins related to wax and cutin synthesis were altered in *A. lentiformis* plants grown at high temperature.

To further understand the biosynthetic machinery required for the lipid phenotype conversion, I specifically targeted the transcripts involved in glycerolipid pathways. In the case where more than one *A. lentiformis* transcript hit the same AGI protein in *Arabidopsis*, normalized transcript expression values measured in FPKM were used to allow direct comparisons between transcript levels. The transcript with the highest FPKM value (and presumably highest expression level) was assigned as a representative transcript of the AGI group and mapped to the custom diagram depicting glycerolipid pathways (Appendix B and Figure 3.10). Consistent with lipid compositional analysis, the transcript level of *ACT1* was reduced 3.3 fold in *A. lentiformis* when grown at 43℃. The *FAD5*, which encodes a key enzyme of the prokaryotic pathway, was down-regulated 2.0 fold. Expression of *FAD7* was also reduced

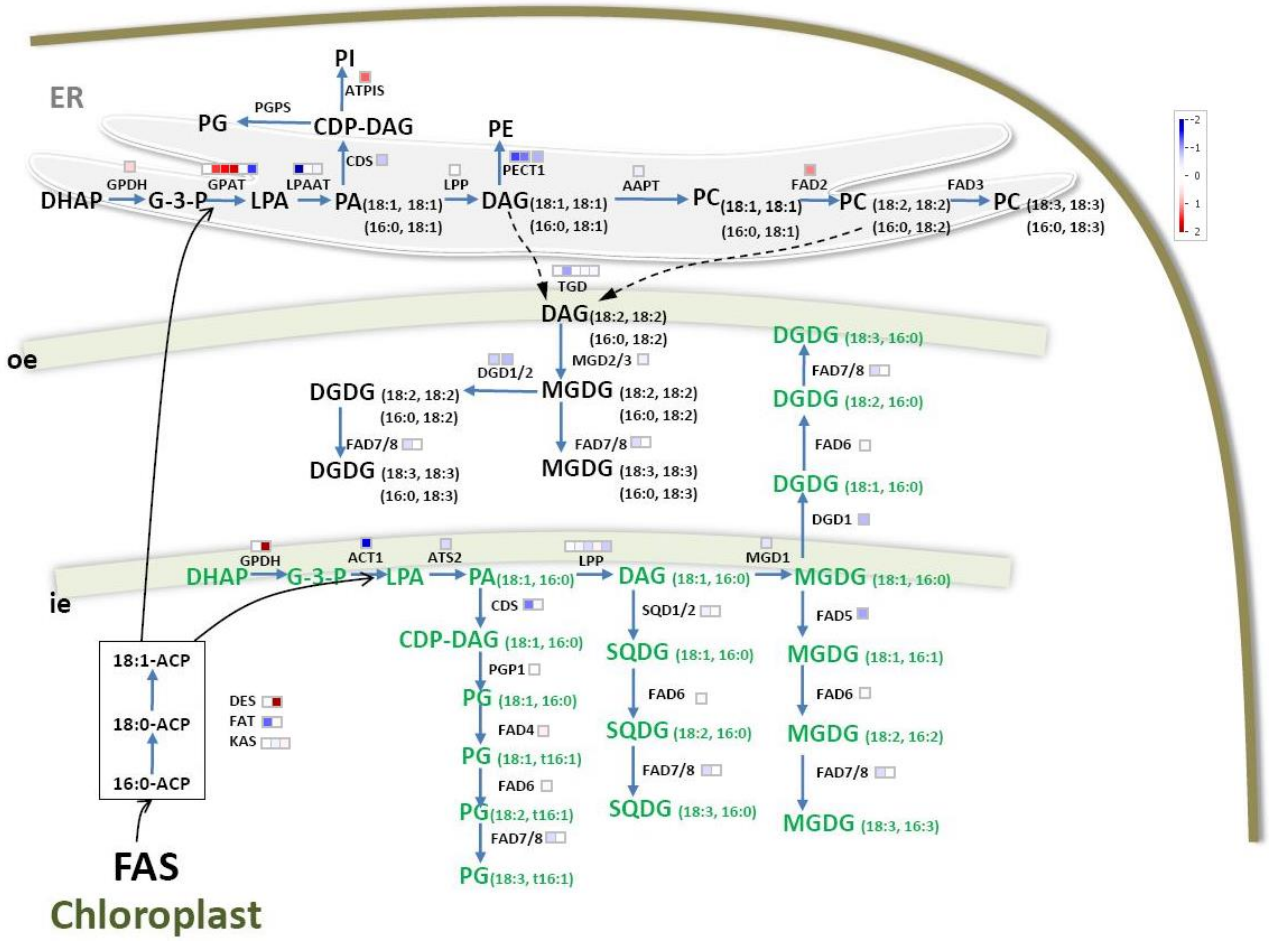

Figure 3.10 Schematic view of glycerolipid biosynthesis pathways integrated with RNA-seq data.

To visualize the relative transcript levels in leaves of *A. lentiformis* plants grown at 23℃ or 43℃, expression data from RNA-seq (Appendix B) were mapped to the customized glycerolipid pathway diagrams using the MapMan program (Thimm et al., 2004). MapMan BINcodes for glycerolipid genes in *A. lentiformis* were manually assigned. The scale used for coloration of counts (log2 ratios) between plants grown at 43℃ relative to 23℃ is presented. Red squares displayed up-regulated and blue squares represents down-regulated transcripts. Different lipid species are derived either from the eukaryotic pathway (*sn-1*/*sn-2*, C18/C18 or C16/C18) or from the prokaryotic pathway (*sn-1*/*sn-2*, C18/C16). Dashed lines represent possible channeling between the ER and chloroplasts. FAS, fatty acid biosynthesis.

(1.5 fold). In addition, the chloroplast *CYTIDINEDIPHOSPHATE DIACYLGLYCEROL SYNTHASE 4* (*CDS4*) which is involved in PG synthesis was suppressed significantly (2.3 fold). This transcript change was consistent with the reduced amount of PG synthesized from the prokaryotic pathway. In the eukaryotic pathway, *FAD2* was significantly up-regulated (2.2 fold) at 43℃. However, the increased *FAD2* expression did not result in any increase in 18:2 in total lipids or in PC (Table 3.6 and Table 3.7). The induction of *FAD2* gene expression further demonstrates that desaturases are not always regulated by temperature to subsequently modulate overall fatty acid desaturation at transcript level. Expression of *ATPIS1* was up-regulated 2.4 fold, and was consistent with an increased amount of PI detected in *A. lentiformis* grown at high temperature. Hence, glycerolipid pathway genes in the ER and chloroplast were differentially regulated to orchestrate the conversion of *A. lentiformis* from a 16:3 to 18:3 lipid phenotype. Importantly, *FAD2*, *FAD5* and *ACT1* identified previously as key genes influencing glycerolipid pathway balance in *Arabidopsis*, were again captured in *A. lentiformis*.

3.3 Lipid redistribution in *T. aestivum* grown at low temperature

Results from both *Arabidopsis* and *A. lentiformis* provide evidence of differential channeling of DAG moieties from the ER to the chloroplast. These changes impact the molecular composition of MGDG and DGDG, and have a significant influence on the degree of desaturation of chloroplast lipids. In 18:3 plants, the prokaryotic pathway only contributes meaningfully to PG synthesis (Browse et al., 1986) while MGDG and DGDG are derived from the eukaryotic pathway. For this reason, I was interested in determining if the differential channeling of DAG moieties also takes place in 18:3 species.

3.3.1 Fatty acid flux in *T. aestivum* grown at low temperature was altered

Lipid profile changes of *T. aestivum* L. cv Manitou (wheat) under low temperature treatment were examined. Total fatty acid analysis showed a significant increase in 18:3 while the proportion of 16:0 and 18:2 were decreased when grown at 4℃ (Table 3.11).

Table 3.11 Total fatty acid composition in leaves of *T. aestivum* plants grown at 23 or 4℃.

T. aestivum plants (cultivar, spring Manitou) were grown at 23℃ for two weeks and then transferred to 4℃ for additional two weeks treatment. Leaves were then harvested for FAME analysis. Leaves from two weeks plants grown at 23℃ were harvested as control. Values are means ± SD of mol % (n = 4). Statistically significant differences (Student t-test; *, p value < 0.05) were calculated. DBI, double bond index. C16 represents the sum of 16: 0 and 16: l; C18 represents the sum of 18:0, 18:1, 18:2 and 18:3.

	Fatty acid composition (mol %)						C16/C18	DBI
	16:0	16:1[a]	18:0	18:1	18:2	18:3		
23℃	14.4 ± 0.27	2.4 ± 0.23	0.7 ± 0.04	1.1 ± 0.21	14.5 ± 1.41	67 ± 1.28	0.2 ± 0.01	2.33 ± 0.01
4℃	12.2 ± 0.11*	3.1 ± 0.12*	1.4 ± 0.15*	1 ± 0.06	11.5 ± 0.45*	70.8 ± 0.44*	0.18 ± 0.00*	2.4 ± 0.01*

[a] represents sum of *cis* and *trans*-16:1

Table 3.12 Glycerolipid composition of leaves from *T. aestivum* grown at 23 or 4℃.

Values are means ± SD (n = 3). Statistically significant differences (*, p value < 0.05) were calculated between 4 and 23℃. C16 represents the sum of 16: 0 and 16: l; C18 represents the sum of 18:0, 18:1, 18:2 and 18:3.

Glycerolipids		Total Polar Lipids (%)	Fatty acid composition (mol%)						C16/C18
			16:0	16:1[a]	18:0	18:1	18:2	18:3	
DGDG									
	23℃	24.9 ± 0.50	9 ± 0.08		1.1 ± 0.07	0.7 ± 0.01	2.2 ± 0.04	87 ± 0.18	0.10 ± 0.00
	4℃	26.4 ± 0.23*	7.7 ± 0.15*		0.9 ± 0.05*	0.8 ± 0.26	1.8 ± 0.47	88.8 ± 0.91*	0.08 ± 0.00*
MGDG									
	23℃	42.7 ± 2.06	1 ± 0.03		0.2 ± 0.02	0.4 ± 0.01	3.7 ± 0.03	94.6 ± 0.08	0.01 ± 0.00
	4℃	35.1 ± 0.25*	1.1 ± 0.04		0.2 ± 0.01	0.4 ± 0.04	1.9 ± 0.06*	96.4 ± 0.08*	0.01 ± 0.00
PC									
	23℃	11.1 ± 0.40	24.3 ± 0.09		1.4 ± 0.09	4.6 ± 0.11	42.8 ± 0.5	26.8 ± 0.62	0.32 ± 0.00
	4℃	15.5 ± 0.50*	21.4 ± 0.86*		1.3 ± 0.1	3.5 ± 0.57	39.2 ± 0.65*	34.6 ± 0.86*	0.27 ± 0.01*
PE									
	23℃	4.6 ± 0.34	25 ± 0.44		1.5 ± 0.14	1.4 ± 0.33	49.3 ± 0.58	22.8 ± 0.21	0.33 ± 0.01
	4℃	8.0 ± 0.25*	24.3 ± 0.52		1 ± 0.23*	0.9 ± 0.01*	41.4 ± 0.33*	32.4 ± 0.47*	0.32 ± 0.01
PG									
	23℃	10.2 ± 0.48	14.5 ± 0.13	37.5 ± 0.22	0.9 ± 0.18	1 ± 0.02	6.2 ± 0.09	39.8 ± 0.41	1.08 ± 0.01
	4℃	9.9 ± 0.28	20.6 ± 0.26*	28.8 ± 0.72*	0.8 ± 0.08	1 ± 0.07	6.6 ± 0.34	42.1 ± 0.44*	0.98 ± 0.03*
PI									
	23℃	1.3 ± 0.17	52.9 ± 3.78		4.1 ± 3.96	0	23 ± 1.05	20 ± 0.82	1.13 ± 0.18
	4℃	1.4 ± 0.03	46.4 ± 2.22		3.3 ± 0.1	1 ± 1.78	21.4 ± 0.67	27.9 ± 1.11*	0.87 ± 0.08
SQDG									
	23℃	5.3 ± 0.30	25.5 ± 0.64		2 ± 0.41	0	4.6 ± 0.69	68 ± 1.33	0.34 ± 0.01
	4℃	3.7 ± 0.11*	25.3 ± 1.1		1.9 ± 0.11	0	1.4 ± 0.31*	71.3 ± 1.3	0.34 ± 0.02

[a] represents sum of *cis* and *trans*-16:1

Glycerolipid compositional analysis showed that MGDG and SQDG were significantly reduced while PC, DGDG and PE were increased (Table 3.12). The proportion of PG, the only glycerolipid species produced through both pathways in *T. aestivum*, was not changed. However, stereo-specific positional analysis revealed an increase in C18 fatty acids and a decrease in C16 fatty acids at the *sn-2* position (Figure 3.11a). These results suggest an enhanced fatty acid flux through the eukaryotic pathway PG production in *T. aestivum* grown at low temperatures. Overall *T. aestivum* plants produced more phospholipids through the eukaryotic pathway at low temperatures and the percentage of total galactolipids (DGDG and MGDG) was significantly decreased, from 67.6 % to 61.5 % (Table 3.12). Hence, there was a reduction of lipid channeling from the ER to the chloroplast at lower temperatures in *T. aestivum*.

3.3.2 Lipidomics analysis with *T. aestivum* grown at low temperature

Similar results in glycerolipid changes were obtained from a lipidomics study of *T. aestivum* (Figure 3.11b). Lipidomics data verified a decrease in C32 pool with a concomitant increase in C36 pool in PG, indicating an enhanced fatty acid flux for PG synthesis from the eukaryotic pathway (Figure 3.11c).

More importantly, differential channeling of 16:0/C18 DAG and C18/C18 DAG moieties was observed in both 2D TLC data and the lipidomics analysis. 2D-TLC results showed a reduction of 16:0 in DGDG (Table 3.12). An earlier study with *T. aestivum* reported that more than 95 mol% of the *sn-2* fatty acids at PC, PE, MGDG and DGDG were C18 (Arunga and Morrison, 1971). Thus, the reduced 16:0 should be at the *sn-1* position of DGDG. In addition, the C16/18 ratio in DGDG was significantly decreased which also suggests increased partitioning of C18 fatty acids from ER to chloroplast. Lipidomic analysis confirmed a significant reduction of DGDG (34:3; 16:0/18:3) and an increased proportion of DGDG (36:6; 18:3/18:3) (Figure 3.11d). Therefore, consistent with the *Arabidopsis* and *A. lentiformis* data, differential channeling of DAG moieties also occurs in 18:3 plants during low temperature adaptation.

(a)

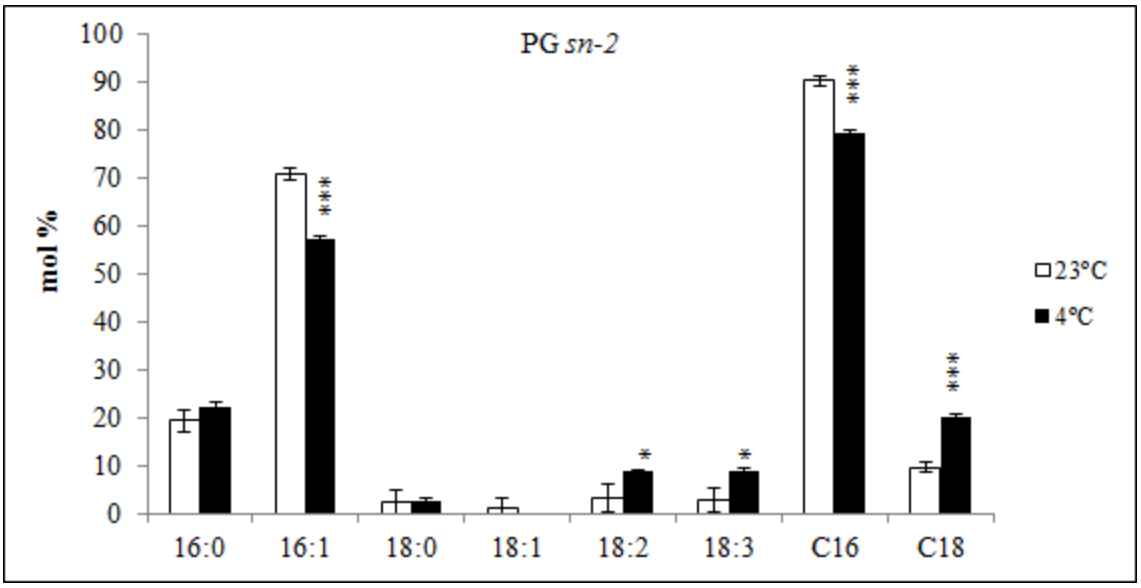
PG sn-2
mol %
100
90
80
70
60
50
40
30
20
10
0
16:0
16:1
18:0
18:1
18:2
18:3
C16
C18
23°C
4°C

(b)

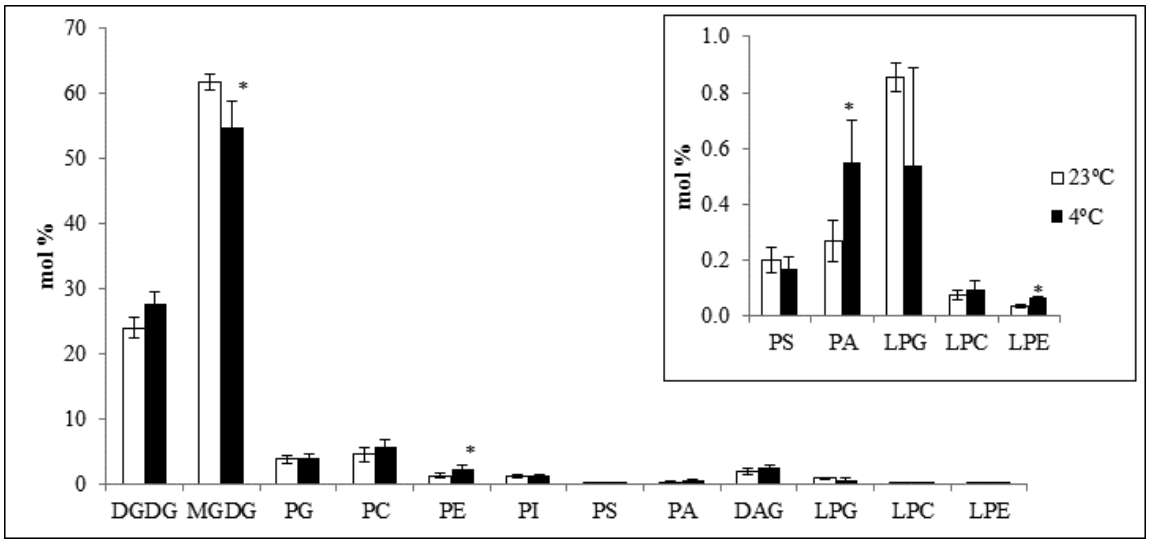
mol %
70
60
50
40
30
20
10
0
DGDG
MGDG
PG
PC
PE
PI
PS
PA
DAG
LPG
LPC
LPE
1.0
0.8
0.6
0.4
0.2
0.0
23°C
4°C

(c)

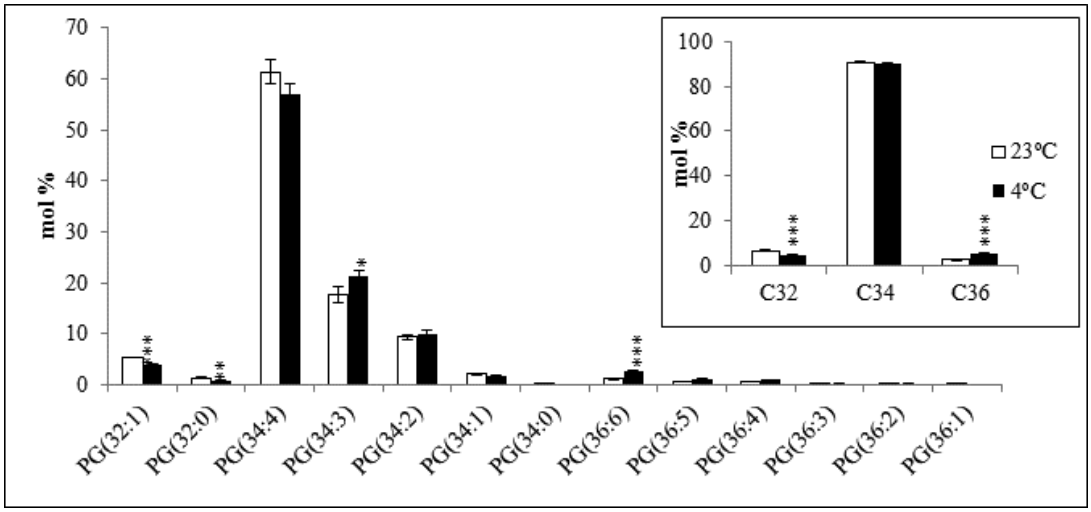

(d)

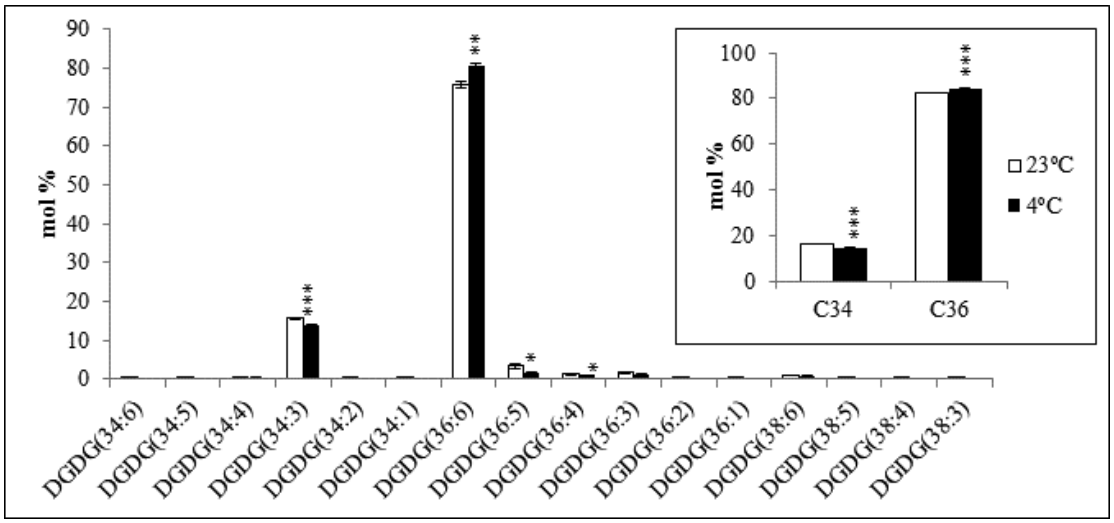

Figure 3.11 Fatty acid flux and differential channeling of lipids from ER to chloroplast in *T. aestivum* grown at 23 or 4°C.

(a) Stereospecific analysis of fatty acid composition at the *sn-2* position of PG. C16 represents the sum of 16:l, 16:2 and 16:3; C18 represents the sum of 18:0, 18:1, 18:2 and 18:3. **(b)** Relative content (mol %) of different lipid species as well as molecular composition of PG **(c)** and DGDG **(d)** in *T. aestivum* plants grown at 23 or 4°C were identified by lipidomics analysis. C32 represents C16/C16 lipid molecules; C34 represents C16/C18 and C18/C16 lipid molecules; C36 represents C18/C18 lipid molecules. Values are means ± SD (n = 3). Student t-test; *, $p < 0.05$; **, $p < 0.01$; ***, $p < 0.001$.

3.4 Temperature treatment of *Arabidopsis* mutant lines

In this study, lipid mutants possessing altered glycerolipid pathways (*fad5, gly1* and *act1*) were included for temperature treatments (Hugly and Somerville, 1992; Miquel et al., 1998; Kunst et al., 1988). FAD5 is critical for MGDG production in the prokaryotic pathway (Hugly and Somerville, 1992). *GLY1* encodes the first glycerol-3-phosphate dehydrogenase (GPDH) in the prokaryotic pathway for the production of glycerol-3-phosphate (G-3-P) (Miquel et al., 1998) while *ACT1* encodes glycerol-3-phosphate acytransferase (GPAT) for the subsequent step in the prokaryotic pathway (Kunst et al., 1988). Hence, each line possesses a mutation that primarily impacts the prokaryotic pathway.

The *fad5* mutant was included as a control for cold treatment in this study as it exhibits chlorosis at 5℃ (Hugly and Somerville, 1992). After three week cold treatment at 5℃, the *gly1* and *fad5* mutants showed chlorosis while no noticeable phenotypes were observed in *act1* mutants (Figure 3.12a). To give a quantitative view of changes in fatty acid compositions and their association with desaturation, total fatty acid composition of leaves from plants grown at 22℃ for 10 days or after 3 weeks at 5℃ was measured. A similar trend in fatty acid changes were observed in plants grown at either 22 or 5℃. However, unlike wild type plants that increased 18:3 and decreased 18:2 at low temperatures, the most significant change in the mutants was the increase in 18:2 and 18:3 (Figure 3.12b). At 22℃, an increase of 18:2, 2.8 mol% in *gly1*, 0.6 mol% in *fad5* and 4.1 mol% in *act1*, was observed compared to wild type. However, the differences were profound in plants grown at 5℃, 8.3 mol% in *gly1*, 3.74 mol% in *fad5* and 9.6 mol% in *act1* between the molar percentage of 18:3 and 18:2. These results suggest that an increase in polyunsaturated fatty acids (18:3) in not always preferred at low temperatures.

(a)

(b)

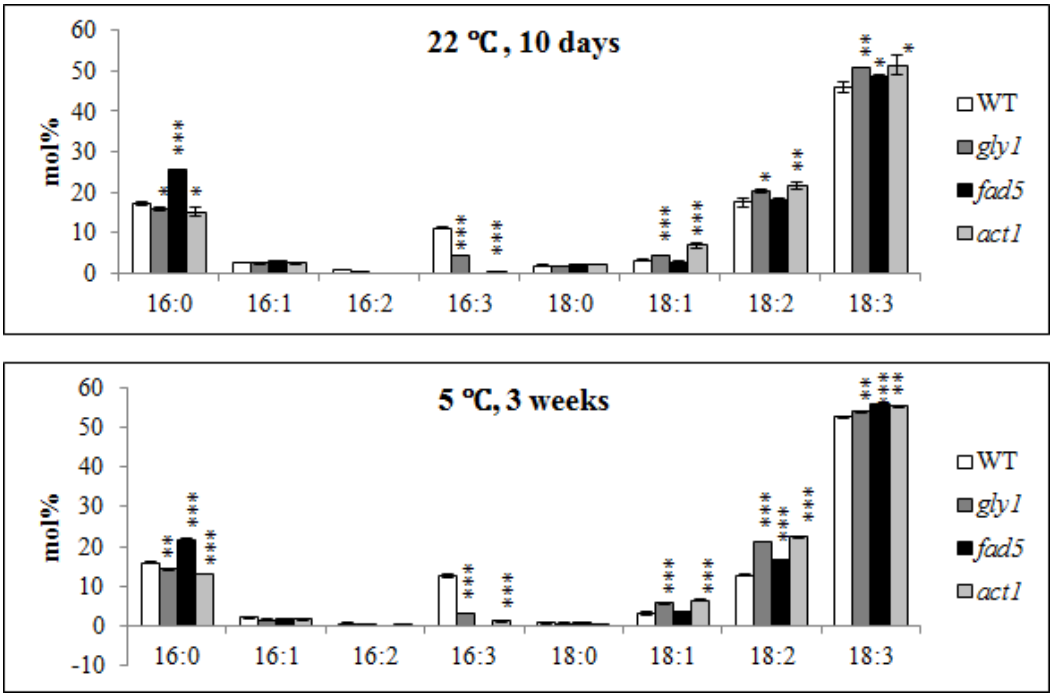

Figure 3.12 Temperature effects on *Arabidopsis* wild type and lipid mutants with altered glycerolipid pathways.

(a) Phenotypes of wild type and mutants grown at 5ºC for three weeks. **(b)** Fatty acid composition of plants grown at 22ºC (10 days) and after exposure to 5ºC for three weeks. Upper panel, fatty acid composition of plants grown at 22ºC for 10 days; lower panel, fatty acid composition of plants after exposure to 5ºC for three weeks. Student t-test was calculated between mutants and wild type. *, p value < 0.05; **, p value < 0.01; ***, p value < 0.001.

4 DISCUSSION

Glycerolipid synthesis in plants involves two major metabolic pathways compartmentalized in the ER and chloroplast that are regulated with considerable flexibility. Moreover, glycerolipids synthesized in the two compartments are distributed to different organelles, e.g. MGDG and DGDG in thylakoid membranes and phospholipids in the cytoplasmic membranes. Thus, the degree of membrane unsaturation is not controlled by desaturases alone but is also determined by the proportion of membrane lipids as well as the molecular composition of each lipid species. It is apparent that plants have evolved biochemical and metabolic adaptations to facilitate their growth and/or survival under unfavorable temperatures. However, the redistribution of membrane lipids, particularly the modulation of fatty acid fluxes between the ER and chloroplast pathways, although noted to occur under different temperatures, has received relatively little attention. In addition, how genes in the glycerolipid pathway are coordinated to mediate the metabolic flexibility in glycerolipid pathways, and precisely, what key factors are involved in lipid redistribution under temperature fluctuations is largely unknown. In this study, the fine tuning of the prokaryotic and eukaryotic glycerolipid biosynthesis pathways in three plant species in response to sub-optimal temperatures was systematically investigated.

4.1 Distinct modes of glycerolipid biosynthesis in three plant species

Plants can be classified according to the presence or absence of 16:3 esterified to galactolipids such as MGDG and DGDG, the main lipids in leaves (Browse et al., 1986). *Arabidopsis* plants are typical 16:3 plants with an almost equal contribution from the prokaryotic and eukaryotic pathways for chloroplast galactolipid biosynthesis. *A. lentiformis* is a notable exception to this rule as they can switch from a 16:3 to 18:3 fatty acid phenotype when grown at high temperatures (Pearcy, 1978). Therefore, *A. lentiformis* plants can be viewed as a natural system acquiring thermotolerance by rebalancing the glycerolipid pathways. In contrast, *T. aestivum* species are typical 18:3 plants. Though the three plant species have been classified into 16:3 and 18:3 plants according to the level of 16:3 in leaves (Arunga and Morrison, 1971; Pearcy,

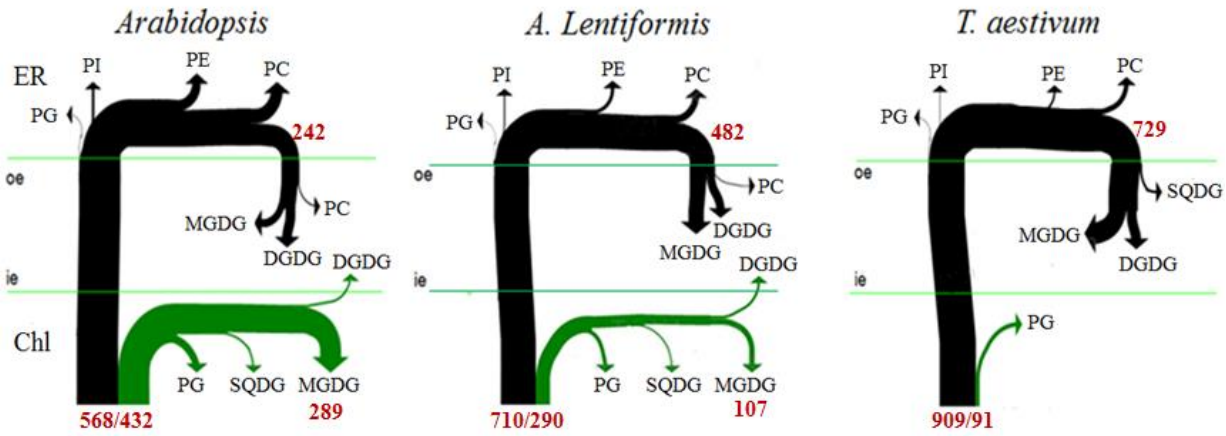

Figure 4.1 Flow diagrams of fatty acid fluxes (mol/1000 mol) during lipid synthesis in *Arabidopsis* (22℃), *A. lentiformis* (23℃) and *T. aestivum* (23℃) plants.

The thickness of the bar and numbers represents the amount of flux as presented in Table 3.5, Table 3.8, Table 3.12 and Figure 3.14. ER, endoplasmic reticulum; Chl, chloroplast; oe, outer envelope; ie, inner envelope.

1978; Wallis and Browse, 2002), the contribution of the two pathways to glycerolipid synthesis has never been investigated or compared. From the data in this study, I have generated three flow diagrams depicting fatty acid fluxes between the two glycerolipid pathways in the three plant species (Figure 4.1). In *Arabidopsis*, the two glycerolipid pathways contribute almost equally for chloroplast glycerolipid synthesis. In contrast, most glycerolipids (79%) are derived from the eukaryotic pathway in *A. lentiformis* while the prokaryotic pathway only accounts for 21% of the total glycerolipids (Table 3.8). *T. aestivum* species are typical 18:3 plants in which only PG is synthesized by the prokaryotic pathway. As a result, the three plant species showed a varied contribution of the prokaryotic pathway for galactolipid synthesis (42.3% in *Arabidopsis*, 27.9% in *A. lentiformis* and 0% in *T. aestivum* at standard conditions) (Figure 4.1).

4.2 Biochemical changes in glycerolipid pathways in response to temperature

4.2.1 Rebalancing of glycerolipid pathways in *Arabidopsis* grown under low and high temperatures

Glycerolipid changes have been observed in plants grown under different growth conditions (Brockman et al., 1990; Härtel et al., 2000). A higher proportion of DGDG has been reported in *Arabidopsis* grown at high temperature while low temperatures induced the synthesis of MGDG in *B. napus* (Chen et al., 2006; Johnson and Williams, 1989). DGDG has been reported to stabilize the activity of PSII against heat stress (Yang et al., 2002). That the desaturation of MGDG occurs more quickly at low temperature than high temperature in *B. napus* was offered as an explanation for possible plant performance advantage for a flexible balance between the two pathways (Johnson and Williams, 1989). These studies, however, mainly focused on lipid composition changes. Since MGDG and DGDG are synthesized by both the prokaryotic and eukaryotic pathways, how plants readjust the relative amount of glycerolipids in the two glycerolipid pathways to adapt to low and high temperatures presents a challenging question. I investigated the balance of glycerolipid pathways in *Arabidopsis* grown at low (10℃), standard (22℃) and high temperature (30℃) conditions. Lipid composition analysis and fatty acid distribution analysis suggested that low temperature induced an enhanced prokaryotic pathway by producing more MGDG, while high temperature resulted in more

DGDG in the chloroplast by redirecting the eukaryotic pathway. Thus, the compositional changes in *Arabidopsis* grown at high and low temperatures were the result of a rebalancing of the two pathways plus lipid transport from the ER to the chloroplast.

4.2.2 Lipid phenotype of *A. lentiformis* is converted from 16:3 to 18:3 by rebalancing of the glycerolipid pathways

Comprehensive lipid profiling and high throughput transcriptomics were employed to explore the biosynthetic machinery of the lipid phenotype conversion in *A. lentiformis*. This analysis revealed a severely repressed prokaryotic pathway in *A. lentiformis* grown at 43℃. Two major lipid species originating exclusively from the prokaryotic pathway, DGDG (34:6, 18:3/16:3) and MGDG (34:6, 18:3/16:3), were dramatically decreased. Therefore, the lipid phenotypic conversion of 16:3 to 18:3 is achieved solely by rebalancing the glycerolipid pathways: a substantial reduction of the prokaryotic pathway and an enhanced eukaryotic pathway. However, unlike 18:3 plants in which galactolipids are entirely derived from the eukaryotic pathway, the repressed prokaryotic pathway still generates chloroplast galactolipids (Figure 4.2). The phenotypic conversion from 16:3 to 18:3 of *A. lentiformis* grown at high temperature points squarely to the utility of lipid pathway adjustment in plant adaptation to temperature fluctuations. Genetically, *A. lentiformis* possess all enzymatic components of a 16:3 plant, and thus fundamentally, it remains a 16:3 plant.

Studies on *A. lentiformis* have revealed several novel aspects of glycerolipid metabolism that are different from a typical 16:3 plant, and are possibly relevant to the conversion from 16:3 to 18:3 plants. First, contribution to the synthesis of chloroplast galactolipids is much lower in *A. lentiformis* (27.9%) compared to 42.3% in *Arabidopsis* (Table 3.5, Table 3.8 and Figure 4.1). Second, interesting changes were identified when comparing the glycerolipid compositional changes of *Arabidopsis* grown at 30℃ and *A. lentiformis* grown at 43℃. As shown in Table 3.4 and Table 3.7, decreased 18:3 and increased 18:2 and 18:1 in MGDG and DGDG were evident in both plant species whereas PC and PE showed opposing responses. In *Arabidopsis*, the decrease of 18:3 with a commitment increase of 18:2 was observed. However, both 18:2 and 18:3 were

reduced while the proportion of 18:1 was significantly increased in *A. lentiformis* at 43℃. Thirdly, *A. lentiformis* plants contain a substantial amount of 34:1 (16:0/18:1) lipid molecules in phospholipids while almost no 34:1 lipids were detected in *Arabidopsis* leaves (Shen et al., 2010). Our results suggest that the significantly increased 34:1 were mainly derived from eukaryotic lipids with 16:0 at the *sn-1* position. These features in *A. lentiformis* once again accentuate the power and utility of rebalancing the glycerolipid pathways when growing at high temperatures.

4.2.3 Transportation of fatty acids from ER to chloroplast is regulated in 18: 3 plants during temperature adaptation

When grown at lower temperatures, 16:3 plants exhibit an enhanced prokaryotic pathway that produces MGDG as demonstrated in both *Arabidopsis* and *A. lentiformis.* 18:3 plants, such as *T. aestivum*, use the prokaryotic pathway solely for PG synthesis while the production of galactolipids relies entirely on the ER-derived lipids. Glycerolipid compositional analysis showed a repression of lipid flux from ER to chloroplast and the production of more phospholipids. The significant decrease of MGDG and increase of phospholipids and DGDG, in *T. aestivum* grown at low temperature, were different from 16:3 plants (*Arabidopsis* and *A. lentiformis*) in which more MGDG was produced from the prokaryotic pathway at lower temperatures. This could be due to different rates of desaturation in the ER-derived MGDG and the chloroplast MGDG. Labeling studies have shown that the desaturation process of chloroplast MGDG is stimulated at lower temperatures while the ER-derived MGDG was desaturated at a much slower rate than the ER-derived DGDG (Johnson and Williams, 1989). Assuming it is also true that the desaturation process is slower for the ER-derived MGDG than DGDG, an increase of DGDG and phospholipids in *T. aestivum* plants would be beneficial for plants grown at low temperatures.

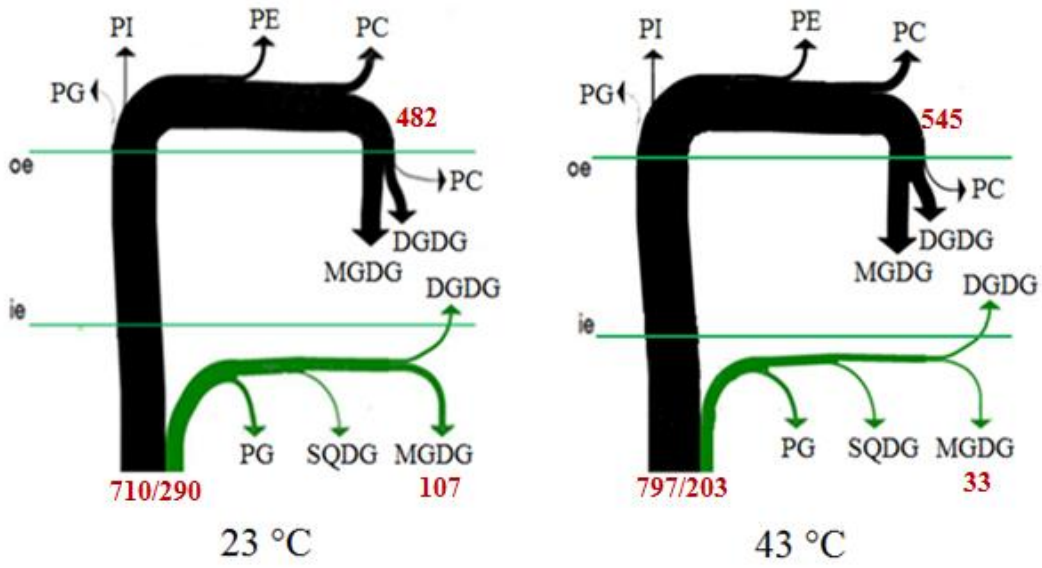

Figure 4.2 Flow diagrams of fatty acid fluxes (mol/1000 mol) during lipid synthesis in *A. lentiformis* plants grown under 23 or 43℃.

The thickness of the bar and numbers represents the amount of fatty acid flux as presented in Table 3.8. ER, endoplasmic reticulum; Chl, chloroplast; oe, outer envelope; ie, inner envelope.

4.3 Differential channeling of DAG moieties from ER to chloroplast

Differential channeling of DAG moieties from ER to chloroplasts offers another layer of metabolic adaptation in plants. PC or PC-derived lipids (DAG, PA and *lyso*-PC) have been proposed to be precursors of the eukaryotic derived galactolipids because the fatty acid pattern of PC resembles that of galactolipids (Benning, 2009; Kelly et al., 2003). It has been shown from labeling experiments in *Arabidopsis* that PC (C18/C18) is preferentially transported to the chloroplast for MGDG and DGDG synthesis while C16 fatty acids are retained in eukaryotic PC (Browse et al., 1986; Miquel and Browse. 1992). In this study, I showed that C16 containing lipid molecules (C34 lipids in DGDG, PC, PE and C32 in PG) in almost all major lipids except MGDG were significantly increased in *A. lentiformis* grown at 43℃. Dramatic increases in 34:1 in phospholipids (such as PC) and 34:3 in DGDG were also observed at high temperatures. This is particularly interesting in the case of DGDG because lipid class analysis and lipidomics indicated that DGDG (34:6) synthesized by the prokaryotic pathway was reduced. The dramatic increase in 34:1 in PC could be mainly responsible for the increase in C34 lipid molecules in DGDG. Like most plant species, PC in *A. lentiformis* contains more than 95 mol% of C18 fatty acyl moieties at the *sn-2* position. Thus, the majority of PC (34:1) had a composition of 16:0/18:1. This was verified by analysis of the fatty acyl moieties at the *sn-1* position of DGDG, MGDG and PC, all of which had an increased percentage of 16:0. These results were consistent with increased 34:1 lipid species in PC and increased 34:3 in DGDG and MGDG. Therefore, the increased DGDG (34:3) in *A. lentiformis* was mainly composed of DGDG (16:0/18:3) derived from the eukaryotic pathway. Together with the increased species of C34 lipid molecules in PC, the DAG moieties with (16:0/C18) from the eukaryotic pathway accumulated at high temperatures. In addition, DAG moieties with (16:0/C18) were preferentially channeled from ER to chloroplast in *A. lentiformis* grown at high temperatures. Based on these observations, I propose that the significant increase of (16:0/18:1) DAG moiety trafficking could be an advantageous adaptation to high temperature in *A. lentiformis* because DGDG (16:0/18:3), which contains fewer double bonds than DGDG (18:3/18:3), and thus has higher saturation, should be favored at high temperatures. It should be noted that an increase in 18:3 at lower temperatures together with an increase in 16:0 at higher temperatures in DGDG were always observed, regardless of whether the plant displayed a 16:3 or an 18:3 fatty acid phenotype. Therefore, high

temperatures promote channeling of DAG moieties with (16:0/C18) from ER to chloroplast while low temperatures stimulate the generation of DGDG (18:3/18:3) from DAG (C18/C18).

Differential channeling of DAG moieties to DGDG synthesis was also observed in *T. aestivum* and confirmed by a reduction of 16:0 in DGDG as well as reduced DGDG (C34) and increased DGDG (C36) (Figure 3.11d). In addition, low temperature nonetheless still leads to a reduced glycerolipid flux from ER to chloroplast (Table 3.12 and Figure 3.11a). Therefore, mediating the fatty acid flux between the two glycerolipid pathways, as well as differential channeling of DAG moieties, was evident in the three plant species with varied contribution of the prokaryotic pathway for galactolipid synthesis.

4.4 Factors involved in mediating fatty acid flux between the glycerolipid pathways revealed at the transcript level

To identify potential factors involved in readjusting the two pathways, expression levels of key genes in the two glycerolipid pathways were investigated. *A. lentiformis* plants showed more dramatic biochemical changes as compared to *Arabidopsis* but transcript level changes as revealed by RNA-seq were consistent with that observed in *Arabidopsis*. In both species, key genes were uncovered by expression analysis. Lower temperatures induce fatty acid unsaturation, while higher temperatures resulted in an opposite response (Wallis and Browse, 2002). Contrary to conventional expectations, the transcript level of *FAD2* in *Arabidopsis* showed a positive association with growth temperatures ranging from 10 to 30℃ compared to 22℃. In *A. lentiformis,* a significant induction of *FAD2* was also observed at high temperatures. An induction of *FAD2-1* and *FAD2-2* expression in soybean seeds at high temperatures has previously been reported (Heppard et al., 1996), but this was rationalized in the context of an up-regulation of degradation of the soybean FAD2-1 at the higher growing temperatures (Tang et al., 2005). Our results suggest that induction of *FAD2* at high temperatures has metabolic consequences in enhancing lipid flux from ER to chloroplast in both *Arabidopsis* and *A. lentiformis*. *FAD2* encodes the major desaturase converting 18:1 to 18:2 in PC (Miquel et al., 1993), thereby suggesting a role in mediating 18:1 and 18: 2 levels in PC. Disruption of the

FAD2 gene in *Arabidopsis* also resulted in reduced lipid flux from the ER to the chloroplast (Miquel and Browse, 1992). In addition, PC is the precursor of PA, DAG and *lyso*-PC which are proposed to be transported from the ER to the chloroplast (Benning, 2009; Kelly et al., 2003; Ohlrogge and Browse, 1995). DAG moieties enriched in 18:2 are preferentially transported from ER to chloroplast for the synthesis of eukaryotic pathway derived DGDG and MGDG (Browse et al., 1986; Miquel and Browse. 1992). It is likely that the induction of *FAD2* promotes this process.

ACT1 encodes the first glycerol-3-phosphate acytransferase (GPAT) in the prokaryotic pathway (Kunst et al., 1988) while FAD5 is responsible for the desaturation of 16:0 to 16:1 in the synthesis of prokaryotic MGDG (Hugly and Somerville, 1992). In the present study, expression of *ACT1* and *FAD5* was induced at lower temperature, contributing to an enhanced prokaryotic pathway in *Arabidopsis*. In contrast, a significant reduction of *FAD5* and *ACT1*expression was observed in *A. lentiformis* grown at high temperature. Down-regulation of *ACT1* under high temperatures would result in an overall repression of the prokaryotic pathway. More importantly, at high temperatures the decrease of prokaryotic MGDG which largely accounts for the reduced fatty acid flux to the prokaryotic pathway was also attributable to the down-regulation of *FAD5* expression. Thus, *ACT1* and *FAD5* in the prokaryotic pathway and *FAD2* in the eukaryotic pathway were identified as key genes/factors mediating the balance of the two glycerolipid pathways.

Evidence supporting this conclusion can also be found in previous studies with *Arabidopsis* mutants and transgenic plants. Our previous studies with *Arabidopsis* transgenic lines of augmented glycerol-3-phosphate (G-3-P) content also showed that the induction of *FAD5* coincided with an enhanced prokaryotic pathway (Shen et al., 2010). Hence, under standard growth conditions, FAD5 is positively associated with fatty acid flux through the prokaryotic pathway. Studies with *act1*, *fad5* and *fad2* mutants in *Arabidopsis* revealed that both *act1* and *fad5* have thermal tolerance (Falcone. et al., 2004; Kunst, et al., 1988). The enhanced thermal tolerance in *fad5* and *act1* has been previously explained by a reduced degree of fatty acid desaturation (Hugly et al., 1989; Kunst, et al., 1989), however, the double bond index of *act1* mutants is similar to wild type at 17 and 36℃ (Falcone et al., 2004). Thus, the degree of fatty acid desaturation is not the sole factor determining plant tolerance to high temperatures as an

enhanced eukaryotic pathway will also make beneficial contributions.

4.5 Factors affecting lipid trafficking from ER to chloroplast

In this study, differential channeling of DAG moieties from ER to chloroplast was identified in both 16:3 and 18:3 plants grown at different temperatures. This process requires a series of intra-cellular events and much remains unknown (Benning, 2009). The TRIGALACTOSYLDIACYLGLYCEROL (TGD) proteins play an essential role in lipid transfer from ER to chloroplast (Awai *et al.*, 2006). Additional proteins such as lipases, lipid flippases and lipid transporters also could be involved in lipid trafficking from ER to chloroplast (Benning et al., 2006; Benning, 2008). RNA-seq analysis of *A. lentiformis* showed that none of the genes for TGDs was significantly changed at the transcriptional level under high temperature treatment (Appendix B). More than half of the significantly changed lipid transcripts (67 out of the 133 transcripts; fold change >4 and p value < 0.01) encode lipid signaling and lipid transfer proteins (Appendix A). Hence, active lipid signaling and lipid transfer events are probably involved in this process.

4.6 Temperature induced changes in *Arabidopsis* lipid mutants with altered glycerolipid pathways

Previously, *fad5* had been shown to be chlorotic when grown at 5℃ (Hugly and Somerville, 1992) my results supported the suggestion that *FAD5* is critical for low temperature tolerance in plants. I further explored the growth performance of mutants with altered glycerolipid pathways. The *gly1* (Miquel et al., 1998) and *act1* mutants (Kunst et al., 1988), both with compromised prokaryotic pathway, were grown at 5℃ for three weeks after growing at standard condition for one week. After this treatment, *gly1* mutants exhibited chlorosis that has not been reported before in leaves. No noticeable phenotypes were observed in *act1* mutants grown at 5℃, but it has been reported that *act1* mutants possess enhanced thermal tolerance to high temperatures (Hugly et al., 1989). Total fatty acid analysis of wild type, *gly1*, *fad5* and *act1*

grown at 22 or 5℃ showed higher levels of 18:2 relative to 18:3, compared to wild type, when grown at 5℃. These results suggested that it is not always necessary to increase polyunsaturated fatty acids (18:3) at low temperatures but alterations between glycerolipid pathways may play a more important role in temperature tolerance in plants.

5 CONCLUSIONS AND FUTURE STUDIES

5.1 Rebalancing the glycerolipid pathways is a strategy for plant adaptation to temperature changes

My study investigated the fine tuning of the two glycerolipid pathways in three plants species when subjected to sub-optimal temperatures. My results revealed that coordination in fatty acid flux sharing between the two glycerolipid pathways, as well as differential channeling of DAG moieties, occurs with changing temperatures (Figure 5.1). The model, for the first time, describes the biochemical basis of increased fatty acid desaturation under low temperature and decreased fatty acid unsaturation at high temperature attributable to fatty acid flux sharing between the two pathways as well as a differential channeling of DAG moieties from the ER to the chloroplast. Higher temperature represses fatty acid flux through the prokaryotic pathway and promotes channeling from ER to chloroplast. In 18:3 plants, this metabolic regulation mainly occurred in the eukaryotic pathway with lipid flux from ER to chloroplast.

5.2 Differential channeling of DAG moieties from ER to chloroplast offers another layer of biochemical regulation in plant adaptation to temperature fluctuations

The regulation of fatty acid flux during temperature adaptation in plants takes place primarily at two metabolic junctures, the prokaryotic pathway and lipid trafficking from ER to chloroplast, as revealed in three plant species. Importantly, my study also revealed that DAG moieties with different combination of fatty acids are differentially transported. That such a differential trafficking of DAG moieties from ER to chloroplast occurs in three species with

distinct modes of glycerolipid pathway coordination strongly suggests the regulation of unsaturation levels in galactolipids under different temperatures. High temperatures promote channeling of 16:0/C18 DAG moieties from ER to chloroplast while low temperatures stimulate generation of 18:3/18:3 DGDG from C18/C18 DAG (Figure 5.1).

5.3 Regulation of glycerolipid pathway balance by *ACT1* and *FAD5* in the prokaryotic pathway

In the prokaryotic pathway, *ACT1* and *FAD5* are identified as key genes/factors. *ACT1* encodes the glycerol-3-phosphate acytransferase (GPAT) of the prokaryotic pathway (Kunst et al., 1988) while FAD5 is responsible for the desaturation of 16:0 to 16:1 in the synthesis of prokaryotic MGDG (Hugly and Somerville, 1992). In this study, *A. lentiformis* lipid phenotype conversion from 16:3 to 18:3 at high temperature is a result of greatly reduced lipid flux through the prokaryotic pathway by dramatic repression of *ACT1* and *FAD5*. In addition, both *ACT1* and *FAD5* were up-regulated in *Arabidopsis* grown at low temperature, correlating with an enhanced prokaryotic pathway. These results suggest that *ACT1* and *FAD5* participate in mediating glycerolipid pathway balance by regulating the prokaryotic pathway. Since ACT1 governs the first step in the prokaryotic pathway, regulation of *ACT1* expression is suggested to be more important.

5.4 Role of FAD2 in lipid transportation from ER to chloroplast during temperature adaptation

In *Arabidopsis,* transcript levels of *FAD2* showed positive association with growth temperature ranging from 10 to 30℃. In *A. lentiformis,* a significant increase in *FAD2* transcript was also observed at high temperature. While this observation has often been rationalized in the context of post-transcriptional regulation of enhanced degradation of FAD2 protein at high growth temperatures (Tang et al., 2005), my study suggests that induction of *FAD2* at high temperature has metabolic consequences in enhancing lipid flux from ER to chloroplast in both

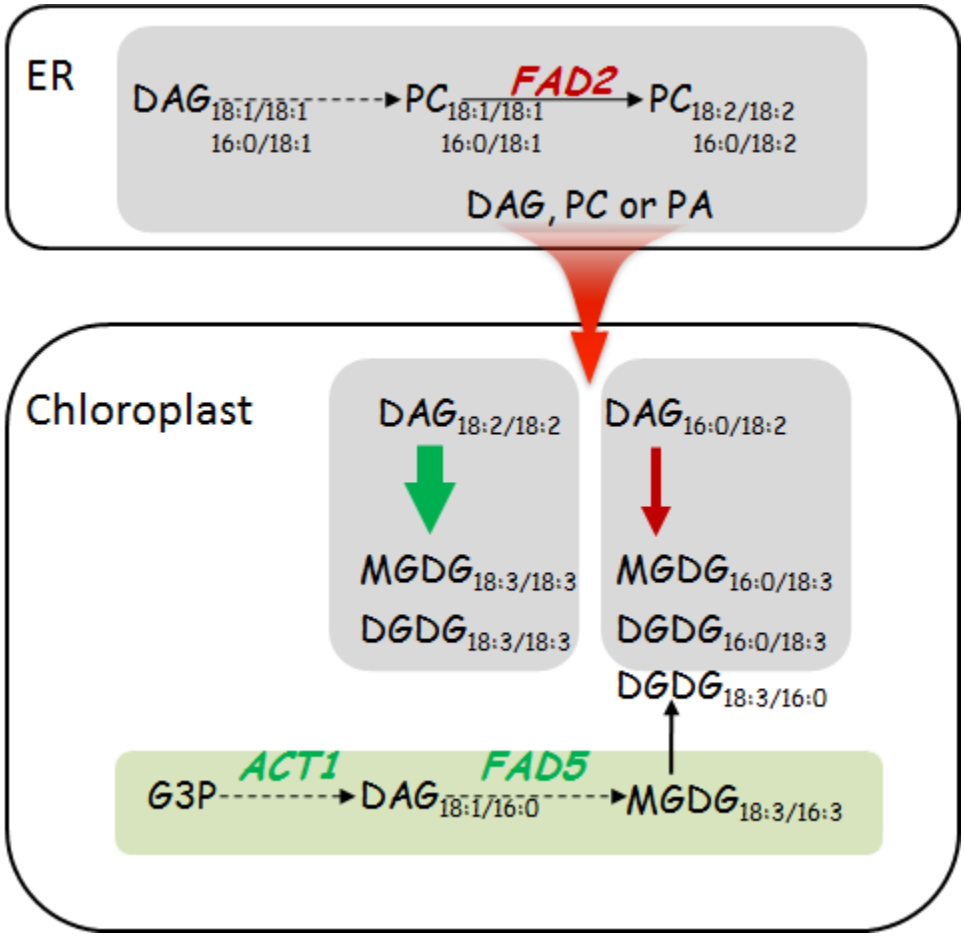

Figure 5.1 Glycerolipid pathway coordination in response to growth temperature change.

Glycerolipid species derived from the eukaryotic pathway are shown in grey (*sn-1*/*sn-2*, C18/C18 or C16/C18); glycerolipids originating from the prokaryotic pathway are in green (*sn-1*/*sn-2*, C18/C16). Red arrows denote trend associated with an increase in growth temperature whereas green arrows indicate changes associated with a decrease in growth temperature. Higher temperatures inhibit the prokaryotic pathway and promote lipid trafficking from ER to chloroplast. DAG moieties of C18/C18 and 16:0/C18 derived from the ER are differentially transported to the chloroplast for the synthesis of MGDG and DGDG. Higher temperatures induce the trafficking of DAG (16:0/C18) while lower temperatures stimulate the channeling of DAG (C18/C18). *FAD2*, *FAD5* and *ACT1* are key genes involved in mediating fatty acid flux in the two glycerolipid pathways. Expression of *FAD2* is up-regulated (highlighted in red) at higher temperature while *FAD5* and *ACT1* are down-regulated (highlighted in green). G3P, glycerol-3-phosphate; DAG, diacylglycerol; PA, phosphatidic acid.

Arabidopsis and *A. lentiformis*. In addition, disruption of the *FAD2* gene in *Arabidopsis* has been shown to result in reduced lipid flux from ER to chloroplast (Miquel and Browse, 1992).

As the major desaturase converting 18:1 to 18:2 in PC (Miquel et al., 1993), how does FAD2 mediate lipid trafficking from ER to chloroplast? This is because PC can be converted to precursors of potential trafficking intermediates, PA and DAG, from ER to chloroplast (Benning, 2009; Kelly et al., 2003; Ohlrogge and Browse, 1995). In addition, studies have shown that DAG moieties enriched in 18:2 are preferentially transported from the ER to chloroplasts for the synthesis of eukaryotic pathway derived DGDG and MGDG (Browse et al., 1986; Miquel and Browse. 1992). Regulation of *FAD2* expression would change 18:1 and 18:2 levels in PC, thereby, regulating trafficking of the intermediates PA and DAG from the ER to chloroplasts. Hence, FAD2 is not only involved in fatty acid desaturation but also plays a role in mediating lipid transport from ER to chloroplast.

5.5 Evolutionary implications

In the present study, similar biochemical changes in response to changes in growing temperatures were revealed in *Arabidopsis*, *A. lentiformis* and *T. aestivum* plants. In addition, the same key factors involved in mediating biochemical changes in the glycerolipid pathways were identified by transcript analysis. Why do plants with different genetic backgrounds display similar metabolic adaptations in response to different temperatures? Many biological systems have intrinsic capacity to maintain specific functions when exposed to particular perturbations and have thus been described as robust (Lempe et al., 2013; Kitano, 2004). From an evolutionary point of view, such environmental robustness ensures plants to develop similar biochemical adaptations in the face of "environmental noise" during development (Kitano, 2004).

Robustness is the ability of a system to maintain its functionality across a wide range of internal and external perturbations such as genetic mutations and environmental fluctuations (Kitano, 2004; Stewart et al., 2012). Membrane lipid biosynthesis is robust and well maintained even in the face of genetic mutations and environmental perturbations. Temperature changes are the major environmental fluctuations that plants encounter consistently in nature. Previous

studies of membrane systems in response to temperature perturbations have often concentrated on individual desaturases (Benning et al., 2006; Benning, 2009; Hamada et al., 1998; Kunst et al., 1988; Miquel et al., 1993; Miquel et al., 1998; Wallis and Browse, 2002). This study demonstrates that maintaining a degree of robustness in cellular membranes requires a responsive network of gene expression and metabolism to accommodate fluctuating conditions. Expression changes in desaturase genes are a means to mount accelerated and transient pulse of gene expression. In the background, the two pathway balance provides a framework for desaturases to impart membrane compositional changes, that at the same time, stabilize the lipid metabolic network against drastic changes to ensure biological robustness.

It is recognized that genetic and environmental perturbations often have similar phenotypic effects on an organism. As a result, environmental stress may accelerate adaptation via "genetic assimilation", promoting populations that will subsequently evolve the adaptive phenotype by mutation (Stewart et al., 2012). Phylogenic data of the glycerolipid phenotype shows that the majority of plant species are 18:3 plants who have abandoned the prokaryotic pathway while a small group of plants (16:3) still retain both pathways (Mongrand et al., 1998). A significant question in plant biology is what triggers or promotes the conversion of 16:3 to 18:3 plants? My studies with both *Arabidopsis* and *A. lentiformis* provide a possible explanation that high temperature represses the prokaryotic pathway by inhibiting the expression of several key genes such as *ACT1*and/or *FAD5*. Unlike the genetic lesion in *act1* mutants, in *A. lentiformis*, the lipid phenotype conversion from 16:3 to 18:3 could be achieved by repressing *ACT1* expression at high temperatures. It is possible that loss of the prokaryotic pathway in different plant species occurred at different rates by inactivating the expression of key genes in the prokaryotic pathway while higher temperatures accelerated this process.

5.6 Future work

5.6.1 Temperature treatments with *Arabidopsis* double and/or triple lipid mutants

In this study, *FAD2* was identified as a potential factor involved in mediating lipid trafficking from ER to chloroplast whereas *ACT1* and *FAD5* were major factors in controlling prokaryotic

pathway activity. Studies with single mutants of *Arabidopsis* have shown glycerolipid changes and phenotype changes under sub-optimal temperatures (Falcone et al., 2004). However, glycerolipid pathways are highly coordinated and flexible. I would like to investigate biochemical as well as phenotypic changes when two or three factors are simultaneously disrupted. First, *fad2*/*fad5* and *fad2*/*act1*double mutants as well as *fad2*/*fad5*/*act1* triple mutants would be generated. Second, fatty acid composition and lipid changes would be analyzed with these mutants grown under low, standard and high temperature conditions. Growth performance such as growth rate and chlorophyll content would be recorded. Third, since the two glycerolipid pathways are high flexible, how plants readjust glycerolipid pathways in *fad2*/*fad5* and *fad2*/*act1*double mutants as well as *fad2*/*fad5*/*act1* triple mutants is an interesting question. Microarray analysis with double and triple mutants would help to identify novel factors or mechanisms involved in lipid trafficking.

5.6.2 RNA sequencing analysis of *T. aestivum* grown at normal and low temperatures

As an 18:3 plant, the prokaryotic pathway in wheat (*T. aestivum*) only contributes meaningfully to PG synthesis (Browse et a l., 1986) while MGDG and DGDG are derived from the eukaryotic pathway. Since I have already generated comprehensive lipid data including lipid composition and lipidomics analysis for wheat (Manitou cultivar), combining metabolic changes with transcript changes would provide more insights into lipid redistribution in 18:3 plants under low temperature. Generally, RNA-seq analysis of wheat would provide the following benefits: 1) constructing the genome-wide transcriptome of wheat, 2) examining the existence of *ACT1* and *FAD5* in the wheat genome that would help to understand the loss of chloroplast galactolipids in 18:3 plants, 3) since lipid transfer from ER to chloroplast is the major metabolic adjustment in 18:3 plants, RNA-seq analysis would help the identification of any novel factors involved in lipid transfer in this process, 4) understanding lipid metabolic responses to low temperatures in combination with lipidomics data.

5.6.3 Modifying chloroplast galactolipid production in wheat by the introduction of *FAD5* or *ACT1*

In nature, more than 95% of plant species are 18:3 plants while only ~5% belong to 16:3 plants. It is generally accepted that the prokaryotic pathway has been lost during evolutionary processes. The endosymbiotic theory states that chloroplasts originated from oxygenic-photosynthetic prokaryotes and they are independent for lipid synthesis (Chan and Bhattacharya, 2010). Hence, loss of the prokaryotic pathway can be regarded as a loss of chloroplastic autonomy, where lipid synthesis is concerned. In terms of glycerolipid biosynthesis, original 16:3 plants appear to have evolved by losing the phosphatidate phosphatase activity that is the first enzyme in the prokaryotic pathway, consequently giving rise to 18:3 plants.

While *ACT1* and *FAD5* are critical for glycerolipid synthesis in the prokaryotic pathway, it is possible that either or both have been lost during the evolutionary process. To test the importance of *FAD5* and *ACT1* in producing galactolipids in chloroplast, I would conduct the following experiments: 1) Introducing *Arabidopsis FAD5* and *ACT1* genes into wheat, the coding sequence of *FAD5* and *ACT1* genes will be inserted into the pANIC 6E vector, used for overexpression in the grass family of plants, under the *ZmUbi* promoter (Mann et al., 2012). *ZmUbi*::*FAD5*and *ZmUbi*::*ACT1* transgenic plants will be generated. 2) Identification of positive transgenic wheat plants by medium selection, GUS staining and PCR screening. 3) Overexpression of both *FAD5* and *ACT1* genes in wheat plants. Wheat transgenic plants, *ZmUbi*::*FAD5* and *ZmUbi*::*ACT1,* will be crossed and double mutants carrying both *FAD5* and *ACT1* genes (*ZmUbi*::*FAD5/ZmUbi*::*ACT1*). 4) Biochemical analysis of wheat transgenic plants. Total fatty acid composition in leaves will be analyzed to assess the production of 16:3 fatty acids in both single and double transgenic plants. 5) Plant growth performance such as growth rate and chlorophyll content will be recorded when growing the transgenic plants under sub-optimal temperatures.

6 REFERENCES

Alfonso M, Yruela I, Almárcegui S, Torrado E, Pérez MA, Picorel R. 2001. Unusual tolerance to high temperatures in a new herbicide-resistant D1 mutant from *Glycine max* (L.) Merr. cell cultures deficient in fatty acid desaturation. Planta 212:573-582

Andersson MX, Larsson KE, Tjellstrom H, Liljenberg C, Sandelius AS. 2005. Phosphate-limited oat. The plasma membrane and the tonoplast as major targets for phospholipid-toglycolipid replacement and stimulation of phospholipases in the plasma membrane. J Biol Chem 280:27578-27586

Andersson MX, Stridh MH, Larsson KE, Liljenberg C, Sandelius AS. 2003. Phosphate-deficient oat replaces a major portion of the plasma membrane phospholipids with the galactolipid digalactosyldiacylglycerol. FEBS Lett 537:128-132

Arunga RO, Morrison WR. 1971. The structural analysis of wheat flour glycerolipids. Lipids 6:768-776

Awai K, Maréchal E, Block MA, Brun D, Masuda T, Shimada H, Takamiya K, Ohta H, Joyard J. 2001. Two types of MGDG synthase genes, found widely in both 16:3 and 18:3 plants, differentially mediate galactolipid syntheses in photosynthetic and nonphotosynthetic tissues in *Arabidopsis thaliana*. Proc Natl Acad Sci USA 98:10960-10965

Awai K, Xu C, Tamot B, Benning C. 2006. A phosphatidic acid-binding protein of the chloroplast inner envelope membrane involved in lipid trafficking. Proc Natl Acad Sci USA 103:10817-10822

Babiychuk E, Müller F, Eubel H, Braun HP, Frentzen M, Kushnir S. 2003. *Arabidopsis* phosphatidylglycerophosphate synthase 1 is essential for chloroplast differentiation, but is dispensable for mitochondrial function. Plant J 33:899-909

BeGora MD, Macleod MJ, McCarry BE, Summers PS, Weretilnyk EA. 2010. Identification of phosphomethylethanolamine N-methyltransferase from *Arabidopsis* and its role in choline and phospholipid metabolism. J Biol Chem 285:29147-29155

Beisson F, Koo AJK, Ruuska S, Schwender J, Pollard M, Thelen JJ, Paddock T, Salas JJ, Savage L, Milcamps A, Mhaske VB, Cho Y, Ohlrogge J. 2003. *Arabidopsis* genes involved in acyl lipid metabolism: a 2003 census of the candidates, a study of the distribution of expressed sequence tags in organs, and a web-based database. Plant Physiol 132:681-697

Benning C, Ohta H. 2005. Three enzyme systems for galactoglycerolipid biosynthesis are coordinately regulated in plants. J Biol Chem 280:2397-2400

Benning C, Xu C, Awai K. 2006. Non-vesicular and vesicular lipid trafficking involving plastids. Curr Opin Plant Biol 9:241-247

Benning C. 2008. A role for lipid trafficking in chloroplast biogenesis. Prog Lipid Res 47:381-389

Benning C. 2009. Mechanisms of lipid transport involved in organelle biogenesis in plant cells. Annu Rev Cell Dev Biol 25:71-91

Bolognese CP, McGraw P. 2000. The isolation and characterization in yeast of a gene for *Arabidopsis* S-adenosylmethionine:phospho-ethanolamine N-methyltransferase. Plant Physiol 124:1800-1813

Brockman JA, Norman HA, Hilderbrand DF. 1990. Effects of temperature, light and a chemical modulator on linolenate biosyntheis in mutant and wild type *Arabidopsis* calli. Phytochem 29:1447-1453

Browse J, Somerville C. 1991. Glycerolipids synthesis: biochemistry and regulation. Annu Rev Plant Physiol Plant Mol Biol 42:467-506

Browse J. Warwick N, Somerville CR, Slack CR. 1986. Fluxes through the prokaryotic and eukaryotic pathways of lipid synthesis in the ’16:3’ plant *Arabidopsis thaliana*. Biochem J 235:25-31

Chan CX, Bhattacharya D. 2010. The Origin of Plastids. Nature Education 3:84-85

Chapman KD, Ohlrogge JB. 2012. Compartmentation of triacylglycerol accumulation in plants. J Biol Chem 287:2288-2294

Chen J, Burke JJ, Xin Z, Xu C, Velten J. 2006. Characterization of the *Arabidopsis* thermosensitive mutant atts02 reveals an important role for galactolipids in thermotolerance. Plant Cell Environ 29:1437-1448

Collin S, Justin AM, Cantrel C, Arondel V, Kader JC. 1999. Identification of AtPIS, a phosphatidylinositol synthase from *Arabidopsis*. Eur J Biochem 262:652-658

Cruz-Ramírez A, López-Bucio J, Ramírez-Pimentel G, Zurita-Silva A, Sánchez-Calderon L, Ramírez-Chávez E, González-Ortega E, Herrera-Estrella L. 2004. The *xipotl* mutant of *Arabidopsis* reveals a critical role for phospholipid metabolism in root system development and epidermal cell integrity. Plant Cell 16:2020-2034

Eastmond PJ, Quettier AL, Kroon JT, Craddock C, Adams N, Slabas AR. 2010. Phosphatidic acid phosphohydrolase 1 and 2 regulate phospholipid synthesis at the endoplasmic reticulum in *Arabidopsis*. Plant Cell 22:2796-2811

Falcone DL, Ogas JP, Somerville CR. 2004. Regulation of membrane fatty acid composition by temperature in mutants of *Arabidopsis* with alterations in membrane lipid composition. BMC Plant Biol 4:17-32

Frentzen, M. 1993. Acyltransferases and triacylglycerols. In: Moore TS., ed. Lipid Metabolism in Plants. Boca Raton, FL: CRC Press; pp. 195-231

Gardiner SE, Rough PG. 1983. Relationship between fatty-acyl composition of diacylgalactosylglycerol and turnover of chloroplast phosphatidate. Biochem J 210:949-952

Gao J, Ajjawi I, Manoli A, Sawin A, Xu C, Froehlich JE, Last RL, Benning C. 2009. FATTY ACID DESATURASE4 of *Arabidopsis* encodes a protein distinct from characterized fatty acid desaturases. Plant J 60:832-839

Gibellini F, Smith TK. 2010. The Kennedy pathway-De novo synthesis of phosphatidylethanolamine and phosphatidylcholine. IUBMB Life 62:414-428

Gibson S, Arondel V, Iba K, Somerville C. 1994. Cloning of a temperature-regulated gene encoding a chloroplast ω-3 desaturase from *Arabidopsis thaliana*. Plant Physiol 106:1615-1621

Goode JH, Dewey RE. 1999. Characterization of aminoalcoholphosphotransferases from *Arabidopsis thaliana* and soybean. Plant Physiol Biochem 37:445-457

Gray GR, Ivanov AG, Król M, Williams JP, Kahn MU, Myscich EG, Huner NP. 2005. Temperature and Light modulate the *trans-delta3*-hexadecenoic acid content of phosphatidylglycerol: light-harvesting complex II organization and non-photochemical quenching. Plant Cell Physiol 46:1272-1282

Hagio M, Sakurai I, Sato S, Kato T, Tabata S, Wada H. 2002. Phosphatidylglycerol is essential for the development of thylakoid membranes in *Arabidopsis thaliana*. Plant Cell Physiol 43:1456-1464

Hamada T, Kodama H, Takeshita K, Utsumi H, Iba K. 1998. Characterization of transgenic tobacco with an increased α-linolenic acid level. Plant Physiol 118:591-598

Härtel H, Dörmann P, Benning C. 2000. DGD1-independent biosynthesis of extraplastidic galactolipids after phosphate deprivation in *Arabidopsis*. Proc Natl Acad Sci USA 97:10649-10654

Harwood JL. 1991. Strategies for coping with low environmental temperatures. Trends Biochem Sci 16:126-127

Harwood JL.1994. Environmental factors which can alter lipid metabolism. Prog Lipid Res 33:193-202

Haselier A, Akbari H, Weth A, Baumgartner W, Frentzen M. 2010. Two closely related genes of *Arabidopsis* encode plastidial cytidinediphosphate diacylglycerol synthases essential for photoautotrophic growth. Plant Physiol 153:1372-1384

Heilmann I, Mekhedov S, King B, Browse J, Shanklin J. 2004. Identification of the *Arabidopsis* palmitoyl-monogalactosyldiacylglycerol delta7-desaturase gene *FAD5*, and effects of plastidial retargeting of *Arabidopsis* desaturases on the *fad5* mutant phenotype. Plant Physiol 136:4237-4245

Heinz E, Roughan PG. 1983. Similarities and differences in lipid metabolism of chloroplasts isolated from 18:3 and 16:3 Plants. Plant Physiol 72:273-279

Heppard EP, Kinney AJ, Stecca KL and Miao GH. 1996. Developmental and growth temperature regulation of two different microsomal ω-6 desaturase genes in soybeans. Plant Physiol 110:311-319

Hölzl G, Witt S, Gaude N, Melzer M, Schöttler MA, and Dörmann P. 2009. The role of diglycosyl lipids in photosynthesis and membrane lipid homeostasis in Arabidopsis. Plant Physiol 150:1147-1159

Huang X, Madan A. 1999. CAP3: a DNA sequence assembly program. Genome Res 9:868-877

Huang D, Jaradat MR, Wu W, Ambrose SJ, Ross AR, Abrams SR, Culter A. 2007. Structural analog of ABA reveal novel features of ABA perception and signaling in Arabidopsis. Plant J 50:414-428

Hugly S, Somerville C. 1992. A role for membrane lipid polyunsaturation in chloroplast biogenesis at low temperature. Plant Physiol 99:197-202

Hugly S, Kunst L. Browse J, Somerville C. 1989. Enhanced thermal tolerance of photosynthesis and altered chloroplast ultrastructure in a mutant of *Arabidopsis* deficient in lipid desaturation. Plant Physiol 90:1134-1142

Iba K. 2002. Acclimative response to temperature stress in higher plants: approaches of gene engineering for temperature tolerance. Ann Rev Plant Biol 53:225-245

Inatsugi R, Kawai H, Yamaoka Y, Yu Y, Sekiguchi A, Nakamura M, Nishida I. 2009. Isozyme-specific modes of activation of CTP: phosphorylcholine cytidylyltransferase in *Arabidopsis thaliana* at low temperature. Plant Cell Physiol 50:1727-1735

Johnson G, Williams JP. 1989. Effect of growth temperature on the biosynthesis of chloroplastic galactosyldiacylglycerol molecular species in *Brassica napus* leaves. Plant Physiol 91:924-929

Jouhet J, Marechal E, Baldan B, Bligny R, Joyard J, Block MA. 2004. Phosphate deprivation induces transfer of DGDG galactolipid from chloroplast to mitochondria. J Cell Biol 167:863-874

Kader JC. 1996. Lipid-transfer proteins in plants. Annu Rev Plant Physiol Plant Mol Biol 47:627-654

Kelly AA, Dörmann P. 2002. DGD2, an *Arabidopsis* gene encoding a UDP-galactose-dependent digalactosyldiacylglycerol synthase is expressed during growth under phosphate-limiting conditions. J Biol Chem 277:1166-1173

Kelly AA, Froehlich JE, Dormann P. 2003. Disruption of the two digalactosyldiacylglycerol synthase genes DGD1 and DGD2 in *Arabidopsis* reveals the existence of an additional enzyme of galactolipid synthesis. Plant Cell 15:2694-2706

Kennedy EP, Weiss SB. 1956. The function of cytidine coenzymes in the biosynthesis of phospholipides. J Biol Chem 222:193-214

Kim HU, H. 2004. Plastid lysophosphatidyl acyltransferase is essential for embryo development in *arabidopsis*. Plant Physiol 134:1206-1216

Kim HU, Li Y, Huang A. 2005. Ubiquitous and endoplasmic reticulum-located lysophosphatidyl acyltransferase, LPAT2, is essential for female but not male gametophyte development in *Arabidopsis*. Plant Cell 17:1073-1089

Kitano H. 2004. Biological robustness. Nat Rev Genet 5:826-837

Kobayashi K, Narise T, Sonoike K, Hashimoto H, Sato N, Kondo M, Nishimura M, Sato M, Toyooka K, Sugimoto K, Wada H, Masuda T, Ohta H. 2012. Role of galactolipid biosynthesis in coordinated development of photosynthetic complexes and thylakoid membranes during chloroplast biogenesis in *Arabidopsis*. Plant J 73:250-261

Kong, Y. 2011. Btrim: a fast, lightweight adapter and quality trimming program for next-generation sequencing technologies. Genomics 98:152-153

Kroll D, Meierhoff K, Bechtold N, Kinoshita M, Westphal S, Vothknecht UC, Soll J, Westhoff P. 2001. *VIPP1*, a nuclear gene of *Arabidopsis thaliana* essential for thylakoid membrane formation. Proc Natl Acad Sci USA 98:4238-4242

Kunst L, Browse J, Somerville C. 1988. Altered regulation of lipid biosynthesis in a mutant of *Arabidopsis* deficient in chloroplast glycerol-3-phosphate acyltransferase activity. Proc Natl Acad Sci USA 85:4143-4147

Kunst L, Samuels L. 2009. Plant cuticles shine: advances in wax biosynthesis and export. Curr Opin Plant Biol 12:721-727

Langmead B, Salzberg SL. 2012. Fast gapped-read alignment with Bowtie2. Nature Methods 9:357-359

Lempe J, Lachowiec J, Sullivan AM, Queitsch C. 2013. Molecular mechanisms of robustness in plants. Curr Opin Plant Biol 16:62-69

Lyons JM. 1973. Chilling injury in plants. Annu Rev Plant Physiol 24:445-466

Löfke C, Ischebeck T, König S, Freitag S, Heilmann I. 2008. Alternative metabolic fates of phosphatidylinositol produced by phosphatidylinositol synthase isoforms in *Arabidopsis thaliana*. Biochem J 413:115-124

Mann DG, Lafayette PR, Abercrombie LL, King ZR, Mazarei M, Halter MC, Poovaiah CR, Baxter H, Shen H, Dixon RA, Parrott WA, Neal Stewart C Jr. 2012. Gateway-compatible vectors for high-throughput gene functional analysis in switchgrass (*Panicum virgatum* L.) and other monocot species. Plant Biotech J 10:226-236

Matsuda O, Sakamoto H, Hashimoto T, Iba K. 2005. A temperature-sensitive mechanism that regulates post-translational stability of a plastidial omega-3 fatty acid desaturase (FAD8) in *Arabidopsis* leaf tissues. J Biol Chem 280:3597-3604

McConn M, Hugly S, Browse J, Somerville C. 1994. A mutation at the *fad8* locus of *Arabidopsis* identifies a second chloroplast ω-3 desaturase. Plant Physiol 106:1609-1614

Miquel M and Browse J. 1992. *Arabidopsis* mutants deficient in polyunsaturated fatty acid synthesis.Biochemical and genetic characterization of a plant oleoyl-phosphatidylcholine desaturase. J Biol Chem 267:1502-1509

Miquel M, James D Jr, Dooner H, Browse J. 1993. *Arabidopsis* requires polyunsaturated lipids for low temperature survival. Proc Natl Acad Sci USA 90:6208-6212

Miquel M, Cassagne C, Browse J. 1998. A new class of *Arabidopsis* mutants with reduced hexadecatrienoic acid fatty acid levels. Plant Physiol 117:923-930

Mizoi J, Nakamura M, Nishida I. 2006. Defects in *CTP:PHOSPHORYLETHANOLAMINE CYTIDYLYLTRANSFERASE* affect embryonic and postembryonic development in *Arabidopsis*. Plant Cell 18:3370-3385

Mongrand S, Bessoule J, Cabantous F and Cassagne C. 1998. The C16:3/C18:3 fatty acid balance in photosynthetic tissues from 468 plant species. Phytochem 49:1049-1064

Müller F, Frentzen M. 2001. Phosphatidylglycerophosphate synthases from *Arabidopsis thaliana*. FEBS Lett 509:298-302

Murakami Y, Tsuyama M, Kobayashi Y, Kodama H, and Iba K. 2000.Trienoic fatty acids and plant tolerance of high temperature. Science 287:476-479

Murata N, Los DA. 1997. Membrane fluidity and temperature perception. Plant Physiol 115:875-879

Murata N, Ishizaki-Nishizawa O, Higashi S, Hayashi H, TasakaY. 1992. Genetically engineered alteration in the chilling sensitivity of plants. Nature 356:710-713

Nakamura Y, Awai K, Masuda T, Yoshioka Y, Takamiya K, Ohta H. 2005. A novel phosphatidylcholine-hydrolyzing phospholipase C induced by phosphate starvation in *Arabidopsis*. J Biol Chem 280:7469-7476

Ohlrogge J, Browse J. 1995. Lipid biosynthesis. Plant Cell 7:957-970

Ouyang S, Buell CR. 2004. The TIGR Plant Repeat Databases: a collective resource for the identification of repetitive sequences in plants. Nucl Acids Res 32:360-363

Pearcy RW. 1978. Effects of growth temperature on the fatty acid composition of the leaf lipids in *Atriplex lentiformis* (*Torr.*) Wats. Plant Physiol 61:484-486

Pulsifer IP, Lowe C, Narayaran SA, Busuttil AS, Vishwanath SJ, Domergue F, Rowland O. 2014. Acyl-lipid thioesterase1-4 from *Arabidopsis thaliana* form a novel family of fatty acyl-acyl carrier protein thioesterases with divergent expression patterns and substrate specificities. Plant Mol Biol 84:549-663

Qi Q, Huang YF, Cutler AJ, Abrams SR, Taylor DC. 2003. Molecular and biochemical characterization of an aminoalcoholphosphotransferase (AAPT1) from *Brassica napus*: effects of low temperature and abscisic acid treatments on *AAPT* expression in *Arabidopsis* plants and effects of over-expression of *BnAAPT1* in transgenic *Arabidopsis*. Planta 217:547-558

Raison JK, Lyons JM. 1986. Chilling injury: a plea for uniform terminology. Plant Cell Environ 9:685-686

Robinson MD, McCarthy DJ, Smyth GK. 2010. edgeR: a Bioconductor package for differential expression analysis of digital gene expression data. Bioinformatics 26:139-140

Roston RL, Gao J, Murcha MW, Whelan J, Benning C. 2012. TGD1, -2, and -3 proteins involved in lipid trafficking form ATP-binding cassette (ABC) transporter with multiple substrate-binding proteins. J Biol Chem 287:21406-21415

Samuels L, Kunst L, Jetter R. 2008. Sealing plant surfaces: cuticular wax formation by epidermal cells. Annu Rev Plant Biol 59:683-707

Sanda S, Leustek T, Theisen MJ, Garavito RM, Benning C. 2001. Recombinant *Arabidopsis* SQD1 converts UDP-glucose and sulfite to the sulfolipid head group precursor UDP-sulfoquinovose *in vitro*. J Biol Chem 276:3941-3946

Schmidt H, Heinz E. 1993. Direct desaturation of intact galactolipids by a desaturase solubilized from spinach (*Spinacia oleracea*) chloroplast envelopes. Biochem J 289:777-782

Shen W, Li JQ, Dauk M, Huang Y, Periappuram C, Wei Y and Zou J. 2010. Metabolic and transcriptional responses of glycerolipid pathways to a perturbation of glycerol-3-phosphate metabolism in *Arabidopsis*. J Biol Chem 285:22957-22965

Shimojima M, Ohta H. 2011. Critical regulation of galactolipid synthesis controls membrane differentiation and remodeling in distinct plant organs and following environmental changes. Prog Lipid Res 50:258-266

Somerville C, Browse J. 1991. Plant lipids: metabolism, mutants, and membranes. Science 252:80-87

Stewart AJ, Parsons TL, Plotkin JB. 2012. Environmental robustness and the adaptability of populations. Evolution 66:1598-1612

Tang GQ, Novitzky WP, Carol Griffin H, Huber SC, Dewey RE. 2005. Oleate desaturase enzymes of soybean: evidence of regulation through differential stability and phosphorylation. Plant J 44:433-446

Tasseva G, Richard L, Zachowski A. 2004. Regulation of phosphatidylcholine biosynthesis under salt stress involves choline kinases in *Arabidopsis thaliana*. FEBS Lett 566:115-120

Wallis JG and Browse J. 2002. Mutants of *Arabidopsis* reveal many roles for membrane lipids. Prog Lipid Res 41:254-278

Wang Z, Anderson NS, Benning C. 2013. The phosphatidic acid binding site of the *Arabidopsis* trigalactosyldiacylglycerol 4 (TGD4) protein required for lipid import into chloroplasts. J Biol Chem 288:4763-4771

Welti R, Li W, Li M, Sang Y, Biesiada H, Zhou H, Rajashekar CB, Williams TD, Wang X. 2002. Profiling membrane lipids in plant stress responses: role of phospholipase Dα in freezing-induced lipid changes in *Arabidopsis*, J Biol Chem 277:31994-32002

Wolfe J. 1978. Chilling injury in plants-the role of membrane lipid fluidity. Plant Cell Environ 1:241-247

Wu J, Lightner J, Warwick N, Browse J. 1997. Low-temperature damage and subsequent recovery of *fab1* mutant *Arabidopsis* exposed to 2℃. Plant Physiol 113:347-356

Xu C, Fan J, Froehlich JE, Awai K, Benning C. 2005. Mutation of the TGD1 chloroplast envelope protein affects phosphatidate metabolism in *Arabidopsis*. Plant Cell 17:3094-3110

Xu C, Härtel H, Wada H, Hagio M, Yu B, Eakin C, Benning C. 2002. The *pgp1* mutant locus of *Arabidopsis* encodes a phosphatidylglycerolphosphate synthase with impaired activity. Plant Physiol 129:594-604

Xue HW, Hosaka K, Plesch G, Mueller-Roeber B. 2000. Cloning of *Arabidopsis thaliana* phosphatidylinositol synthase and functional expression in the yeast *pis* mutant. Plant Mol. Biol. 42:757-764

Yang W, Simpson JP, Li-Beisson Y, Beisson F, Pollard M, Ohlrogge JB. 2012. A land-plant-specific glycerol-3-phosphate acyltransferase family in *Arabidopsis*: substrate specificity, *sn-2* preference, and evolution. Plant Physiol 160:638-652

Yang Z, Li L, Kuang T. 2002.Thermal stability of oxygen evolution in photosystem II core complex in the presence of digalactosyl diacylglycerol. Chinese Sci Bull 47:23-26

Yu B, Xu C, Benning C. 2002. *Arabidopsis* disrupted in *SQD2* encoding sulfolipid synthase is impaired in phosphate-limited growth. Proc Natl Acad Sci USA 99:5732-5737

Zhang L, Kato Y, Otters S, Vothknecht UC, Sakamoto W. 2012. Essential role of VIPP1 in chloroplast envelope maintenance in *Arabidopsis*. Plant Cell 24:3695-3707

Zheng Z, Xia Q, Dauk M, Shen W, Selvaraj G, Zou J. 2003. Arabidopsis AtGPAT1, a member of the membrane-bound glycerol-3-phosphate acyltransferase gene family, is essential for tapetum differentiation and male fertility. Plant Cell 15:1872-1887

Zhou Y, Peisker H, Weth A, Baumgartner W, Dörmann P, Frentzen M. 2013. Extraplastidial cytidinediphosphate diacylglycerol synthase activity is required for vegetative development in *Arabidopsis thaliana*. Plant J 75:867-879

APPENDIX A

Differences in transcript levels of genes involved in lipid metabolism in *A. lentiformis* grown at 43°C compared to 23°C. Genes from different categories were compiled from Arabidopsis Acyl-Lipid Metabolism database (http://aralip.plantbiology.msu.edu) (Beisson et al., 2003; Li-Beisson et al., 2013). FDR, false discovery rate.

Category	Transcript	Length	Fold Change (43°C vs 23°C)	FDR	E value (BLASTx)	AGI code	Description
Degradation of Storage Lipids and Straight Fatty Acids	comp51196_c0_seq9	3291	0.09	2.07E-46	0	AT3G06810.1	| Symbols: IBR3 | acyl-CoA dehydrogenase-related
	comp53955_c1_seq22	2078	0.13	0.0002	0	AT1G10740.4	| alpha/beta-Hydrolases superfamily protein
	comp51196_c0_seq2	3206	0.19	0.00525	0	AT3G06810.1	| Symbols: IBR3 | acyl-CoA dehydrogenase-related
	comp51196_c0_seq6	4407	6.11	0.01811	0	AT3G06810.1	| Symbols: IBR3 | acyl-CoA dehydrogenase-related
	comp53955_c1_seq1	2740	6.72	0.01457	0	AT1G10740.2	| alpha/beta-Hydrolases superfamily protein
	comp53955_c1_seq16	2503	8.08	0.12417	0	AT1G10740.2	| alpha/beta-Hydrolases superfamily protein
	comp51196_c0_seq1	3113	8.56	7.39E-05	0	AT3G06810.1	| Symbols: IBR3 | acyl-CoA dehydrogenase-related
	comp51196_c0_seq5	3028	10.75	0.00418	0	AT3G06810.1	| Symbols: IBR3 | acyl-CoA dehydrogenase-related
	comp53955_c1_seq26	1801	45.26	0.00729	3.80E-93	AT1G10740.2	| alpha/beta-Hydrolases superfamily protein
	comp45806_c0_seq1	1710	224.55	6.36E-09	2.70E-95	AT4G19380.1	| Long-chain fatty alcohol dehydrogenase family protein
Fatty Acid Elongation and Wax and Cutin Metabolism	comp41056_c0_seq1	1553	0.07	9.75E-07	3.00E-52	AT3G49190.1	| O-acyltransferase (WSD1-like) family protein
	Contig2298	1412	0.10	0.06486	2.80E-13	AT3G49210.1	| O-acyltransferase (WSD1-like) family protein
	comp45863_c1_seq5	1745	0.11	0.00232	5.40E-17	AT5G12420.1	| O-acyltransferase (WSD1-like) family protein
	Contig2299	2012	0.19	3.99E-09	1.40E-48	AT3G49190.1	| O-acyltransferase (WSD1-like) family protein

	comp15919_c0_seq1	2633	4.81	1.55E-08	0	AT2G45970.1	| Symbols: CYP86A8, LCR | cytochrome P450, family 86, subfamily A, polypeptide 8
	comp49623_c0_seq1	1353	5.28	0.00383	7.50E-128	AT4G33790.1	| Symbols: CER4, G7, FAR3 | Jojoba acyl CoA reductase-related male sterility protein
	comp49540_c0_seq2	1673	6.04	2.53E-06	1.50E-172	AT4G33790.1	| Symbols: CER4, G7, FAR3 | Jojoba acyl CoA reductase-related male sterility protein
	comp42773_c0_seq1	1715	6.04	3.45E-58	1.30E-50	AT3G49190.1	| O-acyltransferase (WSD1-like) family protein
	comp47282_c0_seq1	699	7.27	0.01494	2.80E-37	AT1G67730.1	| Symbols: YBR159, KCR1, ATKCR1 | beta-ketoacyl reductase 1
	comp42416_c0_seq1	1603	8.05	1.39E-34	2.80E-51	AT3G49190.1	| O-acyltransferase (WSD1-like) family protein
	comp37030_c0_seq1	1859	11.63	6.93E-05	0	AT4G33790.1	| Symbols: CER4, G7, FAR3 | Jojoba acyl CoA reductase-related male sterility protein
	comp44691_c0_seq1	1536	19.46	1.95E-18	2.10E-44	AT3G51970.1	| Symbols: ATSAT1, ASAT1, ATASAT1 | acyl-CoA sterol acyl transferase 1
	comp45863_c1_seq4	1249	24.44	7.68E-11	1.00E-25	AT3G49190.1	| O-acyltransferase (WSD1-like) family protein
	comp49540_c0_seq3	1847	43.45	2.30E-83	4.50E-168	AT4G33790.1	| Symbols: CER4, G7, FAR3 | Jojoba acyl CoA reductase-related male sterility protein
Lipid Signaling	Contig3878	4659	0.00	5.05E-09	7.00E-167	AT1G55180.1	| Symbols: PLDEPSILON, PLDALPHA4 | phospholipase D alpha 4
	Contig3869	4356	0.00	2.61E-09	3.00E-176	AT1G55180.1	| Symbols: PLDEPSILON, PLDALPHA4 | phospholipase D alpha 4
	Contig3877	4367	0.00	1.03E-10	3.30E-176	AT1G55180.1	| Symbols: PLDEPSILON, PLDALPHA4 | phospholipase D alpha 4
	Contig3874	4670	0.00	2.06E-11	7.50E-167	AT1G55180.1	| Symbols: PLDEPSILON, PLDALPHA4 | phospholipase D alpha 4
	Contig3893	5011	0.00	4.65E-10	0	AT1G55180.1	| Symbols: PLDEPSILON, PLDALPHA4 | phospholipase D alpha 4
	comp54969_c0_seq28	4910	0.00	1.19E-05	0	AT3G43220.1	| Phosphoinositide phosphatase family protein
	Contig3864	4110	0.01	1.81E-06	5.30E-177	AT1G55180.1	| Symbols: PLDEPSILON, PLDALPHA4 | phospholipase D

						alpha 4
	comp53198_c4_seq17	1624	0.01	6.47E-07	7.40E-129	AT3G45140.1	| Symbols: LOX2, ATLOX2 | lipoxygenase 2
	comp53844_c0_seq8	1061	0.04	0.01415	4.60E-78	AT3G18860.1	| transducin family protein / WD-40 repeat family protein
	comp53526_c0_seq4	485	0.05	8.46E-06	7.40E-36	AT2G06050.3	| Symbols: OPR3 | oxophytodienoate-reductase 3
	Contig8174	1481	0.06	1.67E-31	1.20E-44	AT4G11850.1	| Symbols: PLDGAMMA1, MEE54 | phospholipase D gamma 1
	comp53844_c0_seq1	1134	0.07	0.14338	1.20E-134	AT3G18860.1	| transducin family protein / WD-40 repeat family protein
	comp54989_c2_seq21	1019	0.09	0.00228	4.60E-83	AT5G07360.1	| Amidase family protein
	comp53844_c0_seq18	1847	0.11	0.00022	0	AT3G18860.1	| transducin family protein / WD-40 repeat family protein
	comp47040_c5_seq1	2198	0.14	0.04481	1.20E-97	AT1G22620.1	| Symbols: ATSAC1 | Phosphoinositide phosphatase family protein
	comp43967_c0_seq1	2444	0.15	1.97E-65	7.60E-82	AT4G29070.2	| Phospholipase A2 family protein
	comp49379_c1_seq1	2861	0.17	8.17E-06	0	AT3G51830.1	| Symbols: ATG5, SAC8 | SAC domain-containing protein 8
	comp13097_c0_seq1	1378	0.19	0.00824	2.90E-177	AT2G30550.2	| alpha/beta-Hydrolases superfamily protein
	comp24002_c0_seq2	1053	0.19	0.00189	1.50E-30	AT1G13280.1	| Symbols: Aoc4 | allene oxide cyclase 4
	comp36405_c0_seq1	2069	0.22	0.01356	5.00E-80	AT5G58670.1	| Symbols: ATPLC1, ATPLC, PLC1 | phospholipase C1
	comp43967_c0_seq3	2199	0.22	1.82E-64	1.80E-82	AT4G29070.2	| Phospholipase A2 family protein
	comp44643_c0_seq1	3661	0.23	3.21E-13	0	AT5G64440.1	| Symbols: AtFAAH, FAAH | fatty acid amide hydrolase
	comp33975_c0_seq1	2436	4.00	3.46E-72	0	AT5G24240.1	| Phosphatidylinositol 3- and 4-kinase ;Ubiquitin family protein
	comp27355_c0_seq2	1667	4.32	0.06068	1.60E-109	AT1G33270.1	| Acyl transferase/acyl hydrolase/lysophospholipase superfamily protein
	comp53198_c4_seq5	956	4.94	0.01515	1.00E-15	AT3G45140.1	| Symbols: LOX2, ATLOX2 | lipoxygenase 2
	Contig8173	2310	5.35	0.19355	3.70E-168	AT2G42010.1	| Symbols: PLDBETA1, PLDBETA | phospholipase D beta 1
	Contig3901	4257	5.78	0.02205	5.70E-168	AT1G55180.1	| Symbols: PLDEPSILON, PLDALPHA4 | phospholipase D alpha 4

	Contig8863	1040	6.46	0.00102	3.70E-85	AT1G67560.1	| Symbols: LOX6 | PLAT/LH2 domain-containing lipoxygenase family protein
	comp47662_c0_seq3	5090	8.13	4.46E-05	0	AT2G42010.1	| Symbols: PLDBETA1, PLDBETA | phospholipase D beta 1
	comp36497_c0_seq1	1845	8.37	0.00013	7.60E-107	AT2G44810.1	| Symbols: DAD1 | alpha/beta-Hydrolases superfamily protein
	comp46618_c0_seq1	1846	8.62	1.67E-06	0	AT4G16820.1	| Symbols: PLA-I{beta]2 | alpha/beta-Hydrolases superfamily protein
	comp54989_c2_seq57	2056	12.00	0.00219	1.10E-68	AT5G07360.1	| Amidase family protein
	comp47662_c0_seq2	4132	13.16	0.0085	0	AT2G42010.1	| Symbols: PLDBETA1, PLDBETA | phospholipase D beta 1
	comp54969_c0_seq39	4820	13.83	0.00223	0	AT3G43220.1	| Phosphoinositide phosphatase family protein
	comp53998_c0_seq18	4848	24.23	0.02976	4.30E-96	AT5G20060.3	| alpha/beta-Hydrolases superfamily protein
	comp53844_c0_seq19	2935	36.18	0.00918	0	AT3G18860.1	| transducin family protein / WD-40 repeat family protein
	comp54969_c0_seq36	3684	45.70	0.00084	0	AT3G43220.1	| Phosphoinositide phosphatase family protein
	comp51547_c0_seq64	2272	62.63	4.78E-11	2.40E-175	AT1G55180.1	| Symbols: PLDEPSILON, PLDALPHA4 | phospholipase D alpha 4
	Contig3868	4339	138.85	0.00211	5.20E-175	AT1G55180.1	| Symbols: PLDEPSILON, PLDALPHA4 | phospholipase D alpha 4
	comp54930_c0_seq49	1196	253.79	0.001	4.10E-142	AT5G07360.1	| Amidase family protein
	comp51547_c0_seq92	1945	257.07	1.77E-09	1.10E-175	AT1G55180.1	| Symbols: PLDEPSILON, PLDALPHA4 | phospholipase D alpha 4
	comp53998_c0_seq1	4759	286.21	0.00073	3.60E-96	AT5G20060.3	| alpha/beta-Hydrolases superfamily protein
Lipid Transfer proteins	Contig10348	1282	0.00	3.10E-08	1.40E-83	AT4G10950.1	| SGNH hydrolase-type esterase superfamily protein
	comp54576_c1_seq11	677	0.00	3.04E-10	8.80E-14	AT4G10950.1	| SGNH hydrolase-type esterase superfamily protein
	Contig10337	1086	0.02	0.00379	1.30E-47	AT4G10950.1	| SGNH hydrolase-type esterase superfamily protein
	Contig10343	1584	0.06	0.0021	1.10E-85	AT4G10950.1	| SGNH hydrolase-type esterase superfamily protein
	Contig10349	1433	0.09	0.09374	1.30E-43	AT4G10950.1	| SGNH hydrolase-type esterase superfamily protein
	Contig10330	1878	0.09	0.11091	1.90E-69	AT4G10950.1	| SGNH hydrolase-type esterase

							superfamily protein
	Contig10331	1314	0.12	0.11236	8.70E-82	AT4G10950.1	| SGNH hydrolase-type esterase superfamily protein
	Contig10329	1515	0.16	8.07E-06	3.90E-47	AT4G10950.1	| SGNH hydrolase-type esterase superfamily protein
	comp30799_c0_seq1	757	0.22	2.08E-49	2.50E-22	AT5G59320.1	| Symbols: LTP3 | lipid transfer protein 3
	comp51931_c0_seq4	6203	0.24	1.06E-17	5.30E-126	AT4G02340.1	| alpha/beta-Hydrolases superfamily protein
	comp46125_c0_seq2	2881	4.12	3.94E-14	0	AT1G49430.1	| Symbols: LACS2, LRD2 | long-chain acyl-CoA synthetase 2
	Contig465	368	4.78	0.00641	1.90E-10	AT5G36880.2	| Symbols: ACS | acetyl-CoA synthetase
	comp42629_c0_seq1	1565	4.94	2.82E-76	9.50E-123	AT4G02340.1	| alpha/beta-Hydrolases superfamily protein
	comp36581_c0_seq1	782	5.28	0.00897	1.40E-34	AT2G48140.1	| Symbols: EDA4 | Bifunctional inhibitor/lipid-transfer protein/seed storage 2S albumin superfamily protein
	Contig10341	919	5.32	0.13125	4.30E-67	AT4G10950.1	| SGNH hydrolase-type esterase superfamily protein
	comp53776_c0_seq3	4043	5.46	0.00091	0	AT4G23850.1	| Symbols: LACS4 | AMP-dependent synthetase and ligase family protein
	comp40508_c0_seq1	899	6.44	#######	1.20E-20	AT5G59320.1	| Symbols: LTP3 | lipid transfer protein 3
	Contig2928	2597	6.89	0.00584	6.10E-75	AT3G49050.1	| alpha/beta-Hydrolases superfamily protein
	comp17632_c0_seq1	649	9.33	#######	4.70E-34	AT2G38540.1	| Symbols: LP1, LTP1, ATLTP1 | lipid transfer protein 1
	comp51520_c0_seq19	2055	14.61	0.01485	3.50E-145	AT3G49050.1	| alpha/beta-Hydrolases superfamily protein
	Contig2929	2128	14.79	6.73E-05	0	AT3G49050.1	| alpha/beta-Hydrolases superfamily protein
	comp17452_c0_seq1	1042	29.60	#######	3.20E-23	AT5G59310.1	| Symbols: LTP4 | lipid transfer protein 4
	comp54576_c1_seq17	1593	32.73	8.33E-15	4.70E-90	AT4G10950.1	| SGNH hydrolase-type esterase superfamily protein
	Contig4242	2086	157.65	0.00025	3.90E-156	AT2G42450.1	| alpha/beta-Hydrolases superfamily protein
	comp54576_c1_seq60	1996	217.02	4.48E-05	5.10E-78	AT4G10950.1	| SGNH hydrolase-type esterase superfamily protein
Metabolism of Acyl-Lipids in Mitochondria	comp48714_c1_seq1	2875	0.01	9.88E-05	1.70E-65	AT3G60510.1	| ATP-dependent caseinolytic (Clp) protease/crotonase family protein
	comp54238_c0_seq20	2977	0.13	0.07216	1.90E-114	AT1G04640.2	| Symbols: LIP2 |

							lipoyltransferase 2
	comp54238_c0_seq16	2650	0.13	0.00314	2.00E-115	AT1G04640.2	| Symbols: LIP2 | lipoyltransferase 2
	comp6047_c0_seq1	1419	5.13	0.02471	1.10E-175	AT1G06520.1	| Symbols: ATGPAT1, GPAT1 | glycerol-3-phosphate acyltransferase 1
	comp54238_c0_seq21	3162	19.71	0.00013	5.70E-114	AT1G04640.2	| Symbols: LIP2 | lipoyltransferase 2
	comp54238_c0_seq25	5232	70.38	1.48E-08	2.00E-111	AT1G04640.2	| Symbols: LIP2 | lipoyltransferase 2
	comp54238_c0_seq22	5473	70.41	1.73E-05	3.20E-111	AT1G04640.2	| Symbols: LIP2 | lipoyltransferase 2
	comp54238_c0_seq19	5336	70.74	4.39E-06	2.50E-111	AT1G04640.2	| Symbols: LIP2 | lipoyltransferase 2
	comp51361_c0_seq11	1615	120.66	0.00042	7.50E-95	AT2G04540.1	| Beta-ketoacyl synthase
	comp51120_c0_seq2	5764	0.00	8.23E-08	0	AT5G04930.1	| Symbols: ALA1 | aminophospholipid ATPase 1
	comp51120_c0_seq17	5735	0.00	3.68E-05	0	AT5G04930.1	| Symbols: ALA1 | aminophospholipid ATPase 1
	Contig9294	2826	0.03	0.02323	0	AT4G04320.1	| malonyl-CoA decarboxylase family protein
	comp48543_c0_seq2	3494	0.11	0.04085	0	AT3G23510.1	| Cyclopropane-fatty-acyl-phospholipid synthase
	comp48543_c0_seq5	3569	0.19	0.17758	0	AT3G23510.1	| Cyclopropane-fatty-acyl-phospholipid synthase
	comp50832_c0_seq2	2752	5.27	0.03504	0	AT1G04010.1	| Symbols: PSAT1, ATPSAT1 | phospholipid sterol acyl transferase 1
Miscellaneous	comp50832_c0_seq3	2724	5.67	0.02127	0	AT1G04010.1	| Symbols: PSAT1, ATPSAT1 | phospholipid sterol acyl transferase 1
	Contig3513	5468	5.81	0.00232	0	AT5G04930.1	| Symbols: ALA1 | aminophospholipid ATPase 1
	comp54522_c0_seq1	970	7.65	5.24E-38	4.50E-76	AT3G23510.1	| Cyclopropane-fatty-acyl-phospholipid synthase
	Contig3515	5439	11.85	1.75E-05	0	AT5G04930.1	| Symbols: ALA1 | aminophospholipid ATPase 1
	comp52305_c0_seq6	4930	14.98	7.50E-06	0	AT3G27870.1	| ATPase E1-E2 type family protein / haloacid dehalogenase-like hydrolase family protein
	comp54282_c2_seq5	3048	18.53	0.00505	0	AT4G04320.1	| malonyl-CoA decarboxylase family protein
	Contig4474	1750	82.97	0.00048	7.20E-84	AT3G05420.1	| Symbols: ACBP4 | acyl-CoA binding protein 4
	comp51120_c0_seq3	5581	142.78	0.00073	0	AT5G04930.1	| Symbols: ALA1 | aminophospholipid ATPase 1

	comp51120_c0_seq5	5610	271.50	0.00011	0	AT5G04930.1	| Symbols: ALA1 | aminophospholipid ATPase 1
Synthesis of Fatty Acids in Plastids	comp37751_c0_seq1	588	4.76	0.00457	1.40E-37	AT2G38040.2	| Symbols: CAC3 | acetyl Co-enzyme a carboxylase carboxyltransferase alpha subunit
	comp44487_c0_seq1	1978	5.16	2.47E-84	2.00E-174	AT3G02630.1	| Plant stearoyl-acyl-carrier-protein desaturase family protein
Synthesis of Membrane Lipids in Endomembrane System	Contig6774	4034	0.01	8.64E-05	3.00E-122	AT4G22340.1	| Symbols: CDS2 | cytidinediphosphate diacylglycerol synthase 2
	comp53415_c0_seq30	1982	0.01	0.00747	0	AT4G22340.1	| Symbols: CDS2 | cytidinediphosphate diacylglycerol synthase 2
	comp53415_c0_seq20	1890	0.04	0.02013	0	AT4G22340.1	| Symbols: CDS2 | cytidinediphosphate diacylglycerol synthase 2
	comp48007_c0_seq10	1934	0.08	0.00702	1.00E-159	AT1G15110.1	| phosphatidyl serine synthase family protein
	Contig2731	2893	0.13	0.19785	1.30E-93	AT3G05510.1	| Phospholipid/glycerol acyltransferase family protein
	Contig2251	1889	0.20	0.04819	3.10E-148	AT3G18850.4	| Symbols: LPAT5 | lysophosphatidyl acyltransferase 5
	comp51810_c0_seq11	2096	0.20	0.06788	7.40E-158	AT2G40690.1	| Symbols: GLY1, SFD1 | NAD-dependent glycerol-3-phosphate dehydrogenase family protein
	comp48007_c0_seq12	1495	0.24	0.12098	3.30E-122	AT1G15110.1	| phosphatidyl serine synthase family protein
	Contig4168	2147	6.36	0.01484	1.30E-154	AT2G40690.1	| Symbols: GLY1, SFD1 | NAD-dependent glycerol-3-phosphate dehydrogenase family protein
	comp53392_c0_seq7	2390	6.86	0.0123	2.00E-160	AT1G13580.3	| Symbols: LAG13 | LAG1 longevity assurance homolog 3
	comp51810_c0_seq18	2190	7.44	0.10865	0	AT2G40690.1	| Symbols: GLY1, SFD1 | NAD-dependent glycerol-3-phosphate dehydrogenase family protein
	Contig1857	1708	9.92	0.00388	4.80E-141	AT1G15110.1	| phosphatidyl serine synthase family protein
	Contig6779	3664	35.62	0.00434	2.10E-123	AT4G22340.1	| Symbols: CDS2 | cytidinediphosphate diacylglycerol synthase 2
	comp46325_c0_seq3	1590	4.49	0.01786	1.70E-150	AT5G40610.1	| NAD-dependent glycerol-3-phosphate dehydrogenase family protein

APPENDIX B

Differences in transcript levels of genes in glycerolipid pathways in *A. lentiformis* grown at 43°C compared to 23°C. FPKM, fragments per feature kilobase per million reads mapped. logFC, log (fold change); FDR, false discovery rate.

Transcript	AGI code	Length	FPKM (23°C)	FPKM (43°C)	LogFC (43°C/23°C)	FDR	E value (BLASTx)	Gene Symbol
Contig2251	AT3G18850	1889	0.40	0.08	-2.33	0.0481938	3.10E-148	LPAAT5
comp52583_c0_seq6	AT1G32200	3196	41.12	12.21	-1.76	6.09E-97	8.00E-112	ATS1 / ACT1
comp46938_c0_seq1	AT4G01950	2154	11.05	4.11	-1.44	2.09E-13	1.40E-154	GPAT3
comp34146_c2_seq1	AT1G48600	715	262.70	101.44	-1.38	1.20E-71	7.90E-103	CPUORF31
comp49619_c1_seq1	AT1G08510	1945	97.63	40.97	-1.26	2.95E-54	0	FatB
comp34146_c1_seq1	AT1G73600	2269	95.33	42.07	-1.19	5.07E-46	4.00E-107	
comp50772_c0_seq1	AT2G45150	1551	14.11	6.32	-1.17	1.42E-10	8.80E-142	CDS4
comp48335_c0_seq1	AT1G65260	1613	95.81	49.37	-0.97	5.56E-28	5.20E-142	VIPP1
comp41529_c0_seq1	AT3G15850	1796	120.30	62.30	-0.96	7.54E-25	2.50E-155	FAD5 / ADS3
comp46757_c0_seq1	AT2G38670	2426	18.23	9.98	-0.88	2.18E-15	2.50E-178	PECT1
comp30776_c0_seq1	AT3G11670	3101	53.08	30.18	-0.82	2.54E-20	0	DGD1
Contig6775	AT4G22340	3677	24.40	14.78	-0.73	3.29E-08	0	CSS2; CDP-DAGS
comp45044_c0_seq1	AT4G00550	2008	13.58	8.55	-0.67	2.03E-06	0	DGD2
Contig5346	AT4G30580	2061	6.91	4.55	-0.61	0.0273726	1.70E-114	LPAAT1
comp34917_c0_seq2	AT3G11170	689	5.62	3.77	-0.58	0.2853372	3.60E-60	FAD7
comp52995_c0_seq1	AT4G31780	2302	23.21	16.36	-0.51	6.65E-07	0	MGD1
comp52612_c3_seq1	AT1G13560	2155	31.69	24.29	-0.39	0.0018853	0	AAPT1
comp40211_c0_seq1	AT4G33030	2240	30.36	23.43	-0.38	9.72E-05	0	SQD1
comp43021_c0_seq2	AT5G20410	1952	4.41	3.48	-0.35	0.3239245	0	MGD2
comp17657_c0_seq1	AT1G74960	2710	49.50	39.30	-0.34	5.53E-05	0	KASII
comp50772_c0_seq2	AT3G60620	1471	0.70	0.56	-0.29	0.8642127	5.50E-111	CDS5
comp48525_c0_seq3	AT5G60620	3151	2.58	2.16	-0.27	0.4686397	0	GPAT9
Contig1671	AT3G20320	2047	18.22	15.29	-0.26	0.0380673	4.00E-155	TGD2
comp51810_c0_seq2	AT2G40690	2107	3.45	2.96	-0.22	0.6905215	0	SFD1

comp45389_c0_seq1	AT3G06960	2062	9.22	7.97	-0.22	0.2596021	4.10E-155	TGD4
comp34113_c0_seq1	AT4G30950	2423	165.23	143.40	-0.21	0.0313881	0	FAD6
comp45138_c1_seq1	AT2G43710	1832	103.05	90.27	-0.2	0.0258087	0	FAB2
comp48590_c0_seq1	AT1G19800	1731	16.26	14.42	-0.18	0.2316925	2.20E-163	TGD1
comp51114_c0_seq1	AT5G42870	4140	11.10	10.15	-0.14	0.3236447	1.50E-176	PAH2
comp50093_c0_seq1	AT1G65410	2290	12.00	11.19	-0.11	0.522185	3.60E-164	TGD3
comp49740_c0_seq1	AT5G46290	2381	36.18	35.70	-0.03	0.831816	0	KASI
comp45192_c0_seq1	AT1G01610	2372	74.95	79.05	0.07	0.550197	0	GPAT4
comp45511_c0_seq1	AT3G57650	1987	18.82	20.17	0.09	0.5341236	0	LPAAT2
comp40812_c0_seq1	AT5G03080	1544	16.12	17.27	0.09	0.6009942	1.40E-104	LPP
comp54177_c1_seq1	AT2G39290	1899	16.67	18.40	0.13	0.3823107	2.80E-84	PGP1
comp45087_c0_seq1	AT5G01220	2101	52.48	59.35	0.17	0.0876926	0	SQD2
comp40254_c0_seq1	AT3G25110	1711	19.71	23.92	0.27	0.0345435	9.10E-169	FatA
comp49125_c0_seq2	AT1G62640	1918	7.80	9.97	0.34	0.0634367	0	KASIII
comp35117_c0_seq1	AT4G27030	1866	13.46	17.62	0.38	0.0074512	4.40E-114	FAD4
Contig8105	AT2G41540	2633	9.96	15.83	0.66	1.99E-07	0	GPDHc1
comp45111_c0_seq1	AT3G12120	2019	67.77	146.82	1.11	9.35E-48	0	FAD2
comp46929_c0_seq4	AT1G68000	1596	5.34	12.94	1.27	8.21E-07	4.10E-113	PIS1
comp49916_c1_seq2	AT1G02390	1145	0.18	0.46	1.44	0.3267064	1.60E-35	GPAT2
comp49916_c0_seq1	AT1G06520	646	0.77	2.37	1.6	0.0359231	1.70E-48	GPAT1
comp189560_c0_seq1	AT3G11430	1727	0.22	0.76	1.78	0.0501885	0	GPAT5
comp46325_c0_seq3	AT5G40610	1590	0.10	0.43	2.17	0.0178559	1.70E-150	GPDHP
comp44487_c0_seq1	AT3G02630	1978	22.97	119.11	2.37	2.47E-84	2.00E-174	SAD